Using Natural Archives to Reconstruct Environmental Changes Caused by Human Activities

Lauren Rachel Gallant

Thesis submitted to the University of Ottawa
in partial fulfillment of the requirements for the

PhD of Science

In

Biology

Specializing in Chemical and Environmental Toxicology

Department of Biology
Faculty of Science
University of Ottawa
Ontario, Canada

Abstract

The objective of this thesis was to develop new approaches and perspectives in resolving historical information from natural archives. Paleolimnology, the study of past aquatic environments using lake sediment cores, has greatly advanced our understanding of previous environments. This thesis intended to expand the range of historical information that may be used in paleolimnology and for historical reconstructions. Here I used pond sediments and a bat guano deposit as natural archives that recorded a history of events that I interpreted using a combination of chemical and biological measurements. In particular, I applied sterols and stanols as novel approaches for interpreting historical information in natural archives.

First, I examined the chemical and biological composition of lake sediments to track the human occupation of Dorset and Thule people in Canada's High Arctic. As predicted, sterols, stanols, cadmium, copper, and zinc increased in sediments deposited during known periods of human occupation owing to nutrient addition, whereas these increases were absent in reference sites. These methods were further corroborated in a study of 20th century human occupation at Resolute Bay by examining similar constituents in waterbodies that received wastewater discharge.

Second, I used $\delta^{15}N$ and $\delta^{13}C$ to track the agricultural history of Jamaica using a 4,300-year-old bat guano deposit. I then used C/N, $\delta^{13}C$, and sterol and stanol ratios to detect two periods of increased frugivory relative to insectivory-based foraging. Metals normalized to titanium increased during the Industrial Revolution and $^{206}Pb/^{207}Pb$ values tracked the introduction and subsequent ban of leaded gasoline. I also examined the same chemical constituents in fresh bat guano from frugivorous, insectivorous, and sanguinivorous bats. C/N

values decreased and cholestanol, cholesterol, and cholesterol/(cholesterol+sitosterol) values increased in bat guano according to trophic level.

This thesis demonstrated the strength of examining several independent lines of evidence to reconstruct historical activities in both High Arctic waterbody sediments and a bat guano deposit. I showed that human activities were traceable within natural archives over several thousand years thus demonstrating that the multi-proxy approach is a powerful tool that can conduct a broad range of analyses in various natural archives.

Table of Contents

Dedication

In loving memory of

Dr. John Warkentin

Acknowledgements

First and foremost, I would like to thank my supervisor, Dr. Jules Blais, for the support and guidance over the course of my graduate studies. I really appreciate the time and resources that you put into my education. To Linda Kimpe and Dave Eickmeyer, thank you for the technical support in the lab. To my committee members, Dr. Danielle Fortin, Dr. Alexandre Poulain, and Dr. Jesse Vermaire, thank you for your support and direction over the years, and for continuously providing a new perspective.

To my parents, Steve, Marg, and Jocelyn, thank you for your unwavering encouragement; you were always there for me, in whatever capacity I required. To my brother, Scott, and my sister(in-law), Tine, words cannot express how much I appreciate everything that you two have done for me. I would not be where I am today without you both. You two put me back-together after every setback, listened to my ever concern, and always gave me a reason to smile. To my late grandpa, Dr. John Warkentin, you were the one who inspired my love of science and the reason I started this journey. To my grandma, Erna Warkentin, thank you for your endless support and encouragement, and for being a constant source of positivity.

To my lab family, I cannot thank each of you enough for everything over the past six years. I could not have done this without your help, both in and out of the office. I will be hard-pressed to ever find a work family as hilarious and supportive as you all. Cynthia, thank you for the countless hours of life chats; you are an incredible friend and you constantly helped me find my sanity. You continuously encouraged me and provided the best advice, both in and out of the office; I will miss having you as my desk buddy. Alexandre, thank you for being a continuous source of entertainment and for the endless supply of goldfish. Julie, you are the kindest and most caring human. Thank you for the dinners, the long conversations, and constant support.

Kirsten, thank you for the laughs and the continuous supply of the most random, yet useful, information; and most importantly, thank you for taking care of my plant babies. Kat, I cannot thank you enough for your help in the lab and in the office; you always provided the most positive and constructive feedback. Madison, I am eternally grateful for your help with stats, manuscript structuring, and general ability to problem solve. Jennifer, thank you so much for your continuous positivity, life advice, and hugs. Jon and Sawyer, the ELA boys, thank you for always encouraging second breakfast and for the laughs in the office and on the soccer field. The one and only, Pepe, thank you for showing me a world outside of Excel. Your guidance and continuous sass kept me both sane and level-headed. MC, thank you for everything. You always knew what I needed; whether it was a coffee, a movie night, a weekend in Tremblant, or just time to catch-up, you were always there to support me. Mija, my twin. I will forever be grateful for our shopping trips, IKEA adventures, party planning meetings, coffee breaks, and lengthy life updates. I look forward to a lifetime of coordinating outfits. Jen, thank you for feeding and clothing me, and thank you for being a constant source of laughter throughout this journey. I thoroughly looked forward to and appreciated all of your crazy stories and Piper updates. I also really appreciate your ability to put together a seating arrangement.

Shayne, I am so happy that I got to complete this journey with you by my side. Thank you for always supporting and encouraging me, and for the nights of cookies, breathing exercises, unofficial karaoke, shredded pepperoni, Mr. Christmas mouse conversations, and the continuous supply of fizzy water and Fisherman's Friends.

List of Abbreviations

Aluminum (Al)
Arsenic (As)
Before common era (BCE)
Before present (BP)
Cadmium (Cd)
Carbon (C)
Carbon/nitrogen (C/N)
Cesium (Cs)
Chloride (Cl)
Chlorophyll *a* (Chl *a*)
Chromium (Cr)
Common era (CE)
Constant rate of supply (CRS)
Copper (Cu)
Counts per second (CPS)
Crassulacean acid metabolism (CAM)
Crystal Lake (CRY)
Deuterated cholesterol (d6 cholesterol)
Dichlorodiphenyltrichloroethane (DDT)
Dichloromethane (DCM)
Dissolved inorganic carbon (DIC)
Dissolved organic carbon (DOC)
Dry weight (dw)
Frugivorous (Fru)
Gas chromatography (GC)
Gas chromatography mass spectrometry (GC-MS)
Glass fiber filter (GF/F)
Home Away from Home (HOM)
Iron (Fe)
Inductively coupled plasma mass spectrometry (ICP-MS)
Insectivorous (Ins)
International Biological Program (IBP)
Isotope ratio mass spectrometry (IRMS)
Lead (Pb)
Maximum (max)
Mercury (Hg)
Method detection limit (mdl)
Nitrogen (N)
Minimum (min)
Natural Sciences and Engineering Research Council (NSERC)
N,O-bis(trimethylsilyl)trifluoroacetamide) + trimethylchlorosilane (BSTFA + TMSCl)
Organic (Org)
Organic carbon (OC or C_{org})

Particulate organic carbon (POC)
Particular organic nitrogen (PON)
Percent organic carbon (C_{org})
Persistent organic pollutants (POPs)
Polar Continental Shelf Program (PCSP)
Principle Component Analysis (PCA)
Sample size (n)
Sanguinivorous (San)
Standard deviation (std. dev or SD)
Standard error (std. error)
Strontium (Sr)
Total dissolved nitrogen (TDN)
Total dissolved phosphorus (TDP)
Total phosphorus (TP)
United States Environmental Protection Agency (USEPA)
Vienna PDB (V-PDB)
Wakefield Lake (WAK)
Wet weight (ww)
Zinc (Zn)

List of Tables

Chapter 2

Chapter 3

Chapter 4

Chapter 5

List of Figures

Chapter 2

Chapter 3

Chapter 4

Chapter 5

Preface

This thesis was written by manuscript in accordance with the guidelines provided by the University of Ottawa's Faculty of Graduate and Postdoctoral Studies. Chapter 1 is an introduction to this thesis and provides the necessary information for the manuscripts to follow. Chapter 2 is a manuscript formatted to Elsevier's guidelines for authors provided by the journal *Anthropocene*. Chapter 3 is a manuscript formatted according to the guidelines for authors provided by the journal *Proceedings of the National Academy of Sciences of the United States of America*. Chapter 4 is a manuscript formatted to Elsevier's guidelines for authors provided by the journal *Palaeogeography, Palaeoclimatology, Palaeoecology*. Chapter 5 is a manuscript formatted according to the guidelines for authors provided by *Nature*. Chapter 6 summarizes the manuscripts and provides concluding remarks and future directions.

Chapter 1: General introduction

1 A brief history of human impacts on the environment

Many of humankind's advances have resulted in the alteration of the environment. One of the earliest records of change in the chemical composition of the terrestrial environment can be traced back to the use of fire by Neanderthals, which was evidenced by increased metal concentrations in hearths [1]. Likewise, atmospheric releases of metals due to mining activities can be traced back to ca. 5000 BCE in China, 1400 BCE in Bolivia, and 1400 CE in the Peruvian Andes [2–4]. Moreover, the development and establishment of cities, and the rise of the Industrial Revolution, led to increased atmospheric concentrations of pollutants, including heavy metals [5–7]. Agricultural practices have led to changes in the chemical composition of soils and nearby waterbodies [8–10] and wastewater discharge has increased the concentration of metals in waterbody sediments [11]. Commencing in the 1940s, the manufacturing and use of persistent organic pollutants (POPs) introduced a new human-derived pollutant to the environment. Fortunately, there has been an increase in the understanding of the burdens that humans have placed on the environment, which has led to modified practices to improve the health of the environment. In 1962, Rachel Carson's book, Silent Spring, sparked public outcry against the application of dichlorodiphenyltrichloroethane (DDT), as severe effects became evident in biota [12] and the surrounding landscape [13]. Changes in industry standards, such as the use of scrubbers in refineries, decreased the atmospheric emission of some metals [14], and regulations to limit the release of POPs have been ratified in many countries. The ongoing development and use of monitoring strategies for anthropogenically derived contaminants is thus crucial to help scientists track the long-term impacts of humans on the environment and reduce the legacy impact of these contaminants.

2 Human activities have increased the atmospheric concentration of metals

Human practices have contributed to the release of metals to the atmosphere for thousands of years. Historical mining practices increased the atmospheric concentrations of metals such as arsenic, cadmium, chromium, copper, and manganese [6]. For example, mining and smelting activity in Europe during the Roman Empire caused a significant increase in the atmospheric release of copper ($15{,}000 \times 10^3$ kg yr^{-1}), lead ($90{,}000 \times 10^3$ kg yr^{-1}), zinc ($10{,}000 \times 10^3$ kg yr^{-1}), and mercury (2000 kg yr^{-1}) [7]. Similarly, the development of the Patio Process, an improved mining practice used to extract silver from ore, increased mercury emissions in South and Central America from 1570 to 1900 CE (196×10^6 kg cumulatively) [15]. 20th century industrial practices have also contributed to atmospheric metal concentrations. In 1983, global coal and oil combustion were the two major contributors to the atmospheric release of heavy metals, and of the total global atmospheric metal emissions in that same year, nickel, lead, manganese, vanadium, and zinc were released in the greatest concentrations [16]. Increased industrial practices, such as zinc production, iron and steel manufacturing, and coal and oil combustion, increased atmospheric concentrations of zinc, nickel, and copper by 293 %, 187 %, and 125 %, respectively [6]. It is therefore evident that the processes of natural resource extraction, processing, and product manufacturing, have significantly increased atmospheric concentrations of metals. Further investigation is thus warranted to determine the magnitude of metal distribution in the environment and whether elevated metal concentrations persist today.

3 Natural archives allow for the reconstruction of historical environmental conditions

Contaminants emitted to the atmosphere eventually settle and accumulate in the terrestrial and/or aquatic environment, which allows for the reconstruction of historical

environmental conditions. Ice [17,18], peat bog [19,20], and sediment [21,22] cores commonly act as natural archives that can be used to infer the influence of anthropogenic activity, if any, on the environment. Bat guano deposits can also act as natural archives as cave-dwelling bats excrete guano in the same location, thus providing a long-term record of their exposure to anthropogenic activity [23,24]. Natural archives can thus be analyzed for a suite of anthropogenic contaminants, environmental proxies, and/or biomarkers, which allows for the reconstruction of historical environmental conditions. Changes in the chemical composition of the archive can be evaluated through time and can be used to infer the extent to which anthropogenic activity may have influenced the terrestrial and/or aquatic environment. Natural historical archives have been used by the scientific community to trace the evolution of human technology and the transition of nomadic societies to settled communities. Throughout history, the environmental impacts caused by humans have evolved, and modern scientists seek to reconstruct, and where possible remediate, these ubiquitous anthropogenic legacies of contamination.

3.1 Natural archives record the history of anthropogenic activity

Sediment cores are a useful tool to track the history of anthropogenic influence on metal concentrations in the environment. In particular, lake sediment cores have been extensively used to study the effects of mining on the environment. In Southern Iberia, lead concentrations increased from 28 to 90 μg g^{-1} dry weight (dw) in lake sediment cores as a result of mining during the Bronze Age (ca. 1950 BCE) [25]. Similarly, lead concentrations increased from ~ 0 to 300 μg g^{-1} dw in lake sediments deposited during pre-Colonial mining in the Bolivian Andes [3] and silver metallurgy ca. 1400 CE was traceable within lake sediment cores from Peru as evidenced by a ten-fold rise in lead [21]. These ancient mining techniques left a legacy footprint

of metal production in lake sediment cores. Cores are thus useful tools with which we can reconstruct the historical processes that shaped metal use and cultural development.

The introduction of leaded gasoline in the 1920s increased atmospheric concentrations of lead [6,17,26,27], which resulted in its subsequent ban in the 1970s due to rising environmental concerns [28]. Natural archives have proven to be a useful tool in tracking the history of leaded gasoline use [4,29]. In China, lead concentrations increased from to ~35 μg g^{-1} dw in lake sediments deposited ca. 1950 owing to leaded gasoline use [4]. A similar peak in lead (40 μg g^{-1} dw) was observed in Swiss lake sediments in response to the use of leaded gasoline [30]. Notably, the lead flux in a Swiss peat bog was 1570-fold greater in 1979 CE when compared to the background flux [29]. The use of leaded gasoline was so widespread, that lead concentrations (9.4 pg g^{-1}) peaked in snow deposited between 1969 and 2004 in Antarctica [31]. One can also use lead isotope ratios to confirm the source of lead in environmental archives [19,29]. In the United Kingdom, a decrease in $^{206}Pb/^{207}Pb$ values (from ~1.17 to ~1.1) in soils marked the onset of the worldwide use of leaded gasoline [27]. $^{206}Pb/^{207}Pb$ values also decreased (from ~1.18 to ~1.3) in a Swiss peat bog, coeval with the introduction of leaded gasoline [29]. Similar 20th century $^{206}Pb/^{207}Pb$ values in U.K foliage [27], Swiss peat bogs [29] and Spanish peat bogs [32] were evidence of the ubiquitous effects of coal burning and use of leaded gasoline. Fortunately, leaded gasoline was banned in the 1970s, which is marked by decreased lead concentrations and increased $^{206}Pb/^{207}Pb$ values in lake sediments [30]. This is a prime example of the utility of lake sediment cores to track not only the deposition of lead from anthropogenic sources, but also the effectiveness of implementing practices to reduce metal emissions.

In addition to lead, mercury concentrations also tracked the history of anthropogenic activity in natural archives. In Peru, mercury concentrations were 10-fold greater in mining-

impacted sediments than in pre-mining sediments deposited ca. 1400 BCE [2]. The rise in mercury emissions during the Roman Empire, a time period characteristic of elevated gold and silver mining activity, was also tracked worldwide in ice, peat, and sediment cores [17,19,25,33]. The mercury flux increased 10-fold in lake sediments from South America in response to mining during the colonial period (1400 to 1600 CE) [34]. In addition, by tracking the effect of anthropogenic activity on mercury deposition thousands of years ago, we can also observe increased mercury concentrations owing to 20th century practices. For example, ice cores tracked an approximately 3-fold increase in mercury concentrations during the 20th century owing largely to coal combustion [18,35]. Similar results were observed in a Swiss peat core where the mercury accumulation rate peaked (78 μg m^{-2} yr^{-1}) in the 1970s owing to the incineration of municipal waste [36]. As such, the effects of anthropogenic activity on the distribution of mercury in the environment are well-documented as evidenced by the globally elevated mercury concentrations in natural archives.

Increased concentrations of other heavy metals in natural archives have also tracked the influence of anthropogenic activity over the last 5000 years. Concentrations of copper, nickel, and zinc increased in lake sediments and peat cores during the Bronze Age in China (3000 BCE to 170 BCE), a period marked by an increase in mining and metal use [4,33]. 11th century metallurgy in Peru is evidenced by increased concentrations of zinc and copper [37]. More recently, peak concentrations of antimony (6 μg g^{-1} dw), silver (0.6 μg g^{-1} dw), and tin (0.5 μg g^{-1} dw) were recorded in Bolivian lake sediments coeval with early colonial mining [3]. 20th century lake sediments were also commonly enriched in zinc, cadmium, and copper owing to increased industrial activity [38]. It is thus evident that lake sediment cores are an ideal tool for tracking changes in atmospheric metal fluxes as a result of anthropogenic activity. Consequently,

sediment cores preserve metal concentrations pre, during, and post-impact; this allows for the determination of the magnitude of change (owing to anthropogenic activity) and the extent of recovery (when applicable).

3.2 Lake sediments and migratory species

In addition to anthropogenic activity, the deposition of faeces (e.g. by birds or mammals) into waterbodies can also change the chemical composition of sediments, and consequently reflect the influence of biota on the aquatic environment. One way to study how biota affect the chemical composition of the aquatic environment is by comparing animal-affected sediments to uninfluenced sediments. For example, cadmium, lead, manganese, and mercury were elevated in seabird-influenced Arctic sediments as a result of the birds' diet that was enriched in these elements [39], whereas selenium and mercury concentrations were greater in seal and penguin-influenced sediments relative to uninfluenced sediments owing to dietary enrichment of these elements [40]. Likewise, higher concentrations of cadmium were recorded in lake sediments influenced by northern fulmar [41] and bat [42] guano, relative to unaffected sediments. Copper and zinc concentrations also increased in seabird-influenced Arctic lake sediments [43]. In addition, these sediment cores can be used to infer movement and changes in biota populations. For example, a peak in the cadmium concentration in Arctic lake sediments reflected the arrival of little auks ca. 250 BCE [44]. Xie and Sun reported increased concentrations of arsenic in 1,800-year-old penguin faeces-influenced sediments, which they used to infer changes in penguin population size [45]. Sediment cores can thus be used to assess the historical influence of biota on waterbodies as the addition of faeces changes the chemical composition of the sediments.

4 Lake sediment cores track the history of human-derived effluents

Lake sediments may also be used to track the history of wastewater discharge. Prior to the development of more advanced wastewater treatment plants, raw sewage was commonly deposited directly into nearby waterbodies [11]. The effects of unloading raw sewage into waterbodies are well-documented and can result in increased concentrations of nutrients, heavy metals, pesticides, and personal care products in the water and sediments [46,47]. For example, chlorophyll *a* (chl *a*) decreased by ~80 % in sewage-influenced lakes following a reduction in sewage discharge [47] and wastewater-influenced High Arctic sediments had more eutrophic diatom assemblages than unimpacted ponds [48]. Specifically, a change in the diatom assemblage (from *Fragilaria sensu lato* to *Navicula kriegeri*) was observed in High Arctic lake sediments in response to wastewater input [49]. In remote locations, wastewater management is particularly difficult owing to logistical and geographical constraints [50,51]. As a result, untreated wastewater is often discharged directly into local waterbodies owing to limited infrastructure [49,52–54]. The study of wastewater discharge on remote lakes can be particularly informative as these systems are often depleted in nutrients prior to human impact [55], and thus changes in the chemical composition of the lake sediments are evident from human occupation.

4.1 Metal concentrations in lake sediments track the history of wastewater discharge

Metal concentrations are often greater in raw sewage than in the sediments of uninfluenced waterbodies, and as such, one can examine downcore metal profiles to track the history of wastewater discharge. For example, raw sewage from a wastewater treatment plant in Poland was most concentrated in chromium (260 μg g^{-1} dw), copper (330 μg g^{-1} dw), and zinc (710 μg g^{-1} dw), with lower, but detectable, concentrations of cadmium (1.9 μg g^{-1} dw), nickel (33 μg g^{-1} dw), and lead (35 μg g^{-1} dw) [11]. Cadmium, copper, lead, and zinc were also

approximately 1.3-fold greater in wastewater influenced sediments from Korea, relative to uninfluenced sediments [56]. Metal concentrations were also elevated in sediments from Zhifu Bay, China, as a result of wastewater input (relative to uninfluenced sediments) and concentrations subsequently decreased in sediments following the implementation of a sewage treatment plant [57]. The ratio of metals to titanium (to account for natural weathering) increased in lake sediments in response to wastewater [52]. The ratio of cadmium, lead, and zinc to titanium increased approximately 3-fold, 2-fold, and 5-fold, respectively, in wastewater influenced sediments [52]. Similarly, heavy metals, including copper and cadmium, were enriched in lake sediments from northern Fennoscandia owing to industrial wastewater discharge [58]. Metal concentrations in lake sediment cores can thus be used to determine and assess the extent of wastewater discharge into waterbodies.

4.2 Sterols and stanols in lake sediments track the history of wastewater discharge

Sterols (unsaturated) and stanols (saturated) are subgroups of steroids that are found in all eukaryotes [59]. Stanols are commonly formed by the reduction of sterols in the intestines of higher mammals [60]. Coprostanol, formed from the reduction of cholesterol in the intestines of higher mammals and birds, is frequently used to identify human-derived faeces in water samples as coprostanol constitutes approximately 60 % of all sterols and stanols in human faeces [61]. The elevated concentrations of coprostanol in wastewater (270 μg L^{-1}) [62] are thus reflected within wastewater-influenced sediments. For example, coprostanol increased from ~0 to 40 μg g^{-1} OC in wastewater influenced sediments from Guanabara Bay, Brazil [63] and increased coprostanol concentrations were recorded in wastewater-influenced sediments from the New York Bight [64], Arctic [65], and Antarctic [66]. In fact, increased concentrations of coprostanol were recorded in sediments collected from the Agora, Athens, Greece as a result of wastewater

input during the Roman period [67]. Cholestanol is formed from the microbial reduction of cholesterol [61] and low, but detectable concentrations of cholestanol are also found in human faeces: 70 μg g^{-1} dw; 1.4 % of total sterols [61,68]. As such, higher concentrations of cholestanol were found in lake sediments as a result of sewage input [68,69]. The cholesterol concentration in human faeces is approximately 290 μg g^{-1} dw, [61] and as such, cholesterol concentrations of 260 μg L^{-1} have been recorded in wastewater [62]. Consequently, increased cholesterol concentrations are frequently recorded in lake sediments owing to wastewater input [67,70].

Phytosterols (plant-derived sterols and stanols) include sitosterol and stigmastanol and can also track wastewater input. Sitosterol concentrations are typically elevated in vegetation, contributing to ~40 – 70 % of the sterol composition in High Arctic plants and mosses, for example [71]. Stigmastanol is produced by the microbial reduction of sitosterol in high trophic level mammals and thus stigmastanol is found in mammalian faeces [61]. Consequently, stigmastanol concentrations in lake sediments increased coeval with manure inputs [72], and sitosterol increased in Arctic lake sediments in response to sewage dumping [65].

5 Ancient human settlements near High Arctic waterbodies

Small communities surrounding High Arctic lakes can alter the chemical composition of the sediments. The Thule people were a group of nomadic whalers who were present in Canada's High Arctic from ca. 1200 CE to ca. 1500 CE [73]. They arrived *via* the Bering Strait and moved south approximately 500 years ago as a result of cooling temperatures during the Little Ice Age, which decreased their ability to hunt owing to sea-ice blockages [74–77]. The Thule specialized in hunting bowhead whales: they hunted using spears and seal-skin floats, which they attached to the whales to keep them from diving [78]. One report estimated that the Thule people hunted ~18,500 whales during their time in Greenland and the Canadian Arctic [73]. The whalebones

were used to construct residential structures, such as permanent and semi-permanent homes, and work-related structures, such as temporary whaling camps and kayak stands [73,75,79]. In order to construct these whalebone structures, whales were brought into or in close proximity to, coastal ponds, and consequently, whalebones are visible in many of those ponds today.

5.1 Stable isotopes, sterols, and stanols recorded the history of human occupation in High Arctic lake sediments

$\delta^{15}N$ profiles in pond sediments can track nitrogen sources from higher trophic level species, because carnivorous species, like humans, are enriched in the heavier nitrogen isotope (^{15}N) relative to the lighter nitrogen isotope (^{14}N) [80,81]. $\delta^{15}N$ values in sediments from Thule-occupied ponds increased coeval with Thule arrival [82,83]. $\delta^{15}N$ values also tracked the departure of the Thule people from these sites, as evidenced by a decrease in $\delta^{15}N$ values (from ~7 to 5.5 %) to pre-Thule settlement values in some sites [82].

Sterols and stanols can also track human settlement adjacent to High Arctic waterbodies. Zoosterols and phytosterols are relatively stable in cold and anaerobic environments [65,84], and consequently, fluctuations in zoosterols and phytosterols in lake sediments may result from human occupation, particularly in an otherwise desolate and oligotrophic setting like an Arctic coastline environment. Coprostanol and cholesterol are present in human faeces, and as such, they should be present in lake sediments influenced by human activity. Indeed, coprostanol comprised ~20 % of the total sterol and stanol composition in High Arctic lake sediments as a result of human settlements around the lake [65]. An increase in the ratio of coprostanol to cholesterol in Arctic lake sediments marked the presence of the T'satsaot'ine people [65].

The presence of the Thule people and nutrients from whale carcasses increased primary production in ponds, as evidenced by shifts to more eutrophic diatom species and increased sedimentary chl *a* (up to three-fold greater) during the time of Thule occupation [82,83].

Consequently, phytosterols should also track the history of human settlement adjacent to Arctic ponds as campesterol, sitosterol, and stigmastanol constitute the majority of sterols and stanols in algae and terrestrial and aquatic plants [71,85]. Thus, one would predict increased sediment phytosterol concentrations in response to increased productivity in sediments deposited at the time of Thule settlement.

6 Bat guano deposits can also serve as natural archives on which one can study the effects of anthropogenic activity

Thus far, we have demonstrated the utility of studying changes in the chemical composition of lake sediment cores to infer the effects of industrial practices, wastewater input, and human settlement on the environment. Bat guano deposits can be used in a similar manner, as the accumulation of guano through time allows one to more directly address the exposure of bats to anthropogenic influences in the environment. One can measure the concentration of contaminants in the excrement of biota in order to track historical changes in chemical exposure to the animals that produced them. Furthermore, bats are an excellent study species because they occupy a range of trophic levels owing to their various dietary habits (frugivorous, insectivorous, and sanguinivorous), which allows one to examine the movement of contaminants through the food web. In addition, bats provide a number of ecosystem services (including pollination, seed dispersal, and acting as a natural insecticide [86]), and consequently, it is important to understand how anthropogenic activity affects the chemical composition of their guano as this can be evidence of their exposure to environmental contaminants. Collection of their guano is relatively non-invasive and can be used as an indicator of their overall body burden of a specific contaminant. Increased metal concentrations in bat guano have been correlated to their environmental exposure to anthropogenic activity. For example, the concentration of cadmium

was elevated (2.2 μg g^{-1} dw) in guano from bats inhabiting caves in proximity to a battery recycling factory [87]. As well, bats roosting near a contaminated military site had higher concentrations of mercury in their guano (0.43 μg g^{-1} dw), relative to bats roosting in uncontaminated areas (0.13 μg g^{-1} dw) [88]. Bat guano can therefore be analyzed for environmental contaminants and used to assess the effects of anthropogenic emissions on mammals occupying a range of trophic levels.

6.1 Bat guano preserves a record of anthropogenic activity

Bat guano deposits offers the means to reconstruct historical exposure trends in relation to changing industrial practices, with the advantage of determining whether bats are exposed to these contaminants. For example, lead and copper concentrations in a 30,000-year-old bat guano deposit reached peak concentrations of ~10 and >1000 μg g^{-1} dw, respectively [89]. Similarly, copper concentrations in a 13,000-year-old bat guano deposit from Borneo were elevated (~8,000 μg g^{-1} dw), with lower concentrations of other metals such as chromium (~450 μg g^{-1} dw), vanadium (~250 μg g^{-1} dw), and zinc (2,250 μg g^{-1} dw) [23]. Onac et al. also examined downcore metal concentrations (of copper, lead, and zinc) in a ~3,000-year-old bat guano deposit in Romania [90] but did not link fluctuations in metal concentrations to anthropogenic activity. Given the elevated metal concentrations previously observed in bat guano deposits, it should be possible to examine temporal changes in metal concentrations in association with changes in anthropogenic activity to infer how bat exposure to metals has changed over time.

6.2 Stable isotopes track dietary changes in bat guano

Stable isotopes are also well-preserved in guano deposits and can be used to infer dietary changes and/or exposure to anthropogenic activity [91–93]. Nitrogen stable isotope values increased with trophic level (e.g.: phytoplankton, zooplankton, insects, and mammals), nitrogen

excretion sources, and habitats [81]. This is the result of preferential fractionation of the lighter nitrogen isotope in higher trophic level species [94,95]. For example, $\delta^{15}N$ values in a chimney swift guano deposit tracked a dietary shift in prey owing to the introduction of DDT [92]. As well, $\delta^{15}N$ has been used as an indicator of trophic position in pond-derived sediments influenced by seabirds [96] and bat guano [97,98]. When studying bat guano, a bat's diet should reflect the specific stable nitrogen isotope of their food source [99,100]. Indeed, greater $\delta^{15}N$ values were present in insectivorous bats relative to frugivorous bats [101]. In summary, $\delta^{15}N$ values in bat guano reflect a bat's diet and thus long-term changes in foraging habits may be evidenced by changes in $\delta^{15}N$ values within a bat guano deposit.

$\delta^{13}C$ is another stable isotope that can be analyzed in bat guano deposits to track their dietary changes. $\delta^{13}C$ can be an indicator of diet as the ratio is dependent on the photosynthetic pathway type of the vegetation the bats consume, either directly or indirectly (*via* insects for example) [102,103]. There are three possible carbon-derived food sources: C3, C4 or crassulacean acid metabolism (CAM). C3 plants, characterized by the production of two 3-phosphoglyceric acids from atmospheric CO_2, dominate under cool, moist conditions, when photorespiration is limited. Conversely, C4 plants dominate under high temperatures because their stomata are open less frequently, thereby reducing water loss. CAM plants are even more effective at preserving water because they open their stomata at night thus dominating under arid conditions. C3 and C4 plants are easily distinguished by their varying $\delta^{13}C$ values, averaging -28.1 ‰ and -13.5 ‰, respectively [104]. CAM plants, however, can be more difficult to identify as the isotope ratio is dependent on the light availability during photosynthesis such that $\delta^{13}C$ may reflect typical C3 or C4 values [104]. The majority of CAM plants, however, have the least negative $\delta^{13}C$ values characteristic of their preference for dry habitats. Therefore, photosynthetic

pathways type is species specific resulting in $\delta^{13}C$ values that are mirrored within the consumer [99] thus allowing for the determination of a bat's diet. $\delta^{13}C$ is typically enriched in C4-derived plants and higher trophic level organisms relative to their diet owing to preferential fractionation of ^{12}C [24,104–106] thus allowing one to determine the carbon source and foraging habits of an individual.

6.3 Sterols and stanols in bat guano differ between feeding habits

The sterol and stanol composition of bat guano should be different between frugivorous, insectivorous, and sanguinivorous bats. The faeces of mammalian herbivores is typically enriched in C_{29} 5β-stanols such as sitostanol, stigmastanol, and campestanol [107]. Notably, concentrations of sitosterol and stigmastanol tend to be similar among mammalian herbivores and omnivores owing to overlaps in their diet. For example, the stigmastanol concentration in goat and human faeces was 330 μg g^{-1} dw and 160 μg g^{-1} dw, respectively [85] and the sitosterol concentration in cow and human faeces was 270 μg g^{-1} dw and 313 μg g^{-1} dw, respectively [85]. Campesterol is also abundant in plants (> 300 mg kg^{-1} wet weight) [108,109], and is present in human faeces (300 μg g^{-1} dw [110]) and herbivore faeces (3 to 140 μg g^{-1} dw [111]). Notably, some herbivores are particularly enriched in phytosterols relative to omnivores; for example, stigmastanol in sheep faeces was 1400 μg g^{-1} dw [85] and sitosterol in rabbits was 970 μg g^{-1} dw [111]. Thus, while concentrations of sterols and stanols are generally similar in faeces from herbivores and omnivores, there are species specific exceptions.

Insects tend to have similar concentrations of sterols and stanols to the plants they consume. This is likely because arthropods are unable to synthesize their own cholesterol *de novo* and thus, they require a dietary intake of C_{28} and C_{29} sterols, such as sitosterol, stigmastanol, and campesterol, to synthesize cholesterol [107]. As a result, elevated

concentrations of sitosterol and campesterol are present in arthropods, which can make up > 95 % of their sterol and stanol composition [112,113]. Fucosterol and desmosterol are abundant in arthropods as they are intermediate products in the conversion of sitosterol to cholesterol in the gut of insects [114–116]. Conversely, fucosterol and desmosterol are present in low concentrations in algae and thus are not commonly analyzed in herbivorous mammals [61,111]. Concentrations of sterols and stanols differ in plants, insects, and mammalian faeces based on feeding habits. We thus surmised that these differences in sterol and stanol patterns among plants and animals would reflect different feeding habits in the guano of bats that feed on a range of plants, insects, and mammalian blood.

7 Summary

This thesis aimed to examine a series of paleo-proxies in both lake sediments and a bat guano deposit for the purpose of inferring the effects of anthropogenic activity on the aquatic and terrestrial environment. Using multiple proxies, including metals, lead isotopes, stable isotopes, sterols, and stanols, we examined temporal changes in the chemical composition of natural archives in relation to anthropogenic activity.

This thesis was written by manuscript and contains four data chapters. Chapter two examined sediment cores from High Arctic waterbodies that were influenced by wastewater. We compared a series of proxies in wastewater-influenced pond sediments to sediments in a nearby reference pond to determine the extent to which wastewater discharge altered the chemical composition of the sediments. Chapter three examined the chemical composition of sediment cores taken from ponds that were previously home to the Thule and Dorset people. The objective was to determine whether multiple proxies tracked the arrival and departure of the Thule and Dorset people and the extent to which the Thule and Dorset people altered the chemical

composition of the pond sediments. In Chapter four, we examined changes in the metal and stable isotope profiles within a 4,300-year-old bat guano deposit from Jamaica to infer the exposure of anthropogenic activity on the biotic environment. We applied commonly used techniques in the field of limnology to the guano deposit and demonstrated the effectiveness of using multiple proxies when reconstructing historical environmental conditions. The objective of chapter five was to determine the sterol and stanol composition in fresh guano from bats feeding at different trophic levels (frugivorous, insectivorous, and sanguinivorous) in order to identify chemical differences based on feeding habits. We also reconstructed the sterol and stanol profiles in a ~4,300-year-old bat guano deposit to reconstruct long-term changes in the foraging habits of the bat colony.

In summary, we demonstrated the effectiveness and strength of examining multiple-proxies in natural archives in order to reconstruct historical events. We provided compelling evidence that this multi-proxy approach tracked human influence in High Arctic waterbodies over the past 2000 years and that when applied to bat guano deposits, this multi-proxy approach can be used to monitor the effects of human activity and changes in bat feeding strategies based on the chemical composition of bat guano.

References

1. Monge G, Jimenez-Espejo FJ, García-Alix A, Martínez-Ruiz F, Mattielli N, Finlayson C, et al. Earliest evidence of pollution by heavy metals in archaeological sites. Sci Rep. 2015;5. doi:10.1038/srep14252
2. Cooke CA, Balcom PH, Biester H, Wolfe AP, Brenner M. Over three millennia of mercury pollution in the Peruvian Andes. Proc Natl Acad Sci U S A. 2009;106: 8830–8834.
3. Abbott MB, Wolfe AP. Intensive pre-Incan metallurgy recorded by lake sediments from the Bolivian Andes. Science. 2003;301: 1893–1895. doi:10.1126/science.1087806
4. Lee CSL, Qi S, Zhang G, Luo C, Zhao LYL, Li X. Seven thousand years of records on the mining and utilization of metals from lake sediments in Central China. Environ Sci Technol. 2008;42: 4732–4738. doi:10.1021/es702990n
5. Bollhöfer A, Rosman KJR. Isotopic source signatures for atmospheric lead: The Northern Hemisphere. Geochim Cosmochim Acta. 2001;65: 1727–1740. doi:10.1016/S0016-7037(00)00630-X
6. Nriagu JO, Pacyna JM. Quantitative assessment of worldwide contamination of air, water and soils by trace metals. Nature. 1988;333: 134–139. doi:10.1038/333134a0
7. Nriagu JO. A history of global metal pollution. Science. 1996;272: 223–224. doi:10.1126/science.272.5259.223
8. Ash C, Vacek O, Jakšík O, Tejnecký V, Drábek O. Elevated soil copper content in a Bohemian vineyard as a result of fungicide application. Soil Water Res. 2012;7: 151–158. doi:10.17221/41/2012-SWR
9. Böhlke J-K. Groundwater recharge and agricultural contamination. Hydrogeol J. 2002;10: 153–179. doi:10.1007/s10040-001-0183-3
10. Bull ID, Evershed RP, Betancourt PP. An organic geochemical investigation of the practice of manuring at a Minoan site on Pseira Island, Crete. Geoarchaeology. 2001;16: 223–242. doi:10.1002/1520-6548(200102)16:2<223::AID-GEA1002>3.0.CO;2-7
11. Bartkowska I, Biedka P, Tałałaj IA. Analysis of the quality of stabilized municipal sewage sludge. J Ecol Eng. 2019;20: 200–208. doi:10.12911/22998993/99306
12. Allinson G, Mispagel C, Kajiwara N, Anan Y, Hashimoto J, Laurenson L, et al. Organochlorine and trace metal residues in adult southern bent-wing bat (*Miniopterus schreibersii bassanii*) in southeastern Australia. Chemosphere. 2006;64: 1464–1471. doi:10.1016/j.chemosphere.2005.12.067
13. Blais JM, Kimpe LE, McMahon D, Keatley BE, Mallory ML, Douglas MSV, et al. Arctic seabirds transport marine-derived contaminants. Science. 2005;309: 445–445. doi:10.1126/science.1112658
14. Mecray EL, King JW, Appleby PG, Hunt AS. Historical trace metal accumulation in the sediments of an urbanized region of the Lake Champlain watershed, Burlington, Vermont. Water Air Soil Poll. 2001;125: 201–230.
15. Nriagu JO. Legacy of mercury pollution. Nature. 1993;363: 589–589. doi:10.1038/363589a0
16. Nriagu JO, Pacyna JM. Quantitative assessment of worldwide contamination of air, water and soils by trace metals. Nature. 1988;333: 134–139.
17. Hong S, Candelone J-P, Patterson CC, Boutron CF. Greenland ice evidence of hemispheric lead pollution two millennia ago by Greek and Roman civilizations. Science. 1994;265: 1841–1843.
18. Schuster PF, Krabbenhoft DP, Naftz DL, Cecil LD, Olson ML, Dewild JF, et al. Atmospheric mercury deposition during the last 270 years: A glacial ice core record of

natural and anthropogenic sources. Environ Sci Technol. 2002;36: 2303–2310. doi:10.1021/es0157503
19. Martínez Cortizas A, García-Rodeja E, Pontevedra Pombal X, Nóvoa Muñoz JC, Weiss D, Cheburkin A. Atmospheric Pb deposition in Spain during the last 4600 years recorded by two ombrotrophic peat bogs and implications for the use of peat as archive. Sci Total Environ. 2002;292: 33–44. doi:10.1016/S0048-9697(02)00031-1
20. Zuna M, Mihaljevič M, Šebek O, Ettler V, Handley M, Navrátil T, et al. Recent lead deposition trends in the Czech Republic as recorded by peat bogs and tree rings. Atmos Environ. 2011;45: 4950–4958. doi:10.1016/j.atmosenv.2011.06.007
21. Cooke CA, Abbott MB, Wolfe AP, Kittleson JL. A millennium of metallurgy recorded by lake sediments from Morococha, Peruvian Andes. Environ Sci Technol. 2007;41: 3469–3474.
22. Jin Z, Han Y, Chen L. Past atmospheric Pb deposition in Lake Qinghai, northeastern Tibetan Plateau. J Paleolimnol. 2010;43: 551–563. doi:10.1007/s10933-009-9351-6
23. Wurster CM, Rifai H, Haig J, Titin J, Jacobsen G, Bird M. Stable isotope composition of cave guano from eastern Borneo reveals tropical environments over the past 15,000 cal yr BP. Palaeogeogr Palaeoclimatol Palaeoecol. 2017;473: 73–81. doi:10.1016/j.palaeo.2017.02.029
24. Wurster CM, Patterson WP, McFarlane DA, Wassenaar LI, Hobson KA, Athfield NB, et al. Stable carbon and hydrogen isotopes from bat guano in the Grand Canyon, USA, reveal Younger Dryas and 8.2 ka events. Geology. 2008;36: 683–686. doi:10.1130/G24938A.1
25. García-Alix A, Jimenez-Espejo FJ, Lozano JA, Jiménez-Moreno G, Martinez-Ruiz F, García Sanjuán L, et al. Anthropogenic impact and lead pollution throughout the Holocene in Southern Iberia. Sci Total Environ. 2013;449: 451–460. doi:10.1016/j.scitotenv.2013.01.081
26. Nickerson SP. Tetraethyl lead: A product of American research. J Chem Educ. 1954; 560–571.
27. Bacon JR, Jones KC, McGrath SP, Johnston AE. Isotopic character of lead deposited from the atmosphere at a grassland site in the United Kingdom since 1860. Environ Sci Technol. 1996;30: 2511–2518. doi:10.1021/es950839s
28. Nriagu JO. The rise and fall of leaded gasoline. Sci Total Environ. 1990;92: 13–28.
29. Shotyk W, Weiss D, Appleby PG, Cheburkin AK, Frei R, Gloor M, et al. History of atmospheric lead deposition since 12,370 14C yr BP from a peat bog, Jura Mountains, Switzerland. Science. 1998;281: 1635–1641. doi:10.1126/science.281.5383.1635
30. Brännvall M-L, Bindler R, Renberg I, Emteryd O, Bartnicki J, Billström K. The Medieval metal industry was the cradle of modern large-scale atmospheric lead pollution in Northern Europe. Environ Sci Technol. 1999;33: 4391–4395. doi:10.1021/es990279n
31. Chang C, Han C, Han Y, Hur SD, Lee S, Motoyama H, et al. Persistent Pb pollution in Central East Antarctic snow: A retrospective assessment of sources and control policy implications. Environ Sci Technol. 2016;50: 12138–12145. doi:10.1021/acs.est.6b03209
32. Martínez Cortizas A, García-Rodeja E, Pontevedra Pombal X, Nóvoa Muñoz JC, Weiss D, Cheburkin A. Atmospheric Pb deposition in Spain during the last 4600 years recorded by two ombrotrophic peat bogs and implications for the use of peat as archive. Sci Total Environ. 2002;292: 33–44. doi:10.1016/S0048-9697(02)00031-1
33. Le Roux G, Weiss D, Grattan J, Givelet N, Krachler M, Cheburkin A, et al. Identifying the sources and timing of ancient and medieval atmospheric lead pollution in England using

a peat profile from Lindow bog, Manchester. J Environ Monit. 2004;6: 502–510. doi:10.1039/B401500B
34. Engstrom DR, Fitzgerald WF, Cooke CA, Lamborg CH, Drevnick PE, Swain EB, et al. Atmospheric Hg emissions from preindustrial gold and silver extraction in the Americas: A reevaluation from lake-sediment archives. Environ Sci Technol. 2014;48: 6533–6543. doi:10.1021/es405558e
35. Fain X, Ferrari CP, Dommergue A, Albert MR, Battle M, Severinghaus J, et al. Polar firn air reveals large-scale impact of anthropogenic mercury emissions during the 1970s. Proc Natl Acad Sci U S A. 2009;106: 16114–16119. doi:10.1073/pnas.0905117106
36. Roos-Barraclough F, Martinez-Cortizas A, Garc E, Shotyk W. A 14 500 year record of the accumulation of atmospheric mercury in peat: volcanic signals, anthropogenic influences and a correlation to bromine accumulation. EPSL. 2002; 435–451.
37. Cooke CA, Abbott MB, Wolfe AP, Kittleson JL. A millennium of metallurgy recorded by lake sediments from morococha, Peruvian Andes. Environ Sci Technol. 2007;41: 3469–3474. doi:10.1021/es062930+
38. Cooke CA, Abbott MB. A paleolimnological perspective on industrial-era metal pollution in the central Andes, Peru. Sci Total Environ. 2008;393: 262–272. doi:10.1016/j.scitotenv.2007.12.034
39. Michelutti N, Blais JM, Mallory ML, Brash J, Thienpont J, Kimpe LE, et al. Trophic position influences the efficacy of seabirds as metal biovectors. Proc Natl Acad Sci U S A. 2010;107: 10543–10548. doi:10.1073/pnas.1001333107
40. Yin X, Sun L, Zhu R, Liu X, Ruan D, Wang Y. Mercury-selenium association in Antarctic seal hairs and animal excrements over the past 1,500 years. Environ Toxicol Chem. 2007;26: 381–386. doi:10.1897/06-128.1
41. Brimble SK, Blais JM, Kimpe LE, Mallory ML, Keatley BE, Douglas MSV, et al. Bioenrichment of trace elements in a series of ponds near a northern fulmar (*Fulmarus glacialis*) colony at Cape Vera, Devon Island. Can J Fish Aquat Sci. 2009;66: 949–958. doi:10.1139/f09-053
42. Cuculić V, Cukrov N, Željko Kwokal, Mlakar M. Distribution of trace metals in anchialine caves of Adriatic Sea, Croatia. Estuar Coast Mar Sci. 2011;95: 253–263. doi:10.1016/j.ecss.2011.09.011
43. Evenset A, Christensen GN, Carroll J, Zaborska A, Berger U, Herzke D, et al. Historical trends in persistent organic pollutants and metals recorded in sediment from Lake Ellasjøen, Bjørnøya, Norwegian Arctic. Environ Pollut. 2007;146: 196–205. doi:10.1016/j.envpol.2006.04.038
44. Davidson TA, Wetterich S, Johansen KL, Grønnow B, Windirsch T, Jeppesen E, et al. The history of seabird colonies and the North Water ecosystem: Contributions from palaeoecological and archaeological evidence. Ambio. 2018;47: 175–192. doi:10.1007/s13280-018-1031-1
45. Xie Z, Sun L. A 1,800-year record of arsenic concentration in the penguin dropping sediment, Antarctic. Environ Geol. 2008;55: 1055–1059. doi:10.1007/s00254-007-1054-6
46. Carreón-Palau L, Parrish CC, Pérez-España H. Urban sewage lipids in the suspended particulate matter of a coral reef under river influence in the South West Gulf of Mexico. Water Res. 2017;123: 192–205. doi:10.1016/j.watres.2017.06.061

47. Choulik O, Moore TR. Response of a subarctic lake chain to reduced sewage loading. Can J Fish Aquat Sci. 1992;49: 1236–1245. doi:10.1139/f92-139
48. Stewart EM, McIver R, Michelutti N, Douglas MSV, Smol JP. Assessing the efficacy of chironomid and diatom assemblages in tracking eutrophication in High Arctic sewage ponds. Hydrobiologia. 2014;721: 251–268. doi:10.1007/s10750-013-1667-6
49. Michelutti N, Hermanson MH, Smol JP, Dillon PJ, Douglas MSV. Delayed response of diatom assemblages to sewage inputs in an Arctic lake. Aquat Sci. 2007;69: 523–533. doi:10.1007/s00027-007-0928-8
50. Yates CN, Wootton BC, Murphy SD. Performance assessment of arctic tundra municipal wastewater treatment wetlands through an arctic summer. Ecol Eng. 2012;44: 160–173. doi:10.1016/j.ecoleng.2012.04.011
51. Daley K, Jamieson R, Rainham D, Truelstrup Hansen L, Harper SL. Screening-level microbial risk assessment of acute gastrointestinal illness attributable to wastewater treatment systems in Nunavut, Canada. Sci Total Environ. 2019;657: 1253–1264. doi:10.1016/j.scitotenv.2018.11.408
52. Antoniades D, Michelutti N, Quinlan R, Blais JM, Bonilla S, Douglas MSV, et al. Cultural eutrophication, anoxia, and ecosystem recovery in Meretta Lake, High Arctic Canada. Limnol Oceanogr. 2011;56: 639–650. doi:10.4319/lo.2011.56.2.0639
53. Michelutti N, Douglas MSV, Smol JP. Tracking recent recovery from eutrophication in a high arctic lake (Meretta Lake, Cornwallis Island, Nunavut, Canada) using fossil diatom assemblages. J Paleolimnol. 2002;28: 377–381.
54. Leeming R, Stark JS, Smith JJ. Novel use of faecal sterols to assess human faecal contamination in Antarctica: a likelihood assessment matrix for environmental monitoring. Antarct Sci. 2015;27: 31–43. doi:10.1017/S0954102014000273
55. Douglas MSV, Smol JP. Eutrophication and recovery in the High Arctic: Meretta Lake (Cornwallis Island, Nunavut, Canada) revisited. Hydrobiologia. 2000;431: 193–204.
56. Chae JS, Choi MS, Song YH, Um IK, Kim JG. Source identification of heavy metal contamination using metal association and Pb isotopes in Ulsan Bay sediments, East Sea, Korea. Mar Pollut Bull. 2014;88: 373–382. doi:10.1016/j.marpolbul.2014.07.066
57. Wang Z, Lu X, Zhang K. Distribution and contamination of metals and biogenic elements in sediments from Zhifu Bay of the Yellow Sea, China. J Environ Sci. 2016;41: 6–15. doi:10.1016/j.jes.2015.06.009
58. Dauvalter VA, Kashulin NA. Assessment of the ecological state of the Arctic freshwater system based on concentrations of heavy metals in the bottom sediments. Geochem Int. 2018;56: 842–856. doi:10.1134/S0016702918080037
59. Espenshade PJ, Hughes AL. Regulation of sterol synthesis in eukaryotes. Ennu Rev Genet. 2007;41: 401–427. doi:10.1146/annurev.genet.41.110306.130315
60. Bull ID, Lockheart MJ, Elhmmali MM, Roberts DJ, Evershed RP. The origin of faeces by means of biomarker detection. Environ Int. 2002;27: 647–654. doi:10.1016/S0160-4120(01)00124-6
61. Leeming R, Ball A, Ashbolt N, Nichols P. Using faecal sterols from humans and animals to distinguish faecal pollution in receiving waters. Wat Res. 1996;30: 2893–2900.
62. Walker RW, Wun CK, Litsky W, Dutka BJ. Coprostanol as an indicator of fecal pollution. C R C Crit Rev Environ Control. 1982;12: 91–112. doi:10.1080/10643388209381695

63. Carreira RS, Wagener ALR, Readman JW. Sterols as markers of sewage contamination in a tropical urban estuary (Guanabara Bay, Brazil): space–time variations. Estuar Coast Mar Sci. 2004;60: 587–598. doi:10.1016/j.ecss.2004.02.014
64. Hatcher PG, McGillivary PA. Sewage contamination in the New York Bight. Coprostanol as an indicator. Environ Sci Technol. 1979;13: 1225–1229. doi:10.1021/es60158a015
65. Stewart EM, Hargan KE, Sivarajah B, Kimpe LE, Blais JM, Smol JP. A paleoenvironmental study tracking eutrophication, mining pollution, and climate change in Niven Lake, the first sewage lagoon of Yellowknife (Northwest Territories). Arctic. 2018;71: 201–217. doi:10.14430/arctic4720
66. Tort LFL, Iglesias K, Bueno C, Lizasoain A, Salvo M, Cristina J, et al. Wastewater contamination in Antarctic melt-water streams evidenced by virological and organic molecular markers. Sci Total Environ. 2017;609: 225–231. doi:10.1016/j.scitotenv.2017.07.127
67. Bull ID, Elhmmali MM, Roberts DJ, Evershed RP. The application of steroidal biomarkers to track the abandonment of a Roman wastewater course at the Agora (Athens, Greece). Archaeometry. 2003;45: 149–161. doi:10.1111/1475-4754.00101
68. Sánez J, Froehner S, Hansel F, Parron L, Knapik H, Fernandes C, et al. Bile acids combined with fecal sterols: a multiple biomarker approach for deciphering fecal pollution using river sediments. J Soils Sediments. 2017;17: 861–872. doi:10.1007/s11368-016-1592-1
69. Nishimura M. Geochemical characteristics of the high reduction zone of stenols in Suwa sediments and the environmental factors controlling the conversion of stenols into stanols. Geochim Cosmochim Acta. 1978;42: 349–357. doi:10.1016/0016-7037(78)90265-X
70. Zocatelli R, Lavrieux M, Guillemot T, Chassiot L, Le Milbeau C, Jacob J. Fecal biomarker imprints as indicators of past human land uses: Source distinction and preservation potential in archaeological and natural archives. J Archaeol Sci. 2017;81: 79–89. doi:10.1016/j.jas.2017.03.010
71. Cheng W, Sun L, Kimpe LE, Mallory ML, Smol JP, Gallant LR, et al. Sterols and stanols preserved in pond sediments track seabird biovectors in a High Arctic environment. Environ Sci Technol. 2016;50: 9351–9360. doi:10.1021/acs.est.6b02767
72. Vane CH, Kim AW, McGowan S, Leng MJ, Heaton THE, Kendrick CP, et al. Sedimentary records of sewage pollution using faecal markers in contrasting peri-urban shallow lakes. Sci Total Environ. 2010;409: 345–356. doi:10.1016/j.scitotenv.2010.09.033
73. Savelle JM. Cumulative bowhead whale (Balaena mysticetus) harvest estimates by prehistoric Thule Inuit in the Canadian Arctic 1200–1500 A.D.: Implications for bowhead whale population modeling and Thule demography. Bulletin of National Museum of Ethnology. 2010;34: 26.
74. Morrison D. The earliest Thule migration. CJA. 1999;22: 19.
75. Dawson PC. Interpreting variability in Thule Inuit architecture: A case study from the Canadian High Arctic. Am Antiq. 2001;66: 453–470. doi:10.2307/2694244
76. McCartney AP, Savelle JM. Thule Eskimo whaling in the Central Canadian Arctic. University of Wisconsin Press. 1985;22: 23.
77. Schledermann P. The effect of climatic/ecological changes on the style of Thule culture winter dwellings. Arct Alp Res. 1976;8: 37. doi:10.2307/1550608

78. Douglas MSV, Smol JP, Savelle JM, Blais JM. Prehistoric Inuit whalers affected Arctic freshwater ecosystems. Proc Natl Acad Sci U S A. 2004;101: 1613–1617. doi:10.1073/pnas.0307570100
79. McGuire RH, Schiffer MB. A theory of architectural design. J Anthropol Archaeol. 1983;2: 277–303. doi:10.1016/0278-4165(83)90002-8
80. McCutchan Jr. JH, Lewis Jr. WM, Kendall C, McGrath CC. Variation in trophic shift for stable isotope ratios of carbon, nitrogen, and sulfur. Oikos. 2003;102: 378–390.
81. Minagawa M, Wada E. Stepwise enrichment of 15N along food chains: Further evidence and the relation between $\delta^{15}N$ and animal age. Geochim Cosmochim Acta. 1984;48: 1135–1140.
82. Hadley KR, Douglas MSV, McGhee R, Blais JM, Smol JP. Ecological influences of Thule Inuit whalers on high Arctic pond ecosystems: a comparative paleolimnological study from Bathurst Island (Nunavut, Canada). J Paleolimnol. 2010;44: 85–93. doi:10.1007/s10933-009-9388-6
83. Hadley KR, Douglas MSV, Blais JM, Smol JP. Nutrient enrichment in the High Arctic associated with Thule Inuit whalers: a paleolimnological investigation from Ellesmere Island (Nunavut, Canada). Hydrobiologia. 2010;649: 129–138. doi:10.1007/s10750-010-0235-6
84. Tse TJ, Codling G, Jones PD, Thoms K, Liber K, Giesy JP, et al. Reconstructing long-term trends in municipal sewage discharge into a small lake in northern Manitoba, Canada. Chemosphere. 2014;103: 299–305. doi:10.1016/j.chemosphere.2013.12.019
85. Prost K, Birk JJ, Lehndorff E, Gerlach R, Amelung W. Steroid biomarkers revisited – Improved source identification of faecal remains in archaeological soil material. Bicho N, editor. PLoS One. 2017;12: e0164882. doi:10.1371/journal.pone.0164882
86. Fenton BM, Simmons NB. A World of Science and Mystery. University of Chicago Press; 2014.
87. Clark DRJ, Wenner AS, Moore JF. Metal residues in bat colonies, Jackson County, Florida, 1981 - 1983. Florida Field Naturalist. 1986;14: 8.
88. O'Shea TJ, Everette AL, Ellison LE. Cyclodiene insecticide, DDE, DDT, arsenic, and mercury contamination of big brown bats (*Eptesicus fuscus*) foraging at a Colorado Superfund site. Arch Environ Contam Toxicol. 2001;40: 112–120.
89. Bird MI, Boobyer EM, Bryant C, Lewis HA, Paz V, Stephens WE. A long record of environmental change from bat guano deposits in Makangit Cave, Palawan, Philippines. Earth Environ Sci Trans R Soc Edinb. 2007;98: 59–69. doi:10.1017/s1755691007000059
90. Onac BP, Hutchinson SM, Geantă A, Forray FL, Wynn JG, Giurgiu AM, et al. A 2500-Yr late Holocene multi-proxy record of vegetation and hydrologic changes from a cave guano-clay sequence in SW Romania. Quat Res. 2015;83: 437–448. doi:10.1016/j.yqres.2015.01.007
91. Mizutani H, McFarlane DA, Kabaya Y. Nitrogen and carbon isotope studies of a bat guano core from Eagle Creek Cave, Arizona, USA. J Mass Spectrom Soc Jpn. 1992;40: 57–65.
92. Nocera JJ, Blais JM, Beresford DV, Finity LK, Grooms C, Kimpe LE, et al. Historical pesticide applications coincided with an altered diet of aerially foraging insectivorous chimney swifts. Proc R Soc B. 2012;279: 3114–3120. doi:10.1098/rspb.2012.0445
93. Zhu R, Liu Y, Ma E, Sun J, Xu H, Sun L. Nutrient compositions and potential greenhouse gas production in penguin guano, ornithogenic soils and seal colony soils in coastal Antarctica. Antarct Sci. 2009;21: 427–438. doi:10.1017/S0954102009990204

94. Wurster C, McFarlane D, Bird M, Ascough P, Beavan Athfield N. Stable isotopes of subfossil bat guano as a long-term environmental archive: Insights from a Grand Canyon cave deposit. J Cave Karst Stud. 2010;72: 111–121. doi:10.4311/jcks2009es0109
95. McFarlane DA, Keeler RC, Mizutani H. Ammonia volatilization in a Mexican bat cave ecosystem. Biogeochemistry. 1995;30: 1–8.
96. Michelutti N, Mallory ML, Blais JM, Douglas MSV, Smol JP. Chironomid assemblages from seabird-affected High Arctic ponds. Polar Biol. 2011;34: 799–812. doi:10.1007/s00300-010-0934-5
97. Salvarina I, Yohannes E, Siemers BM, Koselj K. Advantages of using fecal samples for stable isotope analysis in bats: evidence from a triple isotopic experiment. Rapid Commun Mass Spectrom. 2013;27: 1945–1953. doi:10.1002/rcm.6649
98. Siemers BM, Greif S, Borissov I, Voigt-Heucke SL, Voigt CC. Divergent trophic levels in two cryptic sibling bat species. Oecologia. 2011;166: 69–78. doi:10.1007/s00442-011-1940-1
99. DeNiro MJ, Epstein S. Influence of diet on the distribution of carbon isotopes in animals. Geochimica et Cosmochimica Acta. 1978;42: 495–506. doi:10.1016/0016-7037(78)90199-0
100. Hwang YT, Millar JS, Longstaffe FJ. Do $\delta^{15}N$ and $\delta^{13}C$ values of feces reflect the isotopic composition of diets in small mammals? Can J Zool. 2007;85: 388–396. doi:10.1139/Z07-019
101. Painter ML, Chambers CL, Siders M, Doucett RR, Whitaker, Jr. JO, Phillips DL. Diet of spotted bats (*Euderma maculatum*) in Arizona as indicated by fecal analysis and stable isotopes. Can J Zool. 2009;87: 865–875. doi:10.1139/Z09-075
102. Des Marais DJ, Mitchell JM, Meinschein WG, Hayes JM. The carbon isotope biogeochemistry of the individual hydrocarbons in bat guano and the ecology of the insectivorous bats in the region of Carlsbad, New Mexico. Geochim Cosmochim Acta. 1980;44: 2075–2086. doi:10.1016/0016-7037(80)90205-7
103. Wurster CM, McFarlane DA, Bird MI. Spatial and temporal expression of vegetation and atmospheric variability from stable carbon and nitrogen isotope analysis of bat guano in the southern United States. Geochim Cosmochim Acta. 2007;71: 3302–3310. doi:10.1016/j.gca.2007.05.002
104. O'Leary MH. Carbon isotope fractionation in plants. Phytochemistry. 1981;20: 553–567.
105. Voigt CC, Rex K, Michener RH, Speakman JR. Nutrient routing in omnivorous animals tracked by stable carbon isotopes in tissue and exhaled breath. Oecologia. 2008;157: 31–40. doi:10.1007/s00442-008-1057-3
106. Mirón M LL, Herrera Montalvo LG, Ramírez P N, Hobson KA. Effect of diet quality on carbon and nitrogen turnover and isotopic discrimination in blood of a New World nectarivorous bat. J Exp Biol. 2006;209: 541–548. doi:10.1242/jeb.02016
107. Svoboda JA, Feldlaufer MF. Neutral sterol metabolism in insects. Lipids. 1991;26: 614–618. doi:10.1007/BF02536425
108. Nash D, Leeming R, Clemow L, Hannah M, Halliwell D, Allen D. Quantitative determination of sterols and other alcohols in overland flow from grazing land and possible source materials. Wat Res. 2005;39: 2964–2978. doi:10.1016/j.watres.2005.04.063

109. Piironen V, Lindsay DG, Miettinen TA, Toivo J, Lampi A-M. Review Plant sterols: biosynthesis, biological function and their importance to human nutrition. J Sci Food Agric. 2000; 28.
110. Cuevas-Tena M, Alegría A, Lagarda MJ. Determination of fecal sterols following a diet with and without plant sterols. Lipids. 2017;52: 871–884. doi:10.1007/s11745-017-4286-6
111. Shah VG, Dunstan RH, Geary PM, Coombes P, Roberts TK, Von Nagy-Felsobuki E. Evaluating potential applications of faecal sterols in distinguishing sources of faecal contamination from mixed faecal samples. Water Res. 2007;41: 3691–3700. doi:10.1016/j.watres.2007.04.006
112. Nes WD, Lopez M, Zhou W, Guo D, Dowd PF, Norton RA. Sterol utilization and metabolism by Heliothis zea. Lipids. 1997;32: 1317–1323. doi:10.1007/s11745-006-0170-5
113. Clayton RB. The utilization of sterols by insects. J Lipid Res. 1964;5.
114. Behmer ST, Nes WD. Insect sterol nutrition and physiology: A global overview. Adv Insect Physiol. Elsevier; 2003. pp. 1–72. doi:10.1016/S0065-2806(03)31001-X
115. Gilbert LI, Rybczynski R, Warren JT. Control and biochemical nature of the ecdysteroidogenic pathway. Annu Rev Entomol. 2002;47: 883–916. doi:10.1146/annurev.ento.47.091201.145302
116. Ikekawa N, Morisaki M, Fujimoto Y. Sterol metabolism in insects: dealkylation of phytosterol to cholesterol. Acc Chem Res. 1993;26: 139–146. doi:10.1021/ar00028a002

Chapter 2: Tracking the history of 20th century cultural eutrophication in High Arctic waterbodies

Gallant, Lauren R[1]; Kimpe, Linda E[1]; Hargan, Kathryn E[2]; and Blais, Jules M[1]

[1] Department of Biology, University of Ottawa, Ottawa, ON, K1N 6N5, Canada

[2] Department of Biology, Memorial University of Newfoundland, St. John's, NL A1B 3X9, Canada

This manuscript is under review by Anthropocene.

Statement of author contributions:

Gallant, Lauren R: study design, sample collection, lab work, data analysis and interpretation, and manuscript preparation. Kimpe, Linda E: sample collection and data analysis and interpretation. Hargan, Kathryn E: study design, lab work, data analysis and interpretation, and peer review. Blais, Jules M: study design, sample collection, data analysis and interpretation, manuscript preparation, and peer review.

Keywords: paleolimnology, sterols, metals, sewage, isotopes

Abstract

Human activities can greatly affect the chemical and biological composition of High Arctic lakes that otherwise receive only sparse inputs from their watersheds and airsheds. This study examined three High Arctic waterbodies in which wastewater from an airport was released

over the span of several decades. Using sediment cores from these waterbodies, this study reconstructed the history of wastewater inputs using a multiproxy approach consisting of sterols, stanols, metals, and stable isotopes of carbon and nitrogen. This multi-proxy approach showed good concordance between $\delta^{15}N$, coprostanol (a stanol specific to human faecal sources), cholesterol, and cholestanol, which tracked the known history of human wastewater deposition to this High Arctic environment. Concentrations of plant derived sterols, such as campesterol and sitosterol, increased at the time of wastewater input, presumably due to increased plant growth stimulated by wastewater nutrients. Metal(loid)s normalized to titanium showed copper and lead tracked the input of wastewater into R-12, while arsenic, cadmium, chromium, nickel, and zinc increased more than 15 years after the onset of wastewater input. These results demonstrate the ability of sterols and stanols to reconstruct the historical presence of humans in High Arctic locations within the last 80 years and provided compelling evidence that these paleolimnological approaches may be used to track human populations in the Arctic beyond the last century.

1 Introduction

Eutrophication of waterbodies occurs from the presence of excess nutrients and can be the result of both natural and anthropogenic activity. The addition of untreated wastewater to inland lakes often results in signs of eutrophication and can lead to elevated concentrations of phosphorus in Arctic lake sediments (Dauvalter and Kashulin, 2018). Northern communities often lack sewage treatment facilities and thus wastewater is more commonly discharged directly into nearby waterbodies. Signs of eutrophication may not be evident due to short growing seasons; however, chemical and biological changes have been observed in water and sediments. For example, sewage waste can increase the concentration of heavy metals such as cadmium, lead, mercury, and thallium in Arctic lake sediments (Antoniades et al., 2011; Michelutti et al., 2007), increase nutrient availability as evidenced by increases in carbon and nitrogen in lake water (Schindler et al., 1974), and can lead to increased primary productivity, which alters chironomid and diatom communities (Schindler et al., 1974; Stewart et al., 2018). Cadmium, chromium, copper, lead, and zinc also peaked in lake sediments from Antarctica as a result of sewage input (Bueno et al., 2018b; Santos et al., 2005). The flux of lead, cadmium, and mercury to sediments also increased in Annak Lake, Belcher Island, Nunavut, Canada, coeval with sewage input (Michelutti et al., 2007).

In Resolute Bay, Cornwallis Island, Nunavut, Canada, there is a series of waterbodies that received sewage for decades: R-12 and R-13 (both ponds), and Meretta Lake. In 1949, the Department of Transport Airport Base was established, housing an average of 150 permanent residents. From 1949 to 1979, raw sewage was released from the base through two utilidors into nearby waterbodies. A main utilidor ran 1.6 km, depositing sewage into several waterbodies, including R-12 and R-13, with a final destination of Meretta Lake. A second utilidor ran through a series of waterbodies, also ending its route in Meretta Lake. In the 1970s, the permanent

population at the Airport Base more than halved (averaging 65 people), at which time the major utilidor carrying sewage was dismantled, leaving only one utilidor that deposited sewage directly into Meretta Lake. In 1998, the remaining utilidor was closed owing to the construction of a new airport.

The limnology of these waterbodies was studied as a part of the International Biological Program (IBP) (Antoniades et al., 2011; Douglas and Smol, 2000); providing the unique opportunity to examine human impacts on waterbodies in the High Arctic. Meretta Lake was historically defined as an oligotrophic lake owing to low nutrient availability and few ice-free days (Antoniades et al., 2011; Smol and Douglas, 2007). However following the addition of sewage wastewater in 1949, the lake quickly became eutrophic as evidenced by increased phytoplankton and chlorophyll *a* (chl *a*) concentrations (Kalff and Welch, 1974; Schindler et al., 1974). Biological changes have also been documented in sediment cores from these wastewater-receiving waterbodies. For example, shifts in the bacterial composition in Meretta Lake sediments (Antoniades et al., 2011) and changes in the diatom assemblages in Meretta Lake, R-12, and R-13 (Douglas and Smol, 2000; Stewart et al., 2014) have been shown to track the history of wastewater inputs.

There is evidence that High Arctic lakes are able to recover from human-induced eutrophication. For example, the diatom assemblage in Meretta Lake recovered to pre-wastewater conditions as indicated by a decrease in the concentration of diatoms following a reduction in wastewater input; sewage-associated metals, such as cadmium, also decreased as a result of a reduction in wastewater input (Antoniades et al., 2011). Furthermore, the diatom assemblage in Meretta Lake sediments deposited post-1990 is returning to pre-impact sediment assemblages (Michelutti et al., 2002) and total phosphorus and chl *a* concentrations in lake

sediments in the 1990s are lower than those recorded for the IBP in 1968 (Douglas and Smol, 2000).

Sterols and stanols are a powerful and source-specific proxy that can be used to track the onset and termination of human wastewater input in this High Arctic environment. There is a growing interest in sterols and stanols for paleolimnological studies as they can offer more detail in reconstructing historical conditions. Sterols and stanols are a subgroup of steroids, present in varying concentrations and proportions in all eukaryotes. Sterols and stanols can be divided into two categories: phytosterol (naturally occurring sterols and stanols in plant cell membranes) and zoosterols (naturally occurring sterols and stanols in animals). Sterols and stanols are relatively stable within cold aquatic environments, and thus any change in their composition or abundance in a lake system should be preserved within lake sediments (Leeming et al., 2015, 1997). Consequently, sterols and stanols can function as biomarkers of human presence as the specificity of the sterol composition in vegetation and animals can be used to reconstruct long-term trends in waterbody sediments.

Zoosterols, such as coprostanol, cholesterol, and cholestanol, are more source specific than stable isotopes and thus are frequently used to track sewage in lake sediments (e.g. Bull et al. 2003; Walker et al. 1982; Zocatelli et al. 2017). For example, coprostanol is produced in the gut of higher mammals and is typically ten-times more concentrated in humans relative to other animals (Leeming et al., 1996; Shah et al., 2007). As a result, coprostanol has been effectively used to track the presence of human sewage in the New York Bight (Hatcher and McGillivary, 1979), Arctic lake sediments (Stewart et al., 2018), and Antarctic lake sediments (Tort et al., 2017). While coprostanol is the major component of human faeces (57 % of total sterols), cholesterol is also present in elevated concentrations; this differs from other omnivores and

carnivores, where concentrations of cholesterol exceed those of coprostanol (Leeming et al., 1996; Prost et al., 2017). Cholestanol is formed from the microbial reduction of cholesterol (Leeming et al., 1996) and low, but detectable concentrations of cholestanol are also found in human faeces: 70 µg g^{-1} dry weight (dw); 1.4 % of total sterols (Leeming et al., 1996; Sánez et al., 2017). Thus, higher concentrations of cholestanol are commonly found in lake sediments as a result of sewage input (Nishimura, 1978; Sánez et al., 2017).

Common phytosterols include campesterol, sitosterol, and stigmastanol. Vegetation is typically abundant in sitosterol (Behmer and Nes, 2003; Cheng et al., 2016; Pereira et al., 2017); for example, sitosterol makes up ~40 – 70 % of the sterol composition in High Arctic plants and mosses (Cheng et al., 2016). Stigmastanol is produced by the microbial reduction of sitosterol in high trophic level mammals; as a result, stigmastanol is found in herbivore faeces (Leeming et al., 1996). When combined, sitosterols and stigmastanols account for 64 – 89 % of all sterols in herbivore faeces, with sitosterol being the dominant of the two sterols (Leeming et al., 1996; Prost et al., 2017). Stigmastanol concentrations in lake sediments have been correlated to manure inputs from herbivorous animals such as cows and sheep (Vane et al., 2010), and an increase in the concentration of sitosterol was observed in Niven Lake (Yellowknife, Northwest Territories, Canada) in response to wastewater input (Stewart et al., 2018). Campesterol is also commonly found in higher plants as well as in small concentrations in algae, relative to sitosterol and stigmastanol (Patterson, 1994; Pereira et al., 2017). Consequently, campesterol has been used as an indicator of terrestrial organic matter deposition in estuarine mangrove sediments (Ranjan et al., 2015).

The objective of this study was to reconstruct the history of sewage dumping using sterols and stanols in three High Arctic waterbodies (Meretta Lake, R-12, and R-13, Fig 2.1) and

determine the extent to which these proxies persisted following the cessation of wastewater input. We compared the chemical profiles in sewage-influenced waterbodies to a nearby reference pond, Little Char, in order to differentiate between sewage impacted and unimpacted systems. Dated sediment cores from ponds with a known history of sewage dumping provided the opportunity to test explicit hypotheses about the ability of sterols and stanols to track human faecal contamination of surface waters. We thus aimed to answer the following research questions: (1) Is the sterol and stanol composition in wastewater-influenced sediments different from uninfluenced sediments? We hypothesized that sterols and stanols would be more concentrated in sediments receiving wastewater discharge than in uninfluenced sediments. (2) Does the sterol and stanol composition in sediments change during the period of wastewater discharge? We hypothesized that sterols and stanols would increase during the known period of wastewater input based on ^{210}Pb dating. (3) Are stanols (coprostanol and epicoprostanol) specific to human waste and thus do they track wastewater discharge in sediments? We hypothesized that coprostanol and epicoprostanol would increase in wastewater-influenced sediments and this increase would be absent in the reference pond, which did not receive wastewater. This project aimed to better understand historical changes in the chemistry of remote Arctic waterbodies and to relate those changes to human activity.

2 Methods

2.1 Site description

Little Char, located in Resolute Bay, Cornwallis Island, Nunavut, Canada, is so named as it is a small offshoot of nearby Char Lake (Fig 2.1, Table S2.1 for latitudes and longitudes). While there are no records of sewage dumping into Little Char, sediments from the catchment of the inflow stream of Char Lake were used to construct an airstrip into the drainage basin from

1969 – 1972 (Michelutti et al., 2003). Beginning in 1975, Char Lake was used as a source of drinking water. Meretta Lake, R-12, and R-13 (Fig 2.1, Table S2.1 for latitudes and longitudes) were selected as the wastewater-influenced sites as their chemistry and biology are well-documented, thus allowing for a more in depth paleolimnological analysis. All field sample collections were performed in July 2017, under the Nunavut Research Institute Scientific Research License # 02 025 17N-A issued to JMB.

2.2 Water, periphyton, and zooplankton sampling

We compared the chemical composition of near-shore surface water samples in wastewater-influenced waterbodies to the chemical composition of a water sample from a reference pond to determine if influenced waterbodies recovered following the cessation of wastewater input. Electrical conductivity and pH were measured using a YSI meter (model 85, YSI Incorporated). Water bottles were pre-rinsed using 10 % HNO_3 for total metal concentrations. We used 10 % H_2SO_4 to pre-rinse Nalgene bottles for total phosphorus (TP), total dissolved phosphorus (TDP), total dissolved nitrogen (TDN), dissolved organic carbon (DOC), and dissolved inorganic carbon (DIC). Water samples for DOC were filtered through a Sartorious acetate filter (47 mm, 0.45 μm) and stored at 4°C. Water samples for particulate organic carbon (POC) were filtered through a Whatman glass microfiber filter (GF/F) (47 mm, 0.45 μm); the filter was frozen until analysis. All water chemistry data were analyzed by the National Laboratory for Environmental Testing (Burlington, Ontario, Canada).

We also examined the sterol and stanol profiles in zooplankton and periphyton to determine how these potential sources may have affected the sediment sterol and stanol composition. Near-shore periphyton was collected and stored at 4°C until they were sieved (125 μm) and filtered through a pre-heated (3 hours at 400°C) 110 mm Whatman GF/F (42.5 mm, 0.7

μm). Periphyton samples were air-dried and then homogenized. Near-shore zooplankton samples were collected using a 200 μm net; zooplankton samples were stored frozen and ultimately freeze-dried for analysis.

2.3 Sediment core collection

We collected a sediment core from the centre of each waterbody to determine if sterols, stanols, stable isotopes, and metal profiles in waterbody sediments tracked the introduction and cessation of wastewater input into High Arctic waterbodies. The maximum depth of Meretta Lake was determined by bathymetric map while the maximum depth of the remaining ponds was determined visually upon arrival at the site. Sediment cores were collected from the deepest part of each lake; we used a UWITEC© gravity corer (Uwitec, Mondsee, Austria) in Meretta Lake and a push corer in the shallower ponds, R-12, R-13, and Little Char. We sectioned sediments into 0.5 cm intervals using a Glew extruder (Glew, 1988) and froze the sediments in Whirl-Pak® bags at -4°C.

Sedimentation rates and ^{210}Pb activity can be low in Arctic lakes, which can affect the accuracy and precision of ^{210}Pb dating (Douglas and Smol, 2000). Therefore, we explored two methods of ^{210}Pb dating: alpha and gamma counting. Alpha counting offers the advantage of better sensitivity, accuracy, and precision in ^{210}Pb measurements; however, it is a destructive method, meaning extracted sediments cannot be recovered for other analyses. ^{210}Pb measurements by gamma counting are non-destructive. Consequently, we selected a single core (Meretta Lake) to ^{210}Pb date by alpha counting to determine whether there was sufficient ^{210}Pb activity to use gamma counting on the remaining ponds. Alpha counting was conducted at MyCore Scientific using a ^{209}Po tracer (0.839 Bq g^{-1}); background ^{210}Pb was set to 0.030 Bq g^{-1}. Sufficient excess ^{210}Pb activity was present for gamma counting, so cores from the remaining

three ponds were dated using an Ortec High Purity Germanium Gamma Spectrometer (Oak Ridge, TN, USA) at the University of Ottawa. Efficiency corrections were made using Certified Reference Materials from the International Atomic Energy Association (Vienna, Austria). Sediment chronologies were calculated from ^{210}Pb and ^{137}Cs profiles with the Constant Rate of Supply (CRS) model using ScienTissiMe (Barry's Bay, Ontario, Canada).

Freeze-dried sediments were analyzed for percent carbon and nitrogen using a Micro Cube elemental analyzer at the Ján Veizer Stable Isotope Laboratory (formerly G.G. Hatch SIL Laboratory), located at the University of Ottawa, Ontario, Canada. A subsample of sediments was acidified by repeatedly adding 6N HCl to the sample and oven-heating the sample for 20 minutes until no effervescence was observed for two consecutive acid additions. The volume of acid added increased from 10 – 50 µL and the oven temperature increased from 40 – 60°C over the course of the repetitions. Acidified samples were analyzed for organic δ^{13}C (‰ V-PDB), hereafter, referred to as δ^{13}C, and unacidified samples were analyzed for δ^{15}N (‰ air). The analyses were run separately using an elemental analyzer interfaced to an isotope ratio mass spectrometer at the Ján Veizer Stable Isotope Laboratory. Values were normalized to several internal standards: C-51 Nicotiamide (δ^{15}N: 0.07 ‰, δ^{13}C: -22.95 ‰), C-52 ammonium sulphate and sucrose (δ^{15}N: 16.58 ‰, δ^{13}C: -11.94 ‰), and C-54 caffeine (δ^{15}N: -16.61 ‰, δ^{13}C: -34.46 ‰); the blind standard was C-55 glutamic acid (δ^{15}N: -3.98 ‰, δ^{13}C: -28.53 ‰). Results were reported in delta notation (δ), where $\delta = ((Rx-Rstd))/Rstd)*1000$; R = ratio of the abundance of the heavy to light isotope, x = sample, and std = standard. δ^{15}N values were calibrated to the following international standards: IAEA-N1 (0.4 ‰), IAEA-N2 (20.3 ‰), USGS-40 (-4.52 ‰), and USGS-41 (47.57 ‰). δ^{13}C were calibrated to the following international standards: IAEA-CH-6 (-10.4 ‰), NBS-22 (-29.91 ‰), USGS-40 (-26.24 ‰), and USGS-41 (37.76 ‰).

Analytical precision was ± 0.2 ‰ using glutamic acid. Zooplankton and periphyton samples were analyzed following the same protocol, except zooplankton samples were not acidified owing to low sample weight and the absence of carbonates.

We analyzed the sediment cores from R-12 and Little Char for total metals using approximately 0.5 g dw from each interval. Samples were submitted to SGS Minerals Services, Lakefield ON, Canada for analysis. Metal concentrations were determined using an aqua regia digestion and analyzed using inductively coupled plasma mass spectrometry. Concentrations below the method detection limit (MDL) were replaced with $\mathrm{MDL}/\sqrt{2}$. The concentration of each metal was then normalized to the concentration of titanium in order to account for natural weathering (Boës et al., 2011; Last and Smol, 2001).

Sterol and stanol concentrations were determined in the periphyton and sediment cores using methods modified from Birk et al. (2011) and Cheng et al. (2016). 10 mL of dichloromethane (DCM) (high-grade Optima® brand) was added to 0.1 g of copper (Fisher C434-500, laboratory grade copper powder; CAS 7440-50-8) in a glass scintillation vial, sonicated for 10 minutes, and subsequently removed. This process was repeated twice more; the copper was air-dried. 0.1 g of freeze-dried material and 50 µL of 10,000 ng mL^{-1} deuterated cholesterol (d6 cholesterol) was added to the copper. For blanks, d6 cholesterol was spiked directly into the copper. The samples were left for 12 hours at 4°C. To extract the sterols from the sediments, 10 mL of DCM was added, and the samples were sonicated for 10 minutes, and the DCM pipetted into pre-solvent washed Turbovap tubes. This process was repeated twice more to improve extraction efficiency. Samples were then evaporated to 1 mL at 23°C under a gentle stream of nitrogen. 1 g LC-Si SPE columns (Sigma-Aldrich, Oakville, ON, Canada), were conditioned with 6 mL of DCM; this DCM was discarded. The 1 mL sample was transferred to

the SPE column and the Turbovap tube was rinsed three times using 0.4 mL DCM. The sample and an additional 20 mL of DCM was eluted into a pre-solvent washed Turbovap tube. The sample was again evaporated to 1 mL at 23°C under a gentle stream of nitrogen and transferred to a gas chromatography (GC) vial. The sample was then evaporated to dryness under nitrogen and reconstituted in 1 mL of DCM. A 10x dilution was created by transferring 100 µL of the stock sample to a new GC vial and evaporating to dryness. 100 µL of 99 % N,O-bis(trimethylsilyl)trifluoroacetamide) + 1 % trimethylchlorosilane was added and the sample was heated for two hours at 60°C. 0.9 mL of toluene (high-grade (Optima® brand)) and 10 µL, 10,000 ng mL^{-1} of p-terphenyl-d_{14} (Cambridge Isotope Laboratories, Tewksbury, MA, USA) were added to the sample. Samples were analyzed using an Agilent 6890 gas chromatograph – 5973 mass selective detector in electron impact, selected ion monitoring mode (Agilent 19091J-433 HP-5 5 % phenyl methyl siloxane 29.8 m x 250 µm x 0.25 µm column). Analytical conditions include: a pulsed splitless injection at 250°C at 16.26 psi, DB-5MS (Agilent, Santa Clara, CA, USA), oven start at 150°C, ramp 1 at 8°C $minute^{-1}$ to 250°C, ramp 2 at 12°C $minute^{-1}$ to 300°C held for 12 minutes. Mass selective conditions as follows: transfer line 280°C, source 230°C, quad 150°C. Sterol and stanol concentrations were volume corrected to p-terphenyl-d_{14} using MSD ChemStation D.02.00.275. Samples were analyzed using additional dilutions, as required. Zooplankton sterols were extracted following the same protocol, except no d6 cholesterol was added.

Eleven sterols and stanols were measured: coprostanol (5β-cholestan-3β-ol), epicoprostanol (5β-cholestan-3α-ol), coprostanone (5β-cholestan-3-one), cholesterol (cholest-5-en-3β-ol), cholestanol (5α-cholestan-3β-ol), cholestanone (5α-cholestan-3-one), campesterol (campest-5-en-3β-ol), desmosterol (3β-cholesta-5,24-dien-3-ol), fucosterol (stigmasta-5,24-dien-

3β-ol), sitosterol (β-sitosterol), and stigmastanol (5α-stigmastano-3β-ol). Concentrations were interpreted using a limit of quantification set to a signal to noise ratio of three. The sterol and stanol concentrations in each sample were recovery corrected to the concentration of d6 cholesterol (Table S2.2). Sterol and stanol concentrations below the MDL were corrected to the MDL divided by root two (Table S2.3). MDLs were calculated using a five-point calibration curve in triplicate. Sitosterol and stigmastanol are larger compounds that do not ionize as well as smaller compounds, and thus their MDLs were greater. The sterol and stanol concentrations in the blanks were subtracted from the sterol and stanol concentrations in the sample. All concentrations were normalized to the dry sample weight. Concentrations were normalized to the percent organic carbon, when applicable. All data handling was conducted using R statistical computing environment (v3.5.2).

3 Results

3.1 Dating profiles

Sediments from Meretta Lake were dated to the year 1873 (at 7.25 cm) using alpha counting with the majority of excess ^{210}Pb lost by 5 cm below the sediment surface. Excess ^{210}Pb activity in R-12 reached background (based on ^{214}Pb activity) at 8.75 cm, which was dated to an age of 1909 CE (Fig S2.1). Peak ^{137}Cs activity, representing the year 1963 in accordance with the height of above-ground nuclear weapons testing, closely corroborated the CRS dates. Excess ^{210}Pb activity in R-13 reached background by 3.75 cm (2.75 cm = 1956 CE); peak ^{137}Cs activity was recorded at 1.75 cm and thus closely matched the ^{210}Pb dating profile. In Little Char, ^{210}Pb activity reached background by 5.75 cm (4.75 cm = 1949 CE); ^{137}Cs corroborates this dating profile, as peak activity occurred at 4.75 cm.

3.2 Sterols in sediments, periphyton, and zooplankton

Sterol and stanol profiles in the sediment cores are presented in Figs 2.2 and 2.3, and summary concentrations are presented in Table S2.4 (μg g^{-1} organic carbon (OC) dw) and Table S2.5 (μg g^{-1} dw). The maximum cholesterol concentration was observed in R-12 at the CRS date of 1998 (416 μg g^{-1} OC dw), coincident with peaks in $\delta^{15}N$ and $\delta^{13}C$ values (Fig 2.2). Concentrations of coprostanol, cholestanol, campesterol, and sitosterol also increased during the period of sewage dumping, though appeared to lag beyond the time that effluents were released to this environment. In R-12, percent organic carbon increased after wastewater input stopped (Fig 2.2). The sterol, stanol, and percent organic carbon profiles in R-13 were similar to those observed in R-12, although to a lesser magnitude (Fig 2.3). Sterol and stanol concentrations and percent organic carbon in Meretta Lake sediments increased in 1949 at the onset of sewage dumping, but unlike R-12 and R-13, the sterol and stanol concentrations did not decrease in more recently deposited lake sediments. Sterol and stanol concentrations in R-12 generally exceeded those found in R-13 and Meretta Lake. $\delta^{15}N$ increased coeval with wastewater inputs in R-12 but were relatively constant in R-13 and Meretta Lake (Figs 2.2 and 2.3). In both R-13 and Meretta Lake, $\delta^{15}N$ values did not increase at the time of wastewater inputs and $\delta^{15}N$ values in R-13 were more variable (2.3 – 5.0 ‰) than the $\delta^{15}N$ values observed in Meretta Lake (4.0 – 5.6 ‰) (Table S2.6). $\delta^{13}C$ values increased slightly over the timing of wastewater inputs in R-12 and Meretta Lake, increasing by 2 ‰ and 1 ‰, respectively. Conversely, $\delta^{13}C$ did not increase at the time of wastewater emissions to R-13.

Sterol and stanol concentrations in sediments from the reference pond, Little Char, were always lower than the concentrations recorded in the wastewater-influenced waterbodies (Figs 2.2 and 2.3). For example, the maximum concentration of any sterol and stanol observed in sediments from Little Char was stigmastanol at 14.0 μg g^{-1} OC dw versus a maximum of 254 μg

g^{-1} OC dw cholesterol in Meretta Lake, 416 μg g^{-1} OC dw cholesterol in R-12, and 36.6 μg g^{-1} OC dw cholesterol in R-13 (Table S2.4). Percent organic carbon increased in more recently deposited sediments (2.2 – 5.2 %), but the increase was much lower than that observed in wastewater-influenced waterbodies (e.g. 18 – 41.9 % in R-12) (Table S2.7).

The principle component analyses (PCAs) presented in Figs 2.4 and S2.2 show the inter-relatedness of sterols and stanols in sediment through time. In R-12, 89 % of the total variance in the sterol and stanol concentrations in sediment was explained by the first two axes. Coprostanol and epicoprostanol drove the shift in the sterol and stanol composition starting in 1949, corresponding to the onset of wastewater emissions in R-12 (Fig 2.4). Cholesterol, campesterol, and sitosterol also contributed to the change in the sterol and stanol composition. Recently deposited sediments appeared to return to a composition similar to pre-impact sediments, as evidenced by the reversal in direction along the x axis. The PCA for R-13 was very similar to that of R-12, with 78 % of the variation explained by the first two axes (Fig S2.2). In Meretta Lake sediments, coprostanol, cholesterol, campesterol, and sitosterol also drove much of the variation along the first two axes (96.6 % variance explained) (Fig S2.2). There was a clear shift from the pre-wastewater sterol and stanol composition to the present-day sterol and stanol composition. Unlike R-12 and R-13, sterol and stanol concentrations in Meretta Lake continued to increase even after wastewater input stopped. In Little Char, campesterol, sitosterol, and cholesterol explained little of the variation in the sterol and stanol composition down-core, and while coprostanol drove the composition in more recently deposited sediments, coprostanol only explained 9.5 % of the variation along axis 2, which represented sediments deposited in the 20th century.

We also looked at the concentration of sterols and stanols in periphyton and zooplankton in order to determine if primary producers and consumers had higher concentrations of sterols and stanols relative to those in uninfluenced waterbodies. We were unable to collect sufficient zooplankton biomass to analyze for sterols and stanols in the reference pond, Little Char, and as a result, we only presented the sterol and stanol concentrations in zooplankton from the wastewater-influenced waterbodies. The concentration of sterols and stanols in zooplankton and sediments were generally similar (Table S2.5 and Fig S2.3) with a few exceptions: the concentration of cholesterol was approximately three and five-fold greater in zooplankton than in sediments from Meretta Lake and R-13, respectively. Similarly, the concentration of sitosterol was three to five-fold greater in zooplankton than in sediments from wastewater-influenced waterbodies. Stigmastanol was also more concentrated in zooplankton than in sediments from R-12 and R-13. The maximum concentration of any sterol and stanol in zooplankton was always greater than that in periphyton, with the exception of coprostanol in Meretta Lake. The sterol and stanol concentrations in periphyton from the sewage water receiving waterbodies was generally greater than the sterol and stanol concentrations in periphyton from the reference pond, Little Char, with the following exceptions: the concentration of campesterol, cholesterol, and sitosterol in Little Char exceeded the concentration in R-13 and the concentration of coprostanol in Little Char exceeded the concentration in Meretta Lake (Fig S2.3). Periphyton was largely composed of cholesterol and sitosterol, followed by campesterol and stigmastanol; periphyton were very low in coprostanol and cholestanol.

3.3 Metal profiles in sediment cores

The proportion of copper and lead increased in R-12 sediments in 1949, the start of wastewater input; the remaining metals, (with the exception of vanadium, which was constant

through time), increased more than a decade after the onset of wastewater input (Fig 2.5). The proportion of zinc and copper were approximately four and eight-fold, respectively, greater following wastewater input. The proportion of all metals were relatively low and stable throughout sediments in Little Char; for example, the maximum ratio of all the examined metals was 0.12 for zinc (Table S2.8). The concentration of metals in sediments from Little Char were also low, with maximum values ranging from 0.26 μg g^{-1} dw of cadmium to 33 μg g^{-1} dw for zinc (Table S2.9). Conversely, metals concentrations were generally greater in R-12, with maximum values ranging from 0.72 to μg g^{-1} dw of cadmium to 340 μg g^{-1} dw of copper.

4 Discussion

4.1 Using stable isotopes to reconstruct wastewater deposition in High Arctic waterbodies

$\delta^{15}N$ increased in R-12 coeval with sewage input, thus reflecting the elevated $\delta^{15}N$ signal commonly found in human faeces (Fig 2.2). Similar results were observed in sewage-receiving freshwater systems, were $\delta^{15}N$ increased to values of ~10 ‰ (Bueno et al., 2018a; Vane et al., 2010). $\delta^{15}N$ remained relatively low and stable in both R-13 and Meretta Lake. The causes of low $\delta^{15}N$ values in sewage-affected lake sediments were well described by Vane et al. (2010). In short, $\delta^{15}N$ values varied widely depending on their source, for example: while higher trophic level mammals were enriched in $\delta^{15}N$, nitrogen-fixing algae can have $\delta^{15}N$ values closer to 0 ‰ (Cole et al., 2004). In fact, $\delta^{15}N$ values in raw sewage can be less than 3 ‰ (Cabral et al., 2019). While these factors may have contributed to the low and stable $\delta^{15}N$ values in sediments from R-13, the concentration of coprostanol was also low (relative to R-12), which suggests this pond may not have accumulated as much of the sewage-derived suspended matter to its sediments as R-12. The very stable $\delta^{15}N$ profile in Meretta Lake was unexpected, as a previously constructed $\delta^{15}N$ profile in Meretta Lake sediments saw an increase in $\delta^{15}N$ over time of ~6 ‰ at the onset of

sewage input (Antoniades et al., 2011). The difference in the $\delta^{15}N$ profiles may be attributed to differences in coring locations owing to Meretta Lake's large basin.

The range in $\delta^{13}C$ values were similar between waterbodies (Table S2.10). $\delta^{13}C$ values increased following wastewater input in R-12 to a maximum of -25.2 ‰ and then decreased to background values after sewage input stopped. Similarly, $\delta^{13}C$ values were relatively constant in Meretta Lake sediments and then increased to -24.2 ‰ during the period of wastewater input. This is in agreement with $\delta^{13}C$ profiles from other sewage-affected lake sediments, ranging from -26 ‰ to -22 ‰ (Andrews et al., 1999; Barros et al., 2010; Bueno et al., 2018a). In R-13, $\delta^{13}C$ values generally decreased in more recently deposited pond sediments, reaching a minimum value of -26.7 ‰. This is likely explained by a greater input of terrestrial Arctic vegetation, which typically has depleted $\delta^{13}C$ values relative to autochthonous primary producers (Choy et al., 2010; Skrzypek et al., 2008; Zibulski et al., 2017). Notably, there were two periods of increased $\delta^{13}C$, where $\delta^{13}C$ values increased by ~1 ‰ relative to the $\delta^{13}C$ values deposited before and after. The variation in $\delta^{13}C$ values may be explained by the different $\delta^{13}C$ values reported for different Arctic vegetation; for example: sedges (-28.9 ‰), mosses (-22.5 to -37.0 ‰), lichen (-19.2 to -27.5 ‰), and saxifrage (-30.7 to -23.3 ‰) (Choy et al., 2010; Skrzypek et al., 2008; Zibulski et al., 2017). Consequently, the two small peaks in $\delta^{13}C$ values may reflect a greater input of low $\delta^{13}C$ mosses relative to sedges at that time. Similar trends were observed in sewage-influenced lake sediments from South America, where $\delta^{13}C$ values were variable over the period of sewage input (Cabral et al., 2019).

4.2 Reconstructing the history of wastewater discharge using zoosterols

Sterols and stanols are useful tools for reconstructing historical trends in lake sediments as they can often be linked to specific sources (Bull et al., 2002; Leeming et al., 1998, 1996;

Pereira et al., 2017). Coprostanol has been used for sewage identification in environmental samples as far back as the 1980s and earlier (e.g. Vivian 1986 and references therein). In this study, we observed an increase in coprostanol coincident with wastewater input into the High Arctic waterbodies (Figs 2.2 and 2.3). The sediment concentrations at the study sites were at least two-fold lower than those observed in the other sewage-influenced sediments: for example, the concentration of coprostanol peaked at 252 μg g^{-1} OC in lake sediments from Manitoba, Ontario, Canada as a result of sewage input (Tse et al., 2014). Similarly, the concentration of coprostanol was 150 μg g^{-1} OC in surface sediments of an Antarctic stream as a result of sewage input (Tort et al., 2017). Coprostanol in sediments from Guanabara Bay, Brazil, reached 1,400 μg g^{-1} OC as a result of sewage input (Carreira et al., 2004). There was also a nearly 14-fold difference in coprostanol concentrations in R-12, relative to R-13 and Meretta Lake. The greater concentrations of coprostanol recorded in R-12 relative to Meretta Lake may be attributed to the deposition of sewage *via* the two utilidors into R-12 (and other waterbodies) prior to Meretta Lake; sterols, bound to particulate matter, would be largely deposited before reaching Meretta Lake. Furthermore, Meretta Lake is ~82 times larger than R-12 and therefore the sterol and stanol signal would have been diluted to a much larger area in Meretta Lake. R-13, however, is nearly the same size as R-12, and was the first pond (examined in this study) to receive sewage. The difference in response to the wastewater biomarkers in R-12 and R-13 is likely the result of the higher dating resolution in R-12 (1953 is at 8 cm) relative to R-13 (1956 is at 3.5 cm). Consequently, R-13 likely has more intervals of diluted wastewater input than R-12. Stewart et al. (2014) found that diatoms in R-12 recorded a greater eutrophication impact than R-13, which they also attributed to differences in the dating resolution. The concentration of coprostanol in Little Char, the reference site, was very low throughout the sediment core. The small, but

measurable coprostanol concentrations may be explained by *in situ* hydrogenation of cholesterol (Leeming et al., 1996; Nishimura and Koyama, 1977).

Cholesterol and cholestanol concentrations increased coeval with the onset of wastewater emissions into R-12, R-13, and Meretta Lake. As expected, the concentrations of cholesterol and cholestanol decreased in R-12 and R-13 in more recent sediments, however neither the concentration of cholesterol nor cholestanol decreased in post-sewage sediments in Meretta Lake. Conversely, diatom assemblages did change immediately after sewage was stopped from flowing into Meretta Lake (Douglas and Smol, 2000; Michelutti et al., 2002). Although there was no apparent lag in diatom assemblage changes to Meretta Lake following the cessation of sewage inputs, a twenty-year lag in the response of diatoms to sewage input was observed in Annak Lake, Belcher Island, Nunavut, Canada (Michelutti et al., 2007). Similarly, cholesterol concentrations in sediments from Niven Lake, Yellowknife, Northwest Territories, Canada, did not rise until ~25 years after sewage input had ceased (Stewart et al., 2018). There were no measurable concentrations of cholestanol in Little Char as we also did not measure any cholesterol in the sediments.

Epicoprostanol is a minor component in human faeces (Leeming et al., 1996) so the low, but detectable concentrations of epicoprostanol (maximum of 17.3 $\mu g\ g^{-1}$ OC in R-12) in the wastewater-affected waterbodies may have been the result of the sewage itself. For example, sewage-affected lake sediments can be composed of up to 4 % epicoprostanol (compared to 2 % in pre-sewage sediments) (Stewart et al., 2018). Epicoprostanol may also be present in the lake sediments as a result of the aerobic bacterial degradation of coprostanol to epicoprostanol (Battistel et al., 2015). Low concentrations of epicoprostanol can also be indicative of raw sewage (relative to treated sewage) as the prolonged digestion of the sewage allows for greater

microbial transformation of cholesterol to epicoprostanol (McCalley et al., 1981). For example, lake sediments from Brazil had low epicoprostanol concentrations (maximum: 2.24 μg g^{-1}), which reflected the input of untreated sewage (Carreira et al., 2004).

In the wastewater-influenced waterbodies, many sterols and stanols peaked after the cessation of wastewater input. Such a lag may have occurred from a slow release of contaminated sediments from the utilidor, or delayed particle settling due to currents or turbulence. This may be particularly true of R-12 and R-13, both small waterbodies, where any current created by wastewater input may have delayed the analytes from settling.

Faecal sterols appeared to be the main driver of the sterol and stanol composition in R-12 sediments from 1949 to 1990, as evidenced by the shift along axis 1 (Fig 2.4). Similar trends were observed in Meretta Lake and R-13 (Fig S2.2). The general absence of sterols in pre-sewage sediments was also evident within the PCAs: the sterol composition of pre-wastewater sediments appeared in a separate quadrant from wastewater-input sediments and the sterol vectors travelled in the opposite direction of pre-wastewater sediments. The change in the sterol composition in R-12 following wastewater input was also traceable within the PCA: from 1990 to 2017, the sediment composition appeared in a separate quadrant from pre- and wastewater-input quadrants, and the sterol vectors extended in the opposite direction.

4.3 Phytosterols in waterbody sediments

In addition to faecal sterols, we examined an array of phytosterols, including campesterol, fucosterol, sitosterol, and stigmastanol. Campesterol is commonly found in vascular plants, as well as in phytoplankton and algae, although at lower concentrations (Pereira et al., 2017). In R-12, R-13, and Meretta Lake, campesterol concentrations increased in sediments at the onset of sewage input (Figs 2.2 and 2.3). Campesterol concentrations in this study are

comparable to those found in sewage-affected sediments from a lake in northern Manitoba, Canada (peak of ~100 μg g^{-1} OC) (Tse et al., 2014). Fucosterol is abundant in algae (Mouritsen et al., 2017; Patterson, 1994; Pereira et al., 2017) and can be found in concentrations of up to 48.1 μg g^{-1}, more than double that of sitosterol and stigmastanol (Pereira et al., 2017). Accordingly, fucosterol in sediments also tracked sewage input, suggesting an increase in the abundance of algae as a result of the nutrients supplied by wastewater (Figs 2.2 and 2.3).

Sitosterol and stigmastanol are found in vegetation and have therefore been used to track the input of terrestrial vegetation in lake sediments (Nishimura, 1978). Sitosterol, in particular, makes up a large percentage of the sterol composition in plants; for example, ~30 – 70 % in High Arctic moss (Cheng et al., 2016). Consequently, sitosterol is also found in high concentrations in herbivore faeces (e.g. 497 μg g^{-1} in sheep) and human faeces (313 μg g^{-1}) (Prost et al., 2017). Predictably, sitosterol concentrations increased in sediments at the time of wastewater input in R-13 and Meretta Lake (Fig 2.3), likely as a result of the increased plant growth associated with the presence of wastewater. Sitosterol increased after the period of wastewater inputs in R-12, suggesting delayed plant growth in that location. Water from Meretta Lake has greater concentrations of several analytes, including TP, POC, DOC, and zinc, relative to Little Char (Table S2.11). Despite the elevated nutrients available in Meretta Lake, sitosterol was not measurable in periphyton, however sitosterol was present at concentrations in periphyton equal to ~50 % of that in surface sediments from R-12 (Fig S2.3). The generally low concentration of periphyton in Meretta Lake may be attributed to the low number of rocks located at this site and thus an absence of an adequate environment on which the periphyton can grow.

Stigmastanol, while also present in plants, is found in much lower concentrations than sitosterol; consequently, stigmastanol concentrations in human faeces are ~17 % of that of

sitosterol (Prost et al., 2017). This is reflected within the sediments, as the concentration of stigmastanol is about half of that of sitosterol in Meretta Lake and very low in R-12 and R-13 (Table S2.4). The low, but detectable concentrations of stigmastanol before sewage dumping in Meretta Lake, may be the result of freshwater algae producing stigmastanol under low oxygen conditions (Fahrenfeld, 2008). The concentration of phytosterols in Little Char were consistently low, indicating that this pond was historically low in vegetation and algae. The absence of a nutrient source (such as sewage) would explain the low concentration of sterols, and this is further enforced by the water chemistry: Little Char had lower concentrations of many nutrients, including phosphorus, nitrogen, and OC, which are essential for vegetation growth (Table S2.11).

4.4 The effect of wastewater on the concentration of sterols and stanols in periphyton and zooplankton

We measured the concentration of sterols and stanols in periphyton and zooplankton in order to determine if periphyton and zooplankton from wastewater-influenced waterbodies had greater concentrations of sterols and stanols in primary producers and consumers, relative to unaffected waterbodies. Indeed, there was not enough zooplankton biomass to determine the sterol and stanol concentrations in zooplankton, and the concentration of sterols and stanols in periphyton was generally greater in wastewater-influenced waterbodies relative to the reference pond, Little Char. The only exceptions were the lower concentrations of campesterol, cholesterol, and sitosterol in periphyton from R-13 and the lower concentration of coprostanol in periphyton from Meretta Lake, relative to Little Char (Fig S2.3).

4.5 Metals show a delayed response to wastewater input

Wastewater can increase the concentration of certain biogenic metals in lake sediments. In particular, cadmium, chromium, lead, and zinc are commonly elevated in sewage-influenced lake sediments (Andrews et al., 1999; Antoniades et al., 2011; Bartkowska et al., 2019; Karthikeyan et al., 2018; Wang et al., 2016). With the exception of copper, metals decreased slightly and subsequently increased to baseline prior to wastewater input. In R-12, arsenic, cadmium, chromium, nickel, and zinc first surpassed background either ~15 years after wastewater input began or increased after wastewater input stopped (Fig 2.5). A delayed rise in these elements could be due in part to dissolution and diffusion in sediment porewaters (particularly for arsenic; (Pan et al. 2019)) or from sediment resuspension from turbulence of the wastewater discharge itself. Copper and lead increased slowly with wastewater input and peaked after wastewater input stopped. In R-12, cadmium and zinc increased by two and four-fold, respectively, after wastewater input stopped. Similarly, cadmium and zinc increased in sediments previously collected from Meretta Lake (Antoniades et al., 2011), however the ratio of cadmium and zinc was at least four-times greater in R-12 than that previously observed in Meretta Lake. Similarly, chromium and lead were also more concentrated in wastewater-affected sediments from R-12; a similar rise in chromium and lead was observed in lake sediments from Antarctica (Bueno et al., 2018b). Conversely, metal ratios in the reference pond, Little Char, were generally low and were relatively constant through time. This is expected as there was no wastewater discharge into this pond. Similarly, low concentrations of cadmium and zinc were observed in a reference lake in a study of remote high Arctic lakes (Brimble et al., 2009), and pond sediments before impact by seabird guano (Evenset et al., 2007).

4.6 Tracking the return of lake sediments to pre-wastewater conditions

In R-12 and R-13, sterol and stanol concentrations in sediments increased at the time of wastewater discharge, however unlike R-12 and R-13, sterol and stanol concentrations in Meretta Lake continued to rise in more recently deposited sediments. Wastewater discharge continued into Meretta Lake until 1998, 19 years longer than the discharge into R-12 and R-13, thus resulting in the elevated sterol and stanol concentrations. Furthermore, Meretta Lake is larger than both R-12 and R-13, and thus it may take more time for analytes to settle to the sediment-water interface. This is not the first instance that a delay in the response of a proxy has been observed in Meretta Lake: Michelutti et al. (2007) reported a lag of several decades before diatom assemblages responded to wastewater inputs in Meretta Lake. In this case, these authors attributed this delay to prolonged periods of ice cover, which would have prevented the establishment of new diatom species.

5 Conclusions

We presented a case study that examined sterols, stanols, metals, $\delta^{15}N$, and $\delta^{13}C$ in a multiproxy analysis to reconstruct wastewater input in High Arctic waterbodies. First, this study demonstrated that wastewater-receiving sediments had greater sterol and stanol concentrations than uninfluenced sediments. Second, sterol and stanol profiles in waterbody sediments tracked the introduction and cessation (in the case of R-12 and R-13) of wastewater input whereas sterols and stanols in reference pond sediments remained stable through time. This study found that sterol and stanol concentrations in R-12 and R-13 pond sediments approached pre-wastewater concentrations following the cessation of wastewater input, whereas elevated sterol and stanol concentrations persisted in Meretta Lake, likely due to its larger volume and longer period of wastewater input. Lastly, this study found that coprostanol and epicoprostanol were sensitive

wastewater tracers as evidenced by the low to undetectable concentrations in sediments prior to wastewater input and greater concentrations in wastewater-influenced sediments.

This study highlighted the importance of using multiple proxies when studying paleo-archives. We demonstrated that in addition to stable isotopes and metals, sterols and stanols also tracked historical wastewater discharge. Sterols and stanols have the added advantage of being more source specific than stable isotopes and metals, and as such, they provide additional certainty when reconstructing historical environmental conditions. Furthermore, proxies can be influenced by several factors and thus examining multiple proxies allows for a more accurate reconstruction of historical events.

Acknowledgements

This research was supported by a Natural Sciences and Engineering Research Council (NSERC) Canada grant to JMB (RGPIN-2018-04248) and in-kind support from the Polar Continental Shelf Program (PCSP) awarded to JMB and JPS (PCSP # 654-17) to support lodging and logistics at Resolute Bay.

The authors declare no competing interests.

Figure 2.1: Map of study sites in Resolute Bay, Nunavut, Canada.

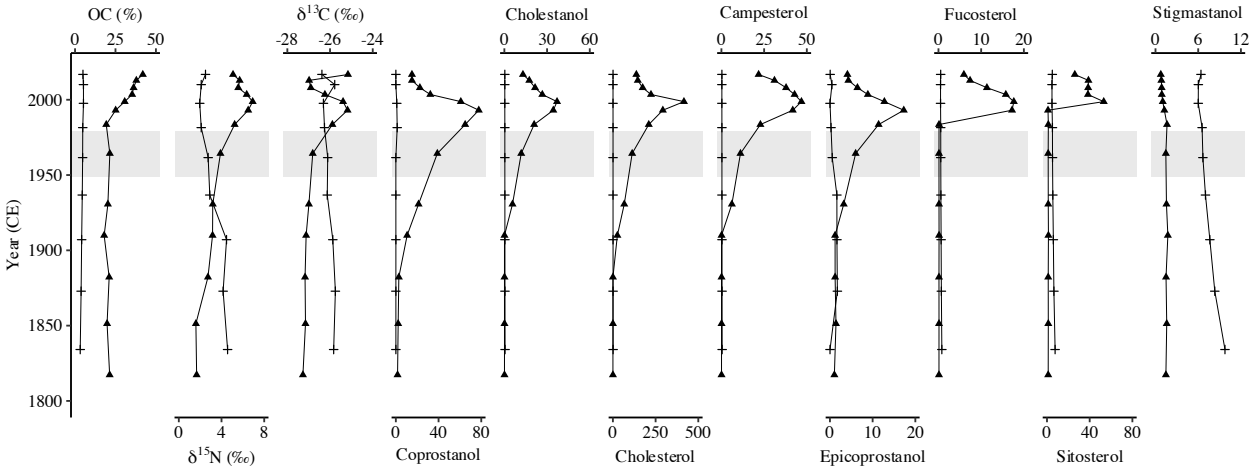

Figure 2.2: Percent organic carbon (OC), stable isotopes, and sterol and stanol concentrations (µg g^{-1} OC dw) in the sewage-water receiving pond, R-12 (▲), and the reference pond, Little Char (+). The shaded area indicates the period of sewage input into R-12.

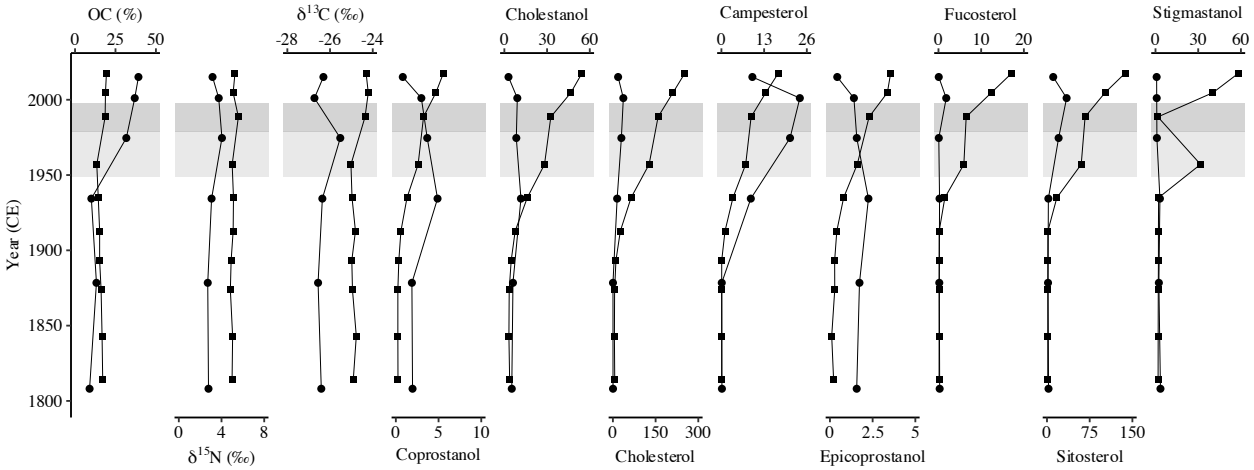

Figure 2.3: Percent organic carbon (OC), stable isotopes, and sterol and stanol concentrations (µg g^{-1} OC dw) in R-13 (●) and Meretta Lake (■), both sewage-receiving waterbodies. The light gray shaded area indicates the period of sewage input from 1949 to 1979; the dark gray shaded area indicates the additional 19 years of sewage input into Meretta Lake, from 1979 to 1998.

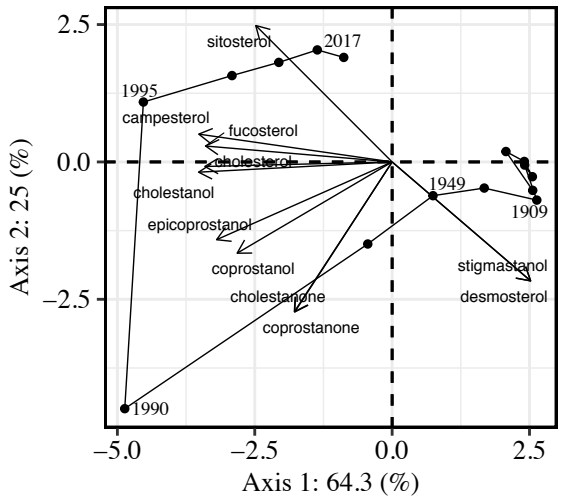

Figure 2.4: Principle Component Analysis (PCA) of the downcore sterol concentrations (µg g^{-1} OC dw) in R-12 (a sewage-influenced pond). Select ^{210}Pb dates are indicated adjacent to their corresponding depth. Principle component axis 1 and axis 2 explain a cumulative 89.3 % of the variation in the sterol and stanol composition of the pond sediments in R-12.

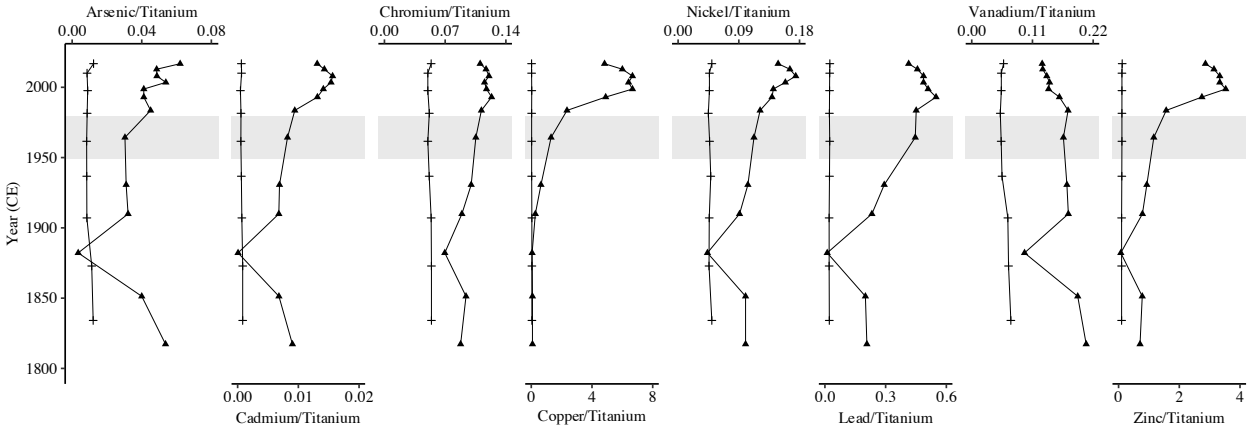

Figure 2.5: Metal ratios (metal concentration normalized to the titanium concentration to account for natural deposition) in the sewage-water receiving pond, R-12 (▲), and the reference pond, Little Char (+). The shaded area indicates the period of sewage input into R-12.

Supplementary information

Table S2.1: Latitude, longitude, area, and elevation above sea level of waterbodies from Cornwallis Island, Nunavut, Canada.

Site	Latitude	Longitude	Waterbody area (m^2)	Elevation above sea level (m)
Meretta Lake	74°41'44.96"N	94°59'34.74"W	239,700	21
Little Char	74°42'01.90"N	94°53'38.06"W	21,740	27
R-12	74°42'32.80"N	94°59'22.61"W	2,910	38
R-13	74°42'37.17"N	94°59'18.82"W	3,250	44

Table S2.2: Percent recoveries ± standard error (std. error) of sterols and stanols in waterbodies; n = sample size.

Waterbody	Median (%)	Std. Error (%)	n
Little Char	124.8	10.2	16
R-12	116.4	5.3	15
R-13	82.7	1.9	15
Meretta Lake	72.3	0.9	21

Table S2.3: Method detection limit (MDLs) (ng g^{-1} dw) of sterols and stanols determined through a calibration curve.

Compound	MDL	MDL/√2
coprostanol	1.08	0.76
epicoprostanol	0.81	0.57
coprostanone	169.49	119.85
cholesterol	52.27	36.96
cholestanol	21.91	15.49
cholestanone	16.90	11.95
desmosterol	123.33	87.21
campesterol	19.36	13.69
fucosterol	35.91	25.39
sitosterol	344.99	243.24
stigmastanol	442.73	312.35

Table S2.4: Summary of sterol and stanol concentrations in the wastewater-impacted waterbodies, Meretta Lake, R-12, and R-13, and the reference pond, Little Char. Sample size (n) represents the number of waterbody sediment intervals analyzed. Standard error = std. error.

		μg g^{-1} OC dw			
Waterbody	Compound	Minimum	Maximum	Median	Std. Error
Little Char (n = 16)	campesterol	0.26	0.61	0.35	0.02
	cholestanol	0.30	0.69	0.40	0.03
	cholestanone	0.23	0.54	0.30	0.02
	cholesterol	0.71	1.66	0.94	0.07
	coprostanol	0.01	1.26	0.02	0.09
	coprostanone	2.30	5.37	3.07	0.21
	desmosterol	1.68	3.91	2.23	0.16
	epicoprostanol	0.01	1.74	0.50	0.16
	fucosterol	0.49	1.14	0.65	0.05
	sitosterol	4.68	10.91	6.22	0.43
	stigmastanol	6.01	14.01	7.98	0.56
Meretta Lake (n = 21)	campesterol	0.06	17.34	0.08	1.09
	cholestanol	0.07	54.53	3.19	3.53
	cholestanone	0.05	13.48	0.07	0.89
	cholesterol	0.16	253.81	5.31	16.71
	coprostanol	0.03	5.57	0.22	0.36
	coprostanone	0.52	0.89	0.62	0.02
	desmosterol	0.38	0.65	0.45	0.02
	epicoprostanol	0.02	3.55	0.16	0.24
	fucosterol	0.11	17.17	0.14	1.01
	sitosterol	1.06	137.29	1.36	8.44
	stigmastanol	1.36	58.36	1.74	3.40
R-12 (n = 15)	campesterol	0.06	46.85	11.15	4.75
	cholestanol	0.07	37.00	11.84	3.28
	cholestanone	0.03	3.19	0.06	0.21
	cholesterol	0.16	415.92	112.84	32.62
	coprostanol	1.60	77.68	15.09	6.52
	coprostanone	0.29	27.52	0.56	1.80
	desmosterol	0.21	0.48	0.41	0.02
	epicoprostanol	1.04	17.29	4.09	1.29
	fucosterol	0.11	17.65	0.14	1.81
	sitosterol	0.97	53.17	1.26	4.95
	stigmastanol	0.75	1.74	1.45	0.09
R-13 (n = 15)	campesterol	0.10	23.87	0.31	2.06

cholestanol	0.22	12.43	5.20	1.12
cholestanone	0.03	0.62	0.17	0.04
cholesterol	0.28	36.63	0.85	3.11
coprostanol	0.02	5.49	1.88	0.43
coprostanone	0.31	3.82	1.38	0.30
desmosterol	0.22	2.78	1.00	0.22
epicoprostanol	0.01	2.25	1.17	0.19
fucosterol	0.06	1.82	0.35	0.11
sitosterol	1.84	34.47	4.46	2.27
stigmastanol	0.80	9.95	3.59	0.77

Table S2.5: Summary of sterol and stanol concentrations in the wastewater-impacted waterbodies, Meretta Lake, R-12, and R-13, and the reference pond, Little Char. Sample size (n) represents the number of waterbody sediment intervals analyzed. Standard error = std. error.

		μg g^{-1} dw			
Waterbody	Compound	Minimum	Maximum	Median	Std. Error
Little Char (n = 16)	campesterol	0.01	0.01	0.01	0.00
	cholestanol	0.02	0.02	0.02	0.00
	cholestanone	0.01	0.01	0.01	0.00
	cholesterol	0.04	0.04	0.04	0.00
	coprostanol	0.00	0.06	0.00	0.00
	coprostanone	0.12	0.12	0.12	0.00
	desmosterol	0.09	0.09	0.09	0.00
	epicoprostanol	0.00	0.07	0.02	0.01
	fucosterol	0.02	0.02	0.02	0.00
	sitosterol	0.24	0.24	0.24	0.00
	stigmastanol	0.31	0.31	0.31	0.00
Meretta Lake (n = 21)	campesterol	0.01	3.36	0.01	0.20
	cholestanol	0.02	10.6	0.53	0.66
	cholestanone	0.01	2.62	0.01	0.17
	cholesterol	0.04	49.1	0.93	3.12
	coprostanol	0.01	1.08	0.04	0.07
	coprostanone	0.12	0.12	0.12	0.00
	desmosterol	0.09	0.09	0.09	0.00
	epicoprostanol	0.01	0.69	0.03	0.04
	fucosterol	0.03	3.33	0.03	0.19
	sitosterol	0.24	26.6	0.24	1.58
	stigmastanol	0.31	11.3	0.31	0.63
R-12 (n = 15)	campesterol	0.01	15.1	2.40	1.58
	cholestanol	0.02	11.4	2.55	1.03
	cholestanone	0.01	0.80	0.01	0.05
	cholesterol	0.04	128	24.3	10.1
	coprostanol	0.34	19.5	5.72	1.68
	coprostanone	0.12	6.91	0.12	0.45
	desmosterol	0.09	0.09	0.09	0.00
	epicoprostanol	0.22	4.34	1.29	0.36
	fucosterol	0.02	5.57	0.02	0.57
	sitosterol	0.24	16.3	0.24	1.74
	stigmastanol	0.31	0.31	0.31	0.00
R-13 (n = 15)	campesterol	0.01	8.81	0.01	0.72

cholestanol	0.02	3.35	0.47	0.26
cholestanone	0.01	0.23	0.01	0.01
cholesterol	0.04	13.5	0.04	1.11
coprostanol	0.00	1.17	0.21	0.09
coprostanone	0.12	0.12	0.12	0.00
desmosterol	0.09	0.09	0.09	0.00
epicoprostanol	0.00	0.52	0.14	0.04
fucosterol	0.02	0.67	0.02	0.04
sitosterol	0.24	12.7	0.24	0.92
stigmastanol	0.31	0.31	0.31	0.00

Table S2.6: Minimum, maximum, median, and standard error (std. error) $\delta^{15}N$ values for the wastewater-impacted waterbodies, Meretta Lake, R-12, and R-13, and the reference pond, Little Char. Sample size (n) represents the number of waterbody sediment intervals analyzed.

	$\delta^{15}N$ (‰)			
Waterbody	Minimum	Maximum	Median	Std. Error
Meretta lake (n = 21)	3.96	5.58	4.8	0.08
R-12 (n = 15)	1.57	6.92	3.9	0.51
R-13 (n = 15)	2.31	4.95	3.2	0.21
Little Char (n = 16)	1.96	5.05	4.3	0.28

Table S2.7: Minimum, maximum, median, and standard error (std. error) percent organic carbon values for the wastewater-influenced waterbodies, Meretta Lake, R-12, and R-13, and the reference pond, Little Char. Sample size (n) represents the number of waterbody sediment intervals analyzed.

	Organic carbon (%)			
Waterbody	Minimum	Maximum	Median	Std. Error
Meretta Lake (n = 21)	13.4	22.9	19.4	0.6
R-12 (n = 15)	18.0	41.9	21.5	2.1
R-13 (n = 15)	3.1	39.2	8.7	3.2
Little Char (n = 16)	2.2	5.2	3.92	0.2

Table S2.8: Minimum, maximum, median, and standard error (std. error) metal ratios (metals normalized to titanium) in the wastewater-influenced pond, R-12, and the reference pond, Little Char. Sample size (n) represents the number of pond sediment intervals analyzed.

Waterbody	Compound	Minimum	Maximum	Median	Std. Error
R-12 (n = 15)	arsenic	0.00	0.07	0.05	0.00
	cadmium	0.00	0.02	0.01	0.00
	chromium	0.07	0.12	0.11	0.00
	copper	0.05	6.67	1.30	0.73
	lead	0.01	0.55	0.41	0.04
	nickel	0.04	0.17	0.11	0.01
	vanadium	0.10	0.21	0.17	0.01
	zinc	0.07	3.53	1.16	0.32
Little Char (n = 16)	arsenic	0.01	0.01	0.01	0.00
	cadmium	0.00	0.00	0.00	0.00
	chromium	0.05	0.06	0.05	0.00
	copper	0.02	0.09	0.04	0.00
	lead	0.02	0.02	0.02	0.00
	nickel	0.04	0.05	0.05	0.00
	vanadium	0.05	0.07	0.06	0.00
	zinc	0.09	0.12	0.10	0.00

Table S2.9: Minimum, maximum, median, and standard error (std. error) metal concentrations (µg g^{-1} dw) in the wastewater-influenced pond, R-12, and the reference pond, Little Char. Sample size (n) represents the number of pond sediment intervals analyzed.

Waterbody	Compound	Minimum	Maximum	Median	Std. Error
R-12 (n = 15)	arsenic	1.60	2.90	2.00	0.08
	cadmium	0.03	0.72	0.46	0.04
	chromium	3.20	32.00	4.70	1.83
	copper	3.20	340.00	73.00	30.26
	lead	5.20	28.00	16.00	1.83
	nickel	4.10	20.00	6.00	0.99
	vanadium	3.70	44.00	8.70	2.48
	zinc	29.00	180.00	65.00	12.41
Little Char (n = 16)	arsenic	1.90	3.20	2.50	0.08
	cadmium	0.13	0.26	0.20	0.01
	chromium	13.00	16.00	13.50	0.23
	copper	5.20	22.00	9.45	0.98
	lead	5.00	7.10	5.35	0.18
	nickel	11.00	15.00	12.00	0.26
	vanadium	15.00	17.00	16.00	0.20
	zinc	24.00	33.00	26.00	0.91

Table S2.10: Minimum, maximum, median, and standard error (std. error) $\delta^{13}C$ values for the wastewater-influenced waterbodies, Meretta Lake, R-12, and R-13, and the reference pond, Little Char. Sample size (n) represents the number of waterbody sediment intervals analyzed.

	$\delta^{13}C$ (‰)			
Waterbody	Minimum	Maximum	Median	Std. Error
Meretta Lake (n = 21)	-25.0	-24.2	-24.7	0.05
R-12 (n = 15)	-27.3	-25.2	-27.0	0.20
R-13 (n = 15)	-26.7	-24.7	-26.3	0.16
Little Char (n = 16)	-26.4	-24.7	-25.8	0.14

Table S2.11: Water chemistry data from wastewater-influenced waterbodies, R-12, R-13, and Meretta Lake, and the reference pond, Little Char. N = 1, except for Meretta Lake, where we presented the average of N = 3. TP = total phosphorus, TDP = total dissolved phosphorus, TDN = total dissolved nitrogen, DOC = dissolved organic carbon, DIC = dissolved inorganic carbon, POC = particulate organic carbon, PON = particulate organic nitrogen.

Analyte	Little Char	Meretta Lake	R-12	R-13
TP µg L^{-1}	1.3	7.2	12.1	12.1
TDP µg L^{-1}	1.3	2.6	6.4	6.1
TDN mg L^{-1}	0.13	0.23	0.30	0.35
NO_3^-/NO_2^- as N mg L^{-1}	0.01	0.01	0.02	0.02
TDN (Kjeldahl) mg L^{-1}	0.16	0.27	0.35	0.40
NH3- as N	130	232	304	346
DOC mg L^{-1}	2.1	3.1	5.4	6.9
DIC mg L^{-1}	20.6	20.3	29.2	28.8
POC mg L^{-1}	0.20	0.45	0.40	0.37
PON mg L^{-1}	0.02	0.05	0.04	0.04
Cl mg L^{-1}	18.4	20.5	14.9	15.0
SO_4^{2-} mg L^{-1}	39.4	8.8	11.7	9.2
Al µg L^{-1}	27.5	10.3	12.3	2.1
As µg L^{-1}	0.10	0.16	0.24	0.20
Cr µg L^{-1}	0.09	0.06	0.08	0.15
Cd µg L^{-1}	<0.001	0.01	0.004	0.006
Cu µg L^{-1}	0.22	0.35	2.58	1.79
Fe µg L^{-1}	29.9	23.4	26.1	26.9
Pb µg L^{-1}	0.02	0.07	0.08	0.04
Zn µg L^{-1}	<0.2	0.8	0.5	0.2
Sr µg L^{-1}	100	70	126	131

Table S2.12: ^{210}Pb dating information for R-12, R-13, and Little Char.

Depth (cm)	Cumulative dry mass (g cm^{-2})	^{210}Pb (Bq kg^{-1})	^{210}Pb error (Bq kg^{-1})	^{214}Pb (Bq kg^{-1})	^{214}Pb error (Bq kg^{-1})	^{137}Cs (Bq kg^{-1})	^{137}Cs error (Bq kg^{-1})	Age (CRS) (year)	Year (CRS) (year)	Error (CRS) (year)
R-12										
0								0	2017.57	0.8561
0.25	0.0769	64.88	11.07	5.43	2.15	14.24	1.89	0.7982	2016.77	0.8659
0.75	0.2183	122.72	19.41	2.36	3.53	13.41	2.53	2.5095	2015.06	0.9626
1.75	0.4811	114.27	14.76	6.94	2.25	22.68	2.47	6.935	2010.64	1.2053
2.75	0.7905	95.24	13.21	4.6	2.14	22.76	2.4	12.2021	2005.37	1.5381
3.75	1.0055	93.58	12.02	7.55	1.92	28.88	2.78	15.9633	2001.61	1.7915
5.75	1.6842	57.06	8.83	8.39	1.59	42.78	3.69	27.3748	1990.2	2.7831
6.75	2.3068	77.36	9.88	9.2	1.54	34.33	3	40.6945	1976.88	4.168
7.75	2.9948	49.75	9.24	6.31	1.63	19.86	2.01	65.8107	1951.76	8.3308
8.75	3.7618	27.57	7.83	9.31	1.57	8.46	1.26	107.9946	1909.58	25.0759
9.75	4.6719	9.09	7.53	8.23	1.64	2.55	0.86			
10.75	5.6856	10.27	6.46	8.09	1.37	0.7	0.79			
R-13										
0								0	2017.57	3.8947
0.25	0.0655	77.57	16.36	6	3.05	10.35	2.15	2.4687	2015.11	3.944
0.75	0.1993	101.93	18.84	6.64	3.31	14.65	2.57	8.2233	2009.35	4.3075
1.75	0.5144	57.26	14.68	7.28	2.56	14.47	2.1	24.7583	1992.82	6.5398
2.75	1.1873	26.44	6.45	7.86	1.25	4.94	0.91	61.207	1956.37	20.503
3.75	2.3631	0	6.65	8.97	1.21	0.97	0.67			
4.75	3.8224	1.06	5.98	9.97	1.24	0.23	0.61			
5.75	5.3695	4.04	5.44	9.89	1.11	0	0.54			
6.75	6.9946	3.68	5.01	10.88	1.09	0	0.51			
7.75	8.7242	13.5	5.39	11.84	1.12	0.79	0.57			
8.75	10.3181	3.19	4.94	10.26	1.06	0	0.54			
9.75	11.8979	16.07	6.29	11.8	1.29	0.13	0.63			
Little Char										
0								0	2017.57	1.525
0.25	0.0737	106.1	15.38	15.77	2.29	10.05	1.69	0.7517	2016.82	1.5314
0.75	0.2996	107.7	14.94	12.24	2.02	8.92	1.52	2.9991	2014.57	1.5965
1.75	0.9964	125.11	15.48	16.17	2.07	12.24	1.79	12.0672	2005.51	2.2579
2.75	1.8201	110.42	15.11	13.74	2.06	10.2	1.61	27.8342	1989.74	3.5299
3.75	2.6029	50.27	10.22	9.83	1.75	7.58	1.31	44.333	1973.24	5.5449
4.75	3.4194	75.65	12.98	14.99	2.01	17.28	2.02	67.6652	1949.91	9.0676
5.75	4.6481	17.96	9.47	15.72	1.6	3.98	1.1			
6.75	6.3026	26.33	8.97	16.04	1.5	0.37	0.88			
7.75	8.0241	18.02	8.38	16.97	1.5	0	0.84			
8.75	9.6580	22.59	8.18	16.42	1.48	0	0.84			

Table S2.13: ^{210}Pb dating information for Meretta Lake.

Depth (cm)	Bulk density (g cm^{-3})	Moisture (%)	Sample weight (g)	^{210}Po measured (Bq g^{-1})	^{210}Pb activity (Bq g^{-1})	Interpolate ^{210}Pb (Bq g^{-1})	^{210}Pb excess (Bq g^{-1})	^{210}Pb excess in the core (Bq g^{-1})	Mass ^{210}Pb excess (Bq)	Age (Year)
0.25	1.178	89.22	0.2888	0.179	0.211	0.211	0.182	0.214	0.645	2017.65
1.25	1.198	88.00	0.3019	0.145	0.171	0.171	0.141	0.169	0.431	2004.68
2.25	1.206	87.54	0.3204	0.140	0.165	0.165	0.136	0.163	0.262	1988.62
3.25	1.236	85.71	0.3154	0.075	0.089	0.089	0.059	0.073	0.098	1957.08
5.25	1.184	88.83	0.2997	0.037	0.044	0.044	0.015	0.017	0.025	1912.81
7.25	1.159	90.36	0.2965	0.033	0.040	0.040	0.010	0.012	0.007	1873.79
9.25	1.169	89.78	0.3075	0.034	0.040	0.040	0.01	0.01		
11.25	1.169	89.73	0.3105	0.032	0.038	0.038	0.01	0.01		
13.25	1.168	89.83	0.3193	0.026	0.031	0.031	0.00	0.00		
15.25	1.197	88.06	0.3019	0.008	0.009	0.009				
20.25	1.014	99.16	0.3182	0.022	0.026	0.026				

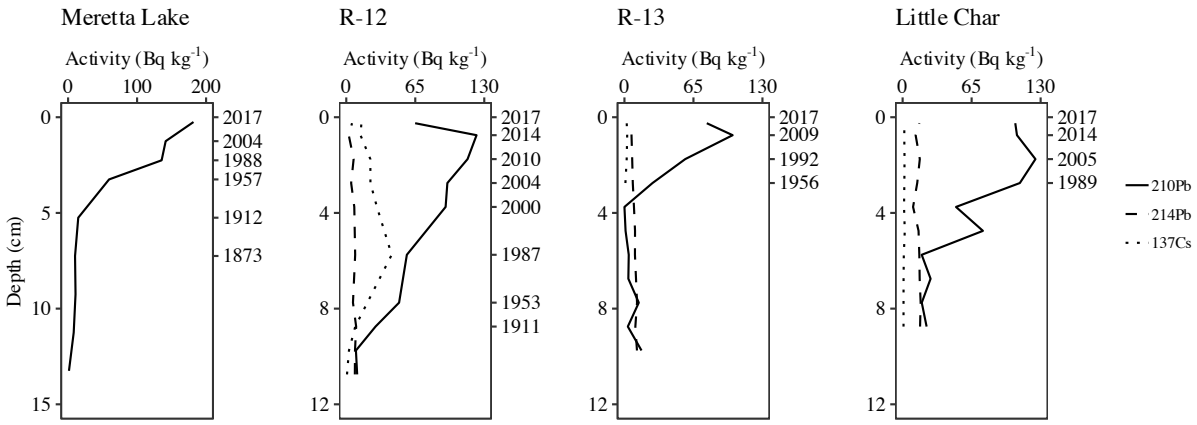

Figure S2.1: ^{210}Pb activity in Meretta Lake (alpha counting), and ^{210}Pb, ^{214}Pb, and ^{137}Cs activity in R-12, R-13, and Little Char (gamma counting). The constant rate of supply (CRS) model was used to infer year and is shown on the right y-axes.

Meretta Lake

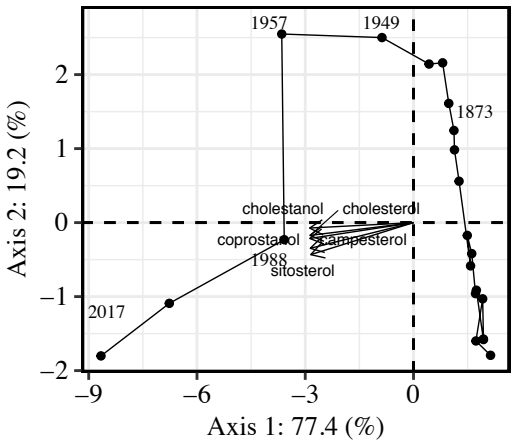

R–13

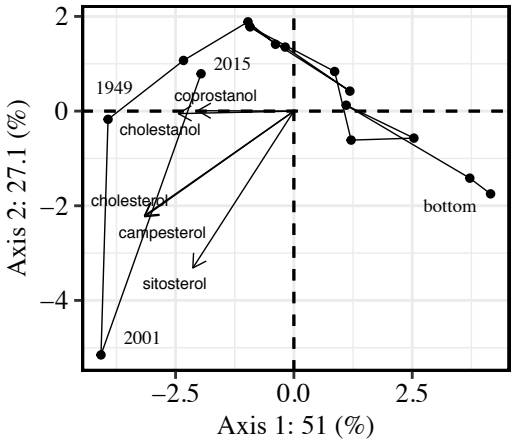

Little Char

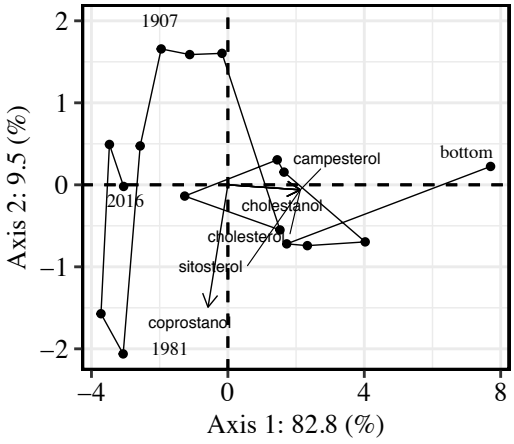

Figure S2.2: Principle component analysis (PCA) of the downcore sterol and stanol concentrations (µg g^{-1} OC dw) in R-13 and Meretta Lake (sewage-influenced waterbodies) and Little Char (reference pond). Select ^{210}Pb dates are indicated adjacent to their corresponding depth.

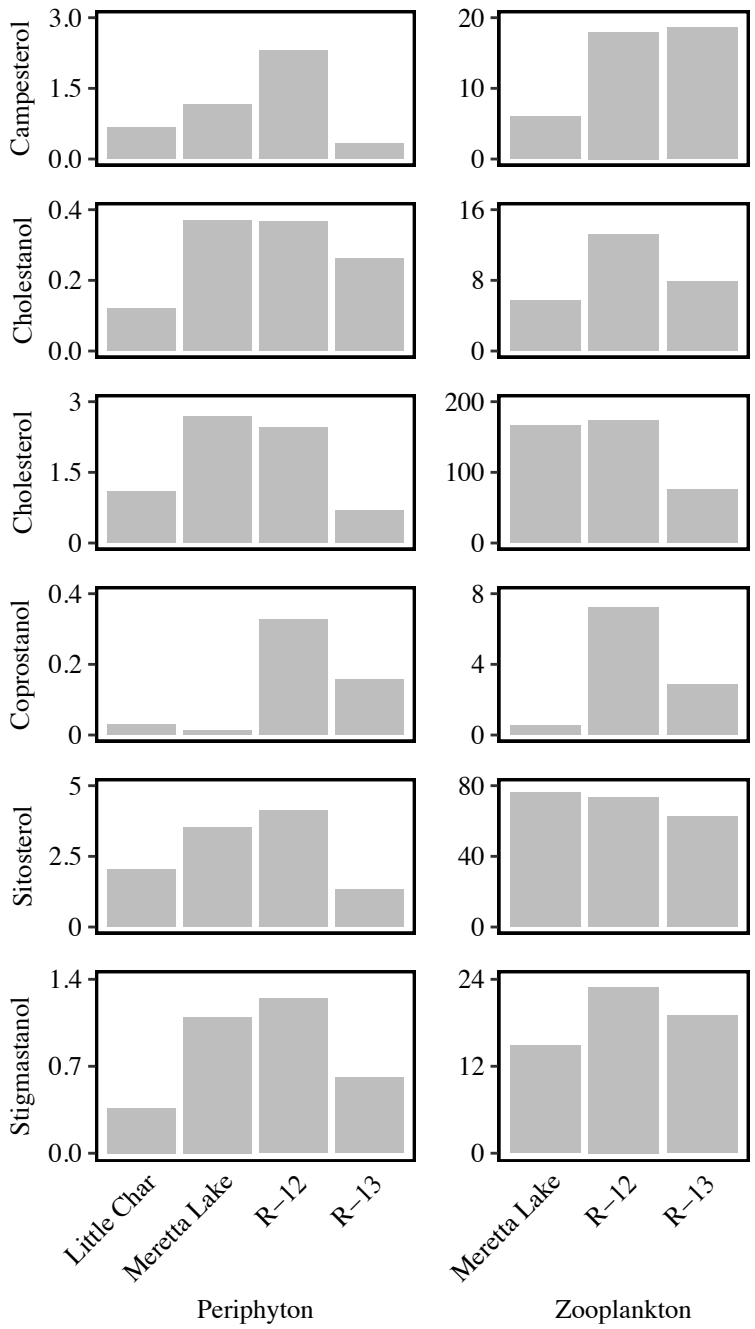

Figure S2.3: Sterol and stanol concentrations (µg g^{-1} dw) in periphyton and zooplankton from sewage influenced waterbodies (R-12, R-13, and Meretta Lake) and the reference pond (Little Char). Note the different y-axis scales for the concentration of sterols and stanols in periphyton and zooplankton.

References

Andrews, J.E., Greenaway, A.M., Bigg, G.R., Webber, D.F., Dennis, P.F., Guthrie, G.A., 1999. Pollution history of a tropical estuary revealed by combined hydrodynamic modelling and sediment geochemistry. J Mar Syst 18, 333–343. https://doi.org/10.1016/S0924-7963(98)00019-0

Antoniades, D., Michelutti, N., Quinlan, R., Blais, J.M., Bonilla, S., Douglas, M.S.V., Pienitz, R., Smol, J.P., Vincent, W.F., 2011. Cultural eutrophication, anoxia, and ecosystem recovery in Meretta Lake, High Arctic Canada. Limnol Oceanogr 56, 639–650. https://doi.org/10.4319/lo.2011.56.2.0639

Barros, G.V., Martinelli, L.A., Oliveira Novais, T.M., Ometto, J.P.H.B., Zuppi, G.M., 2010. Stable isotopes of bulk organic matter to trace carbon and nitrogen dynamics in an estuarine ecosystem in Babitonga Bay (Santa Catarina, Brazil). Sci Total Environ 408, 2226–2232. https://doi.org/10.1016/j.scitotenv.2010.01.060

Bartkowska, I., Biedka, P., Tałałaj, I.A., 2019. Analysis of the quality of stabilized municipal sewage sludge. J Ecol Eng 20, 200–208. https://doi.org/10.12911/22998993/99306

Battistel, D., Piazza, R., Argiriadis, E., Marchiori, E., Radaelli, M., Barbante, C., 2015. GC-MS method for determining faecal sterols as biomarkers of human and pastoral animal presence in freshwater sediments. Anal Bioanal Chem 407, 8505–8514. https://doi.org/10.1007/s00216-015-8998-2

Behmer, S.T., Nes, W.D., 2003. Insect sterol nutrition and physiology: A global overview, in: Advances in Insect Physiology. Elsevier, pp. 1–72. https://doi.org/10.1016/S0065-2806(03)31001-X

Birk, J.J., Teixeira, W.G., Neves, E.G., Glaser, B., 2011. Faeces deposition on Amazonian Anthrosols as assessed from 5β-stanols. J Archaeol Sci 38, 1209–1220. https://doi.org/10.1016/j.jas.2010.12.015

Boës, X., Rydberg, J., Martinez-Cortizas, A., Bindler, R., Renberg, I., 2011. Evaluation of conservative lithogenic elements (Ti, Zr, Al, and Rb) to study anthropogenic element enrichments in lake sediments. J Paleolimnol 46, 75–87. https://doi.org/10.1007/s10933-011-9515-z

Brimble, S.K., Foster, K.L., Mallory, M.L., Macdonald, R.W., Smol, J.P., Blais, J.M., 2009. High Arctic ponds receiving biotransported nutrients from a nearby seabird colony are also subject to potentially toxic loadings of arsenic, cadmium, and zinc. Environ Toxicol Chem 28, 2426–2433. https://doi.org/10.1897/09-235.1

Bueno, C., Brugnoli, E., Bergamino, L., Muniz, P., García-Rodríguez, F., Figueira, R., 2018a. Anthropogenic and natural variability in the composition of sedimentary organic matter of the urbanised coastal zone of Montevideo (Río de la Plata). Mar Pollut Bull 126, 197–203. https://doi.org/10.1016/j.marpolbul.2017.11.009

Bueno, C., Kandratavicius, N., Venturini, N., Figueira, R.C.L., Pérez, L., Iglesias, K., Brugnoli, E., 2018b. An evaluation of trace metal concentration in terrestrial and aquatic environments near Artigas Antarctic Scientific Base (King George Island, Maritime Antarctica). Water Air Soil Poll 229, 398. https://doi.org/10.1007/s11270-018-4045-1

Bull, I.D., Elhmmali, M.M., Roberts, D.J., Evershed, R.P., 2003. The application of steroidal biomarkers to track the abandonment of a Roman wastewater course at the Agora (Athens, Greece). Archaeometry 45, 149–161. https://doi.org/10.1111/1475-4754.00101

Bull, I.D., Lockheart, M.J., Elhmmali, M.M., Roberts, D.J., Evershed, R.P., 2002. The origin of faeces by means of biomarker detection. Environ Int 27, 647–654. https://doi.org/10.1016/S0160-4120(01)00124-6

Cabral, A.C., Wilhelm, M.M., Figueira, R.C.L., Martins, C.C., 2019. Tracking the historical sewage input in South American subtropical estuarine systems based on faecal sterols and bulk organic matter stable isotopes ($\delta^{13}C$ and $\delta^{15}N$). Sci Total Environ 655, 855–864. https://doi.org/10.1016/j.scitotenv.2018.11.150

Carreira, R.S., Wagener, A.L.R., Readman, J.W., 2004. Sterols as markers of sewage contamination in a tropical urban estuary (Guanabara Bay, Brazil): space–time variations. Estuar Coast Mar Sci 60, 587–598. https://doi.org/10.1016/j.ecss.2004.02.014

Cheng, W., Sun, L., Kimpe, L.E., Mallory, M.L., Smol, J.P., Gallant, L.R., Li, J., Blais, J.M., 2016. Sterols and stanols preserved in pond sediments track seabird biovectors in a High Arctic environment. Environ Sci Technol 50, 9351–9360. https://doi.org/10.1021/acs.est.6b02767

Choy, E.S., Gauthier, M., Mallory, M.L., Smol, J.P., Douglas, M.S.V., Lean, D., Blais, J.M., 2010. An isotopic investigation of mercury accumulation in terrestrial food webs adjacent to an Arctic seabird colony. Sci Total Environ 408, 1858–1867. https://doi.org/10.1016/j.scitotenv.2010.01.014

Cole, M.L., Valiela, I., Kroeger, K.D., Tomasky, G.L., Cebrian, J., Wigand, C., McKinney, R.A., Grady, S.P., 2004. Assessment of a $\delta^{15}N$ isotopic method to indicate anthropogenic eutrophication in aquatic ecosystems. J Environ Qual 33, 124–132.

Dauvalter, V.A., Kashulin, N.A., 2018. Assessment of the ecological state of the Arctic freshwater system based on concentrations of heavy metals in the bottom sediments. Geochem Int 56, 842–856. https://doi.org/10.1134/S0016702918080037

Douglas, M.S.V., Smol, J.P., 2000. Eutrophication and recovery in the High Arctic: Meretta Lake (Cornwallis Island, Nunavut, Canada) revisited. Hydrobiologia 431, 193–204.

Evenset, A., Christensen, G.N., Carroll, J., Zaborska, A., Berger, U., Herzke, D., Gregor, D., 2007. Historical trends in persistent organic pollutants and metals recorded in sediment from Lake Ellasjøen, Bjørnøya, Norwegian Arctic. Environ Pollut 146, 196–205. https://doi.org/10.1016/j.envpol.2006.04.038

Glew, J.R., 1988. A portable extruding device for close interval sectioning of unconsolidated core samples. J Paleolimnol 1, 235–239.

Hatcher, P.G., McGillivary, P.A., 1979. Sewage contamination in the New York Bight. Coprostanol as an indicator. Environ Sci Technol 13, 1225–1229. https://doi.org/10.1021/es60158a015

Kalff, J., Welch, H.E., 1974. Phytoplankton production in Char Lake, a natural polar lake, and in Meretta Lake, a polluted polar lake, Cornwallis Island, Northwest Territories. J Fish Res Board Can 31, 621–636. https://doi.org/10.1139/f74-094

Karthikeyan, P., Vennila, G., Venkatachalapathy, R., Subramani, T., Prakash, R., Aswini, M.K., 2018. Assessment of heavy metals in the surface sediments of the Emerald Lake using of spatial distribution and multivariate techniques. Environ Monit Assess 190, 668. https://doi.org/10.1007/s10661-018-7037-0

Last, W.M., Smol, J.P., 2001. Physical and geochemical methods, in: Tracking Environmental Changes Using Lake Sediments. Kluwer Academic Publishers, Dordrecht, The Netherlands.

Leeming, R., Ball, A., Ashbolt, N., Nichols, P., 1996. Using faecal sterols from humans and animals to distinguish faecal pollution in receiving waters. Wat Res 30, 2893–2900.
Leeming, R., Bate, N., Hewlett, R., Nichols, P.D., 1998. Discriminating faecal pollution: a case study of stormwater entering Port Phillip Bay, Australia. Wat Sci Tech 38, 15–22.
Leeming, R., Latham, V., Rayner, M., Nichols, P., 1997. Detecting and distinguishing sources of sewage pollution in Australian inland and coastal waters and sediments, in: Eganhouse, R.P. (Ed.), Molecular Markers in Environmental Geochemistry. American Chemical Society, Washington, DC, pp. 306–319. https://doi.org/10.1021/bk-1997-0671.ch020
Leeming, R., Stark, J.S., Smith, J.J., 2015. Novel use of faecal sterols to assess human faecal contamination in Antarctica: a likelihood assessment matrix for environmental monitoring. Antarct Sci 27, 31–43. https://doi.org/10.1017/S0954102014000273
McCalley, D.V., Cooke, M., Nickless, G., 1981. Effect of sewage treatment on faecal sterols. Water Res 15, 1019–1025. https://doi.org/10.1016/0043-1354(81)90211-6
Michelutti, N., Douglas, M.S.V., Smol, J.P., 2003. Diatom response to recent climatic change in a high arctic lake (Char Lake, Cornwallis Island, Nunavut). Global and Planetary Change 38, 257–271. https://doi.org/10.1016/S0921-8181(02)00260-6
Michelutti, N., Douglas, M.S.V., Smol, J.P., 2002. Tracking recent recovery from eutrophication in a high arctic lake (Meretta Lake, Cornwallis Island, Nunavut, Canada) using fossil diatom assemblages. J Paleolimnol 28, 377–381.
Michelutti, N., Hermanson, M.H., Smol, J.P., Dillon, P.J., Douglas, M.S.V., 2007. Delayed response of diatom assemblages to sewage inputs in an Arctic lake. Aquat Sci 69, 523–533. https://doi.org/10.1007/s00027-007-0928-8
Mouritsen, O.G., Bagatolli, L.A., Duelund, L., Garvik, O., Ipsen, J.H., Simonsen, A.C., 2017. Effects of seaweed sterols fucosterol and desmosterol on lipid membranes. Chem Phys Lipids 205, 1–10. https://doi.org/10.1016/j.chemphyslip.2017.03.010
Nishimura, M., 1978. Geochemical characteristics of the high reduction zone of stenols in Suwa sediments and the environmental factors controlling the conversion of stenols into stanols. Geochim Cosmochim Acta 42, 349–357. https://doi.org/10.1016/0016-7037(78)90265-X
Nishimura, M., Koyama, T., 1977. The occurrence of stanols in various living organisms and the behavior of sterols in contemporary sediments. Geochim Cosmochim Acta 41, 379–385. https://doi.org/10.1016/0016-7037(77)90265-4
Pan, F., Liu, H., Guo, Z., Cai, Y., Fu, Y., Wu, J., Wang, B., Gao, A., 2019. Metal/metalloid and phosphorus characteristics in porewater associated with manganese geochemistry: A case study in the Jiulong River Estuary, China. Environ Pollut 255, 113134. https://doi.org/10.1016/j.envpol.2019.113134
Patterson, G.W., 1994. Phylogenetic distribution of sterols, in: Nes, W.D. (Ed.), Isopentenoids and Other Natural Products. American Chemical Society, Washington, DC, pp. 90–108. https://doi.org/10.1021/bk-1994-0562.ch005
Pereira, C.M.P., Nunes, C.F.P., Zambotti-Villela, L., Streit, N.M., Dias, D., Pinto, E., Gomes, C.B., Colepicolo, P., 2017. Extraction of sterols in brown macroalgae from Antarctica and their identification by liquid chromatography coupled with tandem mass spectrometry. J Appl Phycol 29, 751–757. https://doi.org/10.1007/s10811-016-0905-5
Prost, K., Birk, J.J., Lehndorff, E., Gerlach, R., Amelung, W., 2017. Steroid biomarkers revisited – Improved source identification of faecal remains in archaeological soil material. PLoS One 12, e0164882. https://doi.org/10.1371/journal.pone.0164882

Ranjan, R.K., Routh, J., Val Klump, J., Ramanathan, Al., 2015. Sediment biomarker profiles trace organic matter input in the Pichavaram mangrove complex, southeastern India. Mar Chem 171, 44–57. https://doi.org/10.1016/j.marchem.2015.02.001

Sánez, J., Froehner, S., Hansel, F., Parron, L., Knapik, H., Fernandes, C., Rizzi, J., 2017. Bile acids combined with fecal sterols: a multiple biomarker approach for deciphering fecal pollution using river sediments. J Soils Sediments 17, 861–872. https://doi.org/10.1007/s11368-016-1592-1

Santos, I.R., Silva-Filho, E.V., Schaefer, C.E.G.R., Albuquerque-Filho, M.R., Campos, L.S., 2005. Heavy metal contamination in coastal sediments and soils near the Brazilian Antarctic Station, King George Island. Marine Pollution Bulletin 50, 185–194. https://doi.org/10.1016/j.marpolbul.2004.10.009

Schindler, D.W., Kalff, J., Welch, H.E., Brunskill, G.J., Kling, H., Kritsch, N., 1974. Eutrophication in the High Arctic — Meretta Lake, Cornwallis Island (75° N Lat.). J Fish Res Board Can 31, 647–662. https://doi.org/10.1139/f74-096

Shah, V.G., Dunstan, R.H., Geary, P.M., Coombes, P., Roberts, T.K., Von Nagy-Felsobuki, E., 2007. Evaluating potential applications of faecal sterols in distinguishing sources of faecal contamination from mixed faecal samples. Water Res 41, 3691–3700. https://doi.org/10.1016/j.watres.2007.04.006

Skrzypek, G., Paul, D., Wojtuń, B., 2008. Stable isotope composition of plants and peat from Arctic mire and geothermal area in Iceland. Pol Polar Res 29, 365–376.

Smol, J.P., Douglas, M.S., 2007. From controversy to consensus: making the case for recent climate change in the Arctic using lake sediments. Front Ecol Environ 5, 466–474. https://doi.org/10.1890/060162

Stewart, E.M., Hargan, K.E., Sivarajah, B., Kimpe, L.E., Blais, J.M., Smol, J.P., 2018. A paleoenvironmental study tracking eutrophication, mining pollution, and climate change in Niven Lake, the first sewage lagoon of Yellowknife (Northwest Territories). Arctic 71, 201–217. https://doi.org/10.14430/arctic4720

Stewart, E.M., McIver, R., Michelutti, N., Douglas, M.S.V., Smol, J.P., 2014. Assessing the efficacy of chironomid and diatom assemblages in tracking eutrophication in High Arctic sewage ponds. Hydrobiologia 721, 251–268. https://doi.org/10.1007/s10750-013-1667-6

Tort, L.F.L., Iglesias, K., Bueno, C., Lizasoain, A., Salvo, M., Cristina, J., Kandratavicius, N., Pérez, L., Figueira, R., Bícego, M.C., Taniguchi, S., Venturini, N., Brugnoli, E., Colina, R., Victoria, M., 2017. Wastewater contamination in Antarctic melt-water streams evidenced by virological and organic molecular markers. Sci Total Environ 609, 225–231. https://doi.org/10.1016/j.scitotenv.2017.07.127

Tse, T.J., Codling, G., Jones, P.D., Thoms, K., Liber, K., Giesy, J.P., Wheater, H., Doig, L.E., 2014. Reconstructing long-term trends in municipal sewage discharge into a small lake in northern Manitoba, Canada. Chemosphere 103, 299–305. https://doi.org/10.1016/j.chemosphere.2013.12.019

Vane, C.H., Kim, A.W., McGowan, S., Leng, M.J., Heaton, T.H.E., Kendrick, C.P., Coombs, P., Yang, H., Swann, G.E.A., 2010. Sedimentary records of sewage pollution using faecal markers in contrasting peri-urban shallow lakes. Sci Total Environ 409, 345–356. https://doi.org/10.1016/j.scitotenv.2010.09.033

Vivian, C.M.G., 1986. Tracers of sewage sludge in the marine environment: A review. Sci Total Environ 53, 5–40. https://doi.org/10.1016/0048-9697(86)90091-4

Walker, R.W., Wun, C.K., Litsky, W., Dutka, B.J., 1982. Coprostanol as an indicator of fecal pollution. C R C Crit Rev Environ Control 12, 91–112. https://doi.org/10.1080/10643388209381695

Wang, Z., Lu, X., Zhang, K., 2016. Distribution and contamination of metals and biogenic elements in sediments from Zhifu Bay of the Yellow Sea, China. J Environ Sci 41, 6–15. https://doi.org/10.1016/j.jes.2015.06.009

Zibulski, R., Wesener, F., Wilkes, H., Plessen, B., Pestryakova, L.A., Herzschuh, U., 2017. C/N ratio, stable isotope ($\delta^{13}C$, $\delta^{15}N$), and n-alkane patterns of brown mosses along hydrological gradients of low-centred polygons of the Siberian Arctic. Biogeosciences 14, 1617–1630. https://doi.org/10.5194/bg-14-1617-2017

Zocatelli, R., Lavrieux, M., Guillemot, T., Chassiot, L., Le Milbeau, C., Jacob, J., 2017. Fecal biomarker imprints as indicators of past human land uses: Source distinction and preservation potential in archaeological and natural archives. J Archaeol Sci 81, 79–89. https://doi.org/10.1016/j.jas.2017.03.010

Chapter 3: Human-derived sterols and stanols track Thule and Dorset occupation in Canadian High Arctic pond sediment cores

Gallant, Lauren R[a]; Hargan, Kathryn E[b]; Kimpe, Linda E[a]; Michelutti, Neal[c]; Grooms, Christopher[c]; Smol, John P[c]; and Blais, Jules M[a]

[a] Department of Biology, University of Ottawa, Ottawa, ON, K1N 6N5, Canada

[b] Department of Biology, Memorial University of Newfoundland, St. John's, NL A1B 3X9, Canada

[c] Paleoecological Environmental Assessment and Research Lab (PEARL), Department of Biology, Queen's University, Kingston, ON, K7L 3N6, Canada

This manuscript is being prepared for submission to PNAS.

Statement of author contributions:

Gallant, Lauren R: study design, sample collection, lab work, data analysis and interpretation, and manuscript preparation. Hargan, Kathryn E: study design, lab work, data analysis and interpretation, and peer review. Kimpe, Linda E: sample collection and data analysis and interpretation. Michelutti, Neal: lab work, data analysis and interpretation, and peer review. Grooms, Christopher: sample collection, lab work, data analysis and interpretation, and peer review. Smol, John P: sample collection and peer review. Blais, Jules M: study design, sample collection, data analysis and interpretation, manuscript preparation, and peer review.

Keywords: metals, stable isotopes, whalebones

Abstract

The High Arctic was home to many previous cultures including both the Dorset people (as early as ca. 550 BCE until ca. 1250 CE) and the Thule people (from ca. 1000 to 1600 CE). Here, we used paleolimnological biomarkers in pond sediments to track Thule and Dorset occupation at archeological sites in Canada's High Arctic. The Thule people were nomadic whalers who built over-wintering houses framed by whalebones on coastlines throughout the Arctic. We compared two Thule/Dorset influenced ponds and two reference ponds without evidence of human occupation, and observed pronounced changes in sterols, stanols, metals, and stable isotopes of carbon and nitrogen in the sediments from Thule/Dorset occupied sites that corresponded to the timing of human occupation. Coprostanol and epicoprostanol, the major stanols in human faeces, consistently increased in sediments adjacent to Thule settlements in ca. 1000 CE, coeval with the timing of Thule occupation. Sitosterol and stigmastanol increased in association with human occupation in one of the Thule/Dorset-influenced ponds, PaJs 3N, while concentrations were undetectable in the other influenced pond, PaJs 13; there was no evidence of nearby human occupation in either reference pond. In PaJs 3N, sterol and stanol concentrations and $\delta^{15}N$ values increased in pre-Thule influenced sediments, coincident with the arrival of the Dorset people in ca. 500 CE. In PaJs 13, $\delta^{15}N$ values and cholestanol and coprostanol concentrations increased prior to Thule occupation, which suggested Dorset occupation. We also compared metal ratios (metals normalized to titanium) in sediments from PaJs 13 to sediments from the reference ponds. Cadmium, copper, and zinc ratios increased in sediments from PaJs 13 during the time of Thule occupation, whereas metal ratios were low and stable in the reference

ponds. Our results demonstrated the strength of using multiple proxies to reconstruct the presence and timing of human influence on High Arctic ponds with potential future applications for archeological investigations of pre-historic Arctic peoples.

1 Introduction

Sediment cores from High Arctic ponds may be well-suited to tracking past human occupation. One prime example is the presence of the Thule people in Canada's High Arctic ~1000 years ago (1–4). The Thule people were a group of nomadic whalers who arrived *via* the Bering Strait; recent studies suggested the Thule people then left their over-wintering homes ~500 years ago for better trading opportunities (5). The Thule specialized in hunting bowhead whales; one report estimated that the Thule people hunted ~18,523 whales over 300 years across Greenland and the Canadian Arctic (5). The whalebones were used to build both over-wintering structures, such as permanent and semi-permanent homes, as well as work-related structures, such as temporary whaling camps and kayak stands (5–7). The Thule camps and settlements are still visible today. Whalebones and house foundations are often observed near High Arctic ponds where the Thule would have derived their drinking water. To date, much of the research on the first inhabitants in the High Arctic were derived from archaeological studies. For example, the number and type of Thule homes has been extensively studied at several sites (2, 4, 5). Whalebones have been ^{14}C dated and the number of whalebones required for each home has been calculated (8, 9). Weapons, pots, and other tools have been ^{14}C dated and their cultural history identified (10). These findings provided the foundation for this study, where we aimed to look at the chemical composition of pond sediments through the historical record and determine to what extent we can observe evidence of historical occupation of these High Arctic ponds using a multi-proxy paleolimnology approach. These ponds have elevated nutrients relative to reference ponds lacking evidence of human habitation and even today are still surrounded by moss and plant substrates (11). We hypothesized that the history of human habitation may be recorded by the sterol and stanol composition in dated pond sediments.

While the Thule people left archeological evidence (primarily in the form of whalebone structures) of their occupation in the High Arctic, they were not always the first to live at these High Arctic sites. The Dorset people were present in the High Arctic as early as 550 BCE to 50 BCE and were present until 750 CE to 1250 CE (12). While there is no evidence that the Thule and Dorset ever met, nor that they are genetically connected, the Thule people did inhabit some of the same locations as the Dorset (13).

$\delta^{15}N$ profiles in pond sediments are commonly employed to track nitrogen sources from higher trophic level species, because carnivorous species, such as humans, are enriched in ^{15}N relative to ^{14}N. For example, $\delta^{15}N$ values in pond sediments from Thule-occupied sites increased at the time of their arrival (11). The presence of the Thule people and nutrients from whale carcasses also increased primary production in ponds, as evidenced by a shift to more eutrophic diatom species and an increase in sedimentary chlorophyll *a* (chl *a*) during the time of Thule occupation (11). $\delta^{13}C$ can also be used to infer human occupation in High Arctic ponds as $\delta^{13}C$ values can reflect productivity and the contribution of organic carbon by vegetation in the nearby catchment. For example, $\delta^{13}C$ values decreased in High Arctic lake sediments following wastewater input as a result of increased phytoplankton productivity (14).

Sterols and stanols are more source specific than stable isotopes and may thus more reliably track human influence on pond sediments. Zoosterols (animal-derived) and phytosterols (plant-derived) are relatively stable in cold and anaerobic environments (15, 16), and consequently fluctuations in zoosterols and phytosterols in lake sediments may be observed as a result of human occupation, particularly in an otherwise barren and oligotrophic setting like an Arctic coastline environment. For example, cholesterol, found in all mammals, increased in High Arctic lake sediments as a result of wastewater input (15, 17). Coprostanol, produced from

cholesterol in the guts of higher organisms, is elevated in human faeces (18), and is often much higher in wastewater-influenced lake sediments compared to reference lake sediments not receiving wastewater (19–22). By contrast, sitosterol is a phytosterol found in terrestrial and aquatic plants as well as phytoplankton (17, 23, 24) and consequently, sitosterol in lake sediments may track changes in allochthonous and/or autochthonous primary production (15).

The objective of this study was to reconstruct human occupation in Canada's High Arctic by examining the chemical and biological markers preserved in dated pond sediments. Specifically, we employed a multi-proxy approach, where we analyzed pond sediments for sterols, stanols, stable isotopes ($\delta^{15}N$, $\delta^{13}C$), metals, and chl *a*. This multi-proxy approach showed evidence of the timing of human occupation at these sites based on multiple lines of evidence in dated pond sediments.

2 Site descriptions

PaJs 13 (Fig S3.1) and PaJs 3N (Fig S3.2) are archaeological sites of significant Thule presence as evidenced by the high number of whalebone houses in the vicinity of the ponds (5). Nine houses at each site were constructed using heavier bones, suggesting long-term occupation of these sites (5). At PaJs 3N, moss and whalebones were present in the area immediately surrounding the pond, and the remainder of the landscape was barren rock, while at PaJs 13 vegetation and whalebones were present in a much larger radius surrounding the pond.

Reference sites, Sav R4 and Sav R5, (Fig 3.1) were selected based on their proximity to the archaeological sites, but with the absence of human-made structures and whalebones in the vicinity of the ponds. Detailed site information (latitudes, longitudes, surface area, and height above sea level) are presented in Table S3.1.

3 Methods

3.1 Periphyton and zooplankton

We collected near-shore periphyton and zooplankton samples and stored them at 4°C. We sieved (125 μm) and filtered periphyton samples through a 110 mm Whatman glass microfiber filter (GF/F) (42.5 mm, 0.7 μm; pre-heated for 3 hours at 400°C). The periphyton and filters were air-dried and homogenized prior to further analysis. Surface water samples were collected near-shore in pre-rinsed (10 % HNO_3 for total metals and 10 % H_2SO_4 for total phosphorous, total dissolved phosphorous, total dissolved nitrogen, dissolved organic carbon, and dissolved inorganic carbon) Nalgene bottles. Water samples for dissolved organic carbon were filtered (Sartorius acetate filter, 47 mm, 0.45 μm) and stored at 4°C; water samples for particulate organic carbon were filtered (Whatman GF/F, 47 mm, 0.45 μm) and frozen until analysis. The National Laboratory for Environmental Testing, Burlington, Ontario, Canada, conducted all water chemistry analyses.

3.2 Sediment cores

We collected sediment cores from the centre of each pond by pushing a 3-inch tube into the sediments; sediments were subsequently sectioned into 0.5 cm intervals using a Glew extruder (25) and frozen at -4°C. ^{210}Pb dates were determined using an Ortec High Purity Germanium Gamma Spectrometer (Oak Ridge, TN, USA) at the University of Ottawa. Efficiency corrections were made using Certified Reference Materials from International Atomic Energy Association (Vienna, Austria). We constructed ^{210}Pb and ^{137}Cs profiles using the constant rate of supply (CRS) model (26) (ScienTissiMe; Barry's Bay, Ontario, Canada).

Sediments pre- and post- 1950, as determined by ^{210}Pb dating, were ^{14}C dated. 1-3 mg organic carbon (OC) of freeze-dried material was weighed into culture tubes. Anthracite and To-

12586 were used as standards for background and 2910 BP ± 50, respectively. We submerged the samples in 5 mL of 1N HCl for 30 minutes in a metal bead bath set to 80°C, removed the HCl, added 5 mL milli-Q water, centrifuged the samples for three minutes at 2700 rpm, removed the water, and freeze-dried the material. Samples were analyzed on a 3MV tandem accelerator mass spectrometer (High Voltage Engineering) at the University of Ottawa. Dates were calibrated using OxCal v4.3 (27) and are reported according to the conventions outlined by Millard (28).

3.3 Stable isotopes

We analyzed acidified freeze-dried pond sediments for organic $\delta^{13}C$ (‰ Vienna Pee Dee Belemnite), hereafter, referred to as $\delta^{13}C$, and unacidified pond sediments for $\delta^{15}N$ (‰ air), following the methodology outlined in Gallant et al. 2020 (under review) (17). Analyses were conducted using a Micro Cube elemental analyzer (analytical precision: ± 0.2 ‰ using glutamic acid) at the Ján Veizer Stable Isotope Laboratory (formerly G.G. Hatch SIL Laboratory), located at the University of Ottawa, Ontario, Canada. We also analyzed acidified periphyton for $\delta^{13}C$ and unacidified periphyton for $\delta^{15}N$. Owing to low sample volume, we analyzed unacidified zooplankton for $\delta^{13}C$ and $\delta^{15}N$ in a single run.

3.4 Metals

We analyzed select pond sediments for metals using 0.5 g dry weight (dw) of sediment. The analysis was conducted using inductively coupled plasma mass spectrometry (prepared using an aqua regia digestion) at SGS Minerals Services, Lakefield ON, Canada; a lab accredited by The Canadian Association for Laboratory Accreditation Inc. Metal concentrations below the method detection limit (MDL) were replaced with MDL/√2 and then normalized to the

concentration of titanium in order to account for natural weathering (29). Summary metal concentrations are presented in Table S3.2.

3.5 Sterols and stanols

We analyzed the pond sediments for sterols and stanols in accordance with the methodology outlined in Gallant et al. 2020 (under review) (17). Briefly, 0.1 g of freeze-dried sediments was extracted in dichloromethane (high-grade, Optima® brand) and separated using a 1 g LC-Si SPE column (Sigma-Aldrich, Oakville, ON, Canada). 100 µL of sample was evaporated to dry, reconstituted in 100 µL of 99 % N,O-bis(trimethylsilyl)trifluoroacetamide) + 1 % trimethylchlorosilane (BSTFA + TMSCl), and heated for two hours at 60°C . 900 µL of toluene (high-grade, Optima® brand) and 10 µL, 10,000 ng mL^{-1} of p-terphenyl-d_{14} (Cambridge Isotope Laboratories, Tewksbury, MA, USA) were added to the sample. Samples were analyzed using an Agilent 6890 gas chromatograph – 5973 mass selective detector in electron impact, selected ion monitoring mode (Agilent 19091J-433 HP-5 5 % phenyl methyl siloxane 29.8 m x 250 µm x 0.25 µm column). Sterol concentrations were volume corrected to p-terphenyl-d_{14} using MSD ChemStation D.02.00.275. Additional dilutions were analyzed, as required. The limit of quantification was set to a signal to noise ratio of three. All data analyses was conducted with R statistical computing environment (v3.5.2). Samples were recovery corrected to d6 cholesterol (Table S3.3). Sterol and stanol concentrations below the limit of detection were corrected to MDL/√2 (Table S3.4); values were previously reported in Gallant et al. 2020, under review (17). Sterol and stanol concentrations are presented in Table S3.5.

4 Results

4.1 Dating profiles

In PaJs 13, ^{210}Pb activity reached background at 7.75 cm and peak ^{137}Cs activity occurred at 4.75 cm, closely matching the ^{210}Pb date of 1964 (Fig S3.3). There is a 640-year difference in the ^{210}Pb date (1924) and ^{14}C date (1284) at 6.25 cm; consequently, we applied a reservoir effect correction of 640 years to all ^{14}C dates. As a result, we achieved a ^{14}C date of 134 BCE in pond sediments at 22.25 cm (Fig S3.4). In PaJs 3N, ^{210}Pb activity reached background at 15.75 cm and peak ^{137}Cs activity occurred at 7.75 cm, which closely matched the ^{210}Pb date of 1961 at 8.75 cm. There is a 453-year difference in the ^{210}Pb (1868 CE) and ^{14}C (1415 CE) date at 13.25 cm and thus we applied a 453-year reservoir effect correction to all the ^{14}C dates. As a result, we achieved a ^{14}C date of 826 CE at 23.75 cm.

In Sav R4, ^{210}Pb activity reached background at 5.75 cm; peak ^{137}Cs activity (80.4 Bq kg^{-1}) occurred at 1.75 cm and had a notable drop at 4.8 cm to 4.5 Bq kg^{-1}. ^{210}Pb dating placed 1963 at 3.75 cm. There is a 655-year difference in the ^{210}Pb date (1905) and ^{14}C date (1250) at 5.25 cm, so we applied a 655-year reservoir effect correction to all of the ^{14}C dates to the Sav R4 core. In Sav R5, ^{210}Pb activity reached background at 4.75 cm and peak ^{137}Cs activity occurred at 1.75 cm (13.5 ± 1.5 Bq kg^{-1}), which supported the ^{210}Pb date at 1.75 cm of 1978. There is a 1,748-year difference in the ^{210}Pb (1829 CE) and ^{14}C age (82 CE) of sediments deposited at 4.75 cm and as such, we applied a 1,748-year-reservior effect. Consequently, sediments reached a maximum age of 868 BCE (at 15.25 cm) in Sav R5.

The reservoir effect corrections that we applied to these pond sediments were generally in the same range as the corrections applied to marine shells (740 years) and bowhead whalebones (400 years) from the same region (Gulf of Boothia) (13). Notably, corrections > 400 years were

also required for bowhead whalebone samples (30); this may be attributed to long ^{14}C residency times in oceans, which can reach up to 2000 years in deep waterbodies (31). Reservoir effect corrections are not specific to Arctic samples; reservoir effect corrections ranging from 200 to 600 years have been applied to lake sediments from South America (32,33) and elsewhere.

4.2 Sterols and stanols

In PaJs 3N, background concentrations of all the sterols were detectable, and comparable to concentrations recorded in sediments deposited between ca. 1000 CE and ca. 1500 CE (Fig 3.2). The concentration of coprostanol, cholestanol, epicoprostanol, and campesterol increased in the influenced pond, PaJs 13 ca. 1200 CE (Fig 3.3). Notably, coprostanol and epicoprostanol peaked between ca. 1000 and ca. 1500 CE, while the concentrations of cholestanol and campesterol continued to increase into present day sediments. The concentration of cholesterol did not increase until after ca. 1800 CE, and interestingly, the phytosterols, sitosterol and stigmastanol, were not detectable throughout the sediment core.

When compared to the reference ponds, the concentration of sterols in the reference ponds was nearly always lower than the influenced ponds; the only exception was the concentration of cholesterol in Sav R4 in 2016 (14.6 μg g^{-1} dw) relative to that in PaJs 13 (maximum: 14.3 μg g^{-1} dw in 2016). In Sav R5, the only sterols to exceed their MDLs were coprostanol and epicoprostanol, whereas in Sav R4, campesterol, cholesterol, coprostanol, and epicoprostanol exceeded their MDLs.

4.3 Metals

We analyzed sediments from one influenced pond, PaJs 13, and sediments from the reference ponds, Sav R4 and Sav R5, for metals (Fig 3.4). The concentration of each metal was normalized to the concentration of titanium in each sample in order to account for natural

weathering. Cadmium, copper, lead, and zinc-titanium ratios in PaJs 13 were generally low prior to ca. 1000 CE and increased thereafter, peaking in the most recently deposited sediments at 0.001, 60, 0.02, and 0.16, respectively. By contrast, metal ratios to titanium were generally stable throughout the sediment cores from both reference ponds. We then examined metal enrichment factors (EFs) in order to determine the extent to which human activity influenced the metal composition in sediments (Table S3.6). Background metal concentrations were determined using sediments deposited pre-Thule and pre-Dorset; two sediment intervals met this criterion: Sav R5, 14.25 cm (520 BCE) and 15.25 cm (870 BCE) (Table S3.6). We divided metal ratios deposited during the time of Thule occupation by background metal ratios to determine sediment metal ratio EFs ($sediment_{EF\_Ti}$): cadmium (4.0), copper (1.7), lead (2.8), and zinc (1.2). We also compared metal concentrations in whale livers to background metal concentrations in sediments to determine which metal would be most affected by an external source of whale flesh. We divided previously reported whale liver metal concentrations (μg g^{-1} dw): cadmium (31), copper (20), lead (0.1), and zinc (140) (34, 35) by background metal concentrations to determine liver metal EFs ($liver_{EF}$): cadmium (3100), copper (1.4), lead (0.07), and zinc (8.2). Titanium concentrations in whale livers were not reported and thus we calculated sediment metal concentration EFs ($sediment_{EF}$) in order to compare $liver_{EF}$ to sediment data. We divided metal concentrations in Thule-influenced sediments by background metal concentrations to determine $sediment_{EF}$: cadmium (12), copper (2.6), lead (4.3), and zinc (1.9).

4.4 Periphyton and zooplankton

Sterol concentrations in the periphyton and zooplankton were MDL corrected. In all instances, the maximum sterol concentration (ng g^{-1} OC dw) in periphyton was below the minimum concentration in zooplankton (Fig 3.5). Cholesterol was the only sterol detected in

periphyton from both reference ponds; fucosterol was only detected in low concentrations (0.15 ng g^{-1} dw) in Sav R4. In Sav R5, there was insufficient zooplankton to analyze for sterols. Zooplankton from Sav R4 were more concentrated in campesterol, cholestanol, coprostanol, epicoprostanol, fucosterol, sitosterol, and stigmastanol than PaJs 3N and PaJs 13 (Fig 3.5). With the exception of fucosterol, the minimum sterol concentration in sediments from PaJs 3N was always greater than the maximum sterol concentration in zooplankton and periphyton. Peak concentrations of campesterol, cholestanol, and cholesterol in influenced pond sediments exceeded the concentrations in zooplankton and periphyton.

4.5 Percent composition and stable isotopes

OC increased in PaJs 3N prior to ca. 1200 CE and remained elevated into present day deposited sediments; in general, OC was high, ranging from 40.7 to 56.9 %. In PaJs 13, OC increased notably in ca. 1800 CE; the range in OC was also much greater than that observed in PaJs 3N, with OC values ranging from 2.55 to 36.4 %. In the reference ponds, Sav R4 (0.49 to 32.1 %) and Sav R5 (0.30 to 2.23 %), OC was generally much lower than observed in the influenced ponds.

In PaJs 3N, $\delta^{15}N$ increased in ca. 1100 CE and decreased in ca. 1800 CE, while in PaJs 13, $\delta^{15}N$ was relatively stable until it decreased in ca. 1800 CE. $\delta^{15}N$ values were low in the reference ponds, never exceeding 3.51 ‰, versus the influenced ponds, where $\delta^{15}N$ values reached a maximum of 6.38 ‰ and 6.77 ‰ in PaJs 3N and PaJs 13, respectively.

In PaJs 3N, $\delta^{13}C$ increased from values generally below -17 ‰ to values ranging from -16.4 to -14.1 ‰ after ca. 1200 CE. In PaJs 13, $\delta^{15}N$ remained relatively constant before decreasing in sediments deposited post-1800 CE; notably, $\delta^{13}C$ values then increased again in the most recently deposited sediments. $\delta^{13}C$ values in both reference ponds were stable through time,

ranging from -28.4 to -24.5 ‰ in Sav R4 and from -26.8 to -24.1 ‰ in Sav R5. Summary stable isotope data are presented in Table S3.7.

4.6 Chlorophyll a

Trends in inferred Chl *a* increased in ca. 1100 CE, just prior to the archaeological evidence suggesting Thule occupation, and remained elevated until ca. 1890s CE; Chl *a* then peaked in 21^{sh} century deposited sediments (Fig 3.6).

5 Discussion

Ponds previously occupied by the Thule people are easily identifiable by the presence of whalebones in and around the ponds, as well as the presence of the whalebone homes themselves. Dorset tent rings were previously observed at PaJs 13 (13), which is in close proximity to PaJs 3N, and thus we hypothesized that marked changes in the chemical composition of sediments would also reflect Dorset-occupation at these sites. Our aim was to determine whether we could reconstruct the presence of the Thule and Dorset people at these sites by examining the chemical composition of the pond sediments.

5.1 Tracking the historical presence of humans using sterols and stanols

The best chemical marker for identifying influenced ponds relative to reference ponds appears to be the presence/absence and overall greater concentration of sterols and stanols. For example, the maximum concentration of cholesterol in PaJs 3N was five-times greater than the maximum concentration of cholesterol in either reference pond (Figs 3.2 and 3.3). Campesterol was only detected in one sediment layer of one of the reference ponds (Sav R4), while campesterol was detected throughout the majority of both influenced sediment cores with concentrations often exceeding 1 μg g^{-1} dw. Similarly, cholestanol was not detected in either

reference pond, but was present in nearly all sediment intervals of the influenced ponds. Increased phytosterol concentrations in sediments deposited post-Thule occupation suggested sustained productivity following Thule departure, as evidence by elevated chl *a* concentrations post-Thule (Fig 3.6). Sustained zoosterol and phytosterol concentrations in post-Thule deposited sediments may also have resulted from continued shoreline run-off of faecal matter or moss substrates, thus supplying a continued source of sterols and stanols to the sediments. Low levels of cholesterol (maximum of 14.6 μg g^{-1} dw in Sav R4; not detected in Sav R5), coprostanol (maximum of 0.14 μg g^{-1} dw in Sav R4), and epicoprostanol (maximum of 0.12 μg g^{-1} dw in Sav R4) were detected in reference ponds, however only in sediments deposited during the 20th century. Low concentrations of cholesterol, coprostanol, and epicoprostanol in the surface sediments of Sav R4 likely reflected the small surface organic layer, which may be composed of decaying zooplankton and phytoplankton. Indeed, low cholesterol concentrations were detected within the phytoplankton and zooplankton of Sav R4 (Fig 3.5). The small surface sediment concentrations of coprostanol and epicoprostanol in Sav R4 may be the result of *in situ* degradation of cholesterol (37).

In PaJs 3N, cholesterol, coprostanol, and epicoprostanol were elevated in sediments deposited in ca. 860 CE, and thus prior to Thule occupation (Fig 3.2), suggesting influence from occupation by the Dorset who pre-dated the Thule at this location (13). Indeed, there was evidence of historical occupation in the form of whalebones (^{14}C dated to 965 CE and 825 CE after a 400-year reservoir age was applied) and relative sea level curves, which demonstrated that the sites were elevated above sea level at the time of Dorset occupation (13). Therefore, the elevated concentration of sterols and stanols in ca. 860 CE may have tracked the historical presence of the Late Dorset people (450 CE to 950 CE) (13). The decrease of sterols and stanols

in sediments in 995 CE and the subsequent increase in 1060 CE marks the approximate timing of the transition from Dorset to Thule occupation (13). The sterol and stanol profiles in PaJs 3N suggest the Thule people did indeed arrive in ca. 1000 CE, which aligns with findings of previous studies (1–4). While a more recent date of 1200 CE has been proposed for the arrival of the Thule people (5), our results suggested occupation at PaJs 3N and PaJs 13 prior to this time, as evidenced by increases in $\delta^{15}N$, sterols, stanols, cadmium, and copper in 1000 CE (Figs 3.2 and 3.3), though we cannot ascribe this occupation to Thule or Dorset based on available evidence. The prior occupation of these sites by the Dorset people is further supported by the presence of Dorset winter houses and longhouses in the immediate area (13). $\delta^{15}N$ values do not peak during the time of Dorset occupation because the earliest sediments in this core do not extend back to pre-Dorset occupation (prior to 450 CE) (13).

Sterol concentrations in the PaJs 13 sediment core were generally ten-fold lower than in PaJs 3N (Figs 3.2 and 3.3). Campesterol, cholestanol, coprostanol, and epicoprostanol concentrations increased in sediments deposited during the 11th century, marking the arrival of the Thule to PaJs 13 (Fig 3.3). Coprostanol, cholestanol, and campesterol concentrations increased slightly beginning in ca. 100 BCE, which closely matched the earliest recorded arrival of the Dorset people to the High Arctic in ca. 550 BCE (13). $\delta^{15}N$ values also increased coeval with the early rise in sterols and stanols, and OC values were similar among Thule-influenced and Dorset-influenced sediments. In addition to the presence of Dorset tent rings (13), these independent proxies lend further evidence that PaJs 13 was occupied by the Dorset people prior to the Thule people.

Sitosterol and stigmastanol were not detected within sediments from PaJs 13. The absence of these two sterols was unexpected as the area immediately surrounding PaJs 13 was

rich in vegetation. OC was elevated in PaJs 13 (maximum of 36.4 %), which suggested increased productivity (37) and therefore increased concentrations of sitosterol and stigmastanol. However, OC was also elevated in the reference pond, Sav R4 (maximum of 32.1 %), suggesting that increased OC alone may not be indicative of elevated sterol concentrations. The absence of a strong sterol signal in sediments from PaJs 13 may be attributed to site size: PaJs 13 is a large site, with whalebones spread for tens of meters beyond the perimeter of the pond itself. By comparison, PaJs 3N is a relatively isolated pond where whalebones were concentrated in the immediate area and the perimeter of vegetation surrounding the pond was much smaller than that observed at PaJs 13. We thus proposed that the input of whalebones and human waste into PaJs 13 was diluted over a wide area, resulting in lower concentrations of sterols and stanols in pond sediment, relative to a more focused input into PaJs 3N, resulting in higher concentrations of sterols and stanols in sediment. Sediment chl *a* values fluctuated in concordance with changes in the concentrations of phytosterols, and thus likely tracked primary productivity in the ponds during the period of Thule occupation (Fig 3.6).

5.2 Historical human activity altered the metal composition of pond sediments

Human practices have altered the metal composition in the environment for thousands of years. We thus examined the concentrations of cadmium, copper, lead, and zinc normalized to titanium in the influenced pond, PaJs 13, and the two reference ponds, Sav R4 and Sav R5, (Fig 3.4) to determine if metal concentrations tracked human occupation at PaJs 13. Cadmium (mean ± standard error: 31 ± 5.8 μg g^{-1} dw), copper (20 ± 1.5 μg g^{-1} dw), and zinc (140 ± 8.8 μg g^{-1} dw) were three of the most concentrated metals in bowhead whale livers (34), thus we expected the flensing of bowhead whales in High Arctic ponds to increase these sediment metal concentrations. Indeed, cadmium (4.0), copper (1.7), and zinc (1.2) $sediment_{EF\_Ti}$ were elevated

between 1000 CE and 1500 CE, coinciding with the arrival of the Thule people (Fig 3.4). The lead sediment$_{EF_Ti}$ (2.8) was higher than predicted given the low lead concentrations in both whale livers (0.1 ± 0.06 μg g^{-1} dw) and bone (0.1 to 0.2 μg g^{-1} dw) (35), suggesting that human excrement or atmospherically deposited lead may have also contributed to lead concentrations in sediment. We also examined the liver$_{EF}$ (based on whale liver concentrations), to determine whether we could predict the extent to which whale-derived materials contributed to metal concentrations in sediments. With the exception of cadmium, previously reported biotic EFs for fulmar guano were similar (cadmium: 23, zinc: 4.4, copper: 0.6, and lead: 0.01) (38) to those reported in this study (cadmium: 3100, zinc: 8.2, copper: 1.4, and lead: 0.07) (Table S3.6). We attributed differences in cadmium EFs to very low background cadmium concentrations in Sav R5 (0.01 μg g^{-1} dw) relative to those in the fulmar study (0.37 μg g^{-1} dw) (38). Aside from cadmium, (which had the highest liver$_{EF}$ and accordingly, the highest sediment$_{EF}$), sediment$_{EFs}$ did not necessarily increase with increasing liver$_{EF}$ (Table S3.6). Instead, liver$_{EF}$ better predicted mean Thule-sediment concentrations, where cadmium had the highest liver$_{EF}$ and thus the highest Thule-influenced sediment concentration while lead had the lowest liver$_{EF}$ and the lowest Thule-influenced sediment concentration. The whale liver zinc concentration was 7-fold greater than copper, which was reflected by a 6-fold greater zinc liver$_{EF}$, relative to the copper liver$_{EF}$. Interestingly, the copper and zinc concentrations were similar among Thule-influenced sediments, which suggested greater copper biogenic enrichment relative to zinc, despite that predicted by the liver$_{EF}$. Whale livers were least concentrated in lead, which was reflected by the lowest liver$_{EF}$. We thus found that biogenic EFs were useful for predicting metal concentrations in whale-influenced pond sediments.

Proportions of cadmium, copper, lead, and zinc peaked in surface sediments at 3-fold, 9-fold, 1-fold, and 2-fold greater than background, respectively. Surface sediment peaks in the proportion of metals were reflective of 20th century increases in the atmospheric emissions of these metals in association with mining and coal combustion (39–41). In contrast, sediment metal ratios in both reference ponds, Sav R4 and Sav R5, were generally low and stable, as expected for ponds uninfluenced by human activity. Notably, cadmium, lead, and zinc ratios increased in surface sediments in Sav R4, which may too reflect the atmospheric deposition of metals by 20th century industrial activity.

5.3 Sources of sterols and stanols in High Arctic ponds

We hypothesized that Thule and Dorset occupation would affect the sterol and stanol composition in the pond sediments. Indeed, the sterols and stanols in sediments from PaJs 3N generally exceeded those of other potential sources to waterbodies, such as zooplankton and periphyton (Fig 3.5). Fucosterol was higher in zooplankton than in periphyton because fucosterol is a phytosterol commonly found in algae, which are consumed by zooplankton (42). The phytosterols, fucosterol, sitosterol, and stigmastanol, were not detected in sediments from PaJs 13, but were detected in zooplankton from the same pond. Zooplankton consume algae, which explains the presence of these phytosterols in zooplankton from PaJs 13. In Sav R4, cholestanol, fucosterol, sitosterol, and stigmastanol were more concentrated in zooplankton than in pond sediments. This was expected for a reference pond because the only major contributors to the sterol and stanol concentrations in Sav R4 pond sediments were periphyton and zooplankton. Phytosterols and zoosterols in sediments, phytoplankton, and zooplankton thus reflected the presence of the Thule and Dorset people in PaJs 13 and PaJs 3N. Conversely, reduced

concentrations of phytosterols and zoosterols reflected the absence of human influence in the reference ponds.

6 Conclusions

We demonstrated the utility of using multiple proxies to infer the presence of human occupation in the High Arctic over 1000-years ago. We found that sterols, and in particular, zoosterols, best tracked the historical occupation of the Thule and Dorset people at High Arctic ponds. Increased ratios of cadmium, copper, lead, and zinc in Thule-influenced sediments reflected the flensing of bowhead whales while surface sediment peaks likely tracked 20th century industrial sources. Sterols, stanols, and metal ratios were low in reference pond sediments, which was consistent with the absence of human and whale-derived nutrients. We also demonstrated that biotic EFs were useful for predicting metal concentrations in whale-influenced sediments. This study provided a first glimpse at changes in the sterol and stanol composition of lake sediments as a result of Thule and Dorset occupation in High Arctic ponds. We surmised that the combined analysis of sterols, stanols, stable isotopes, and metal ratios in waterbody sediments could be used to identify other historically important sites and track the timing of human presence in these locations.

Acknowledgements

This research was supported by a Natural Sciences and Engineering Research Council (NSERC) Canada grant to JMB (RGPIN-2018-04248) and in-kind support from the Polar Continental Shelf Program (PCSP) awarded to JMB and JPS (PCSP # 654-17) to support lodging and logistics at Resolute Bay.

The authors declare no competing interests.

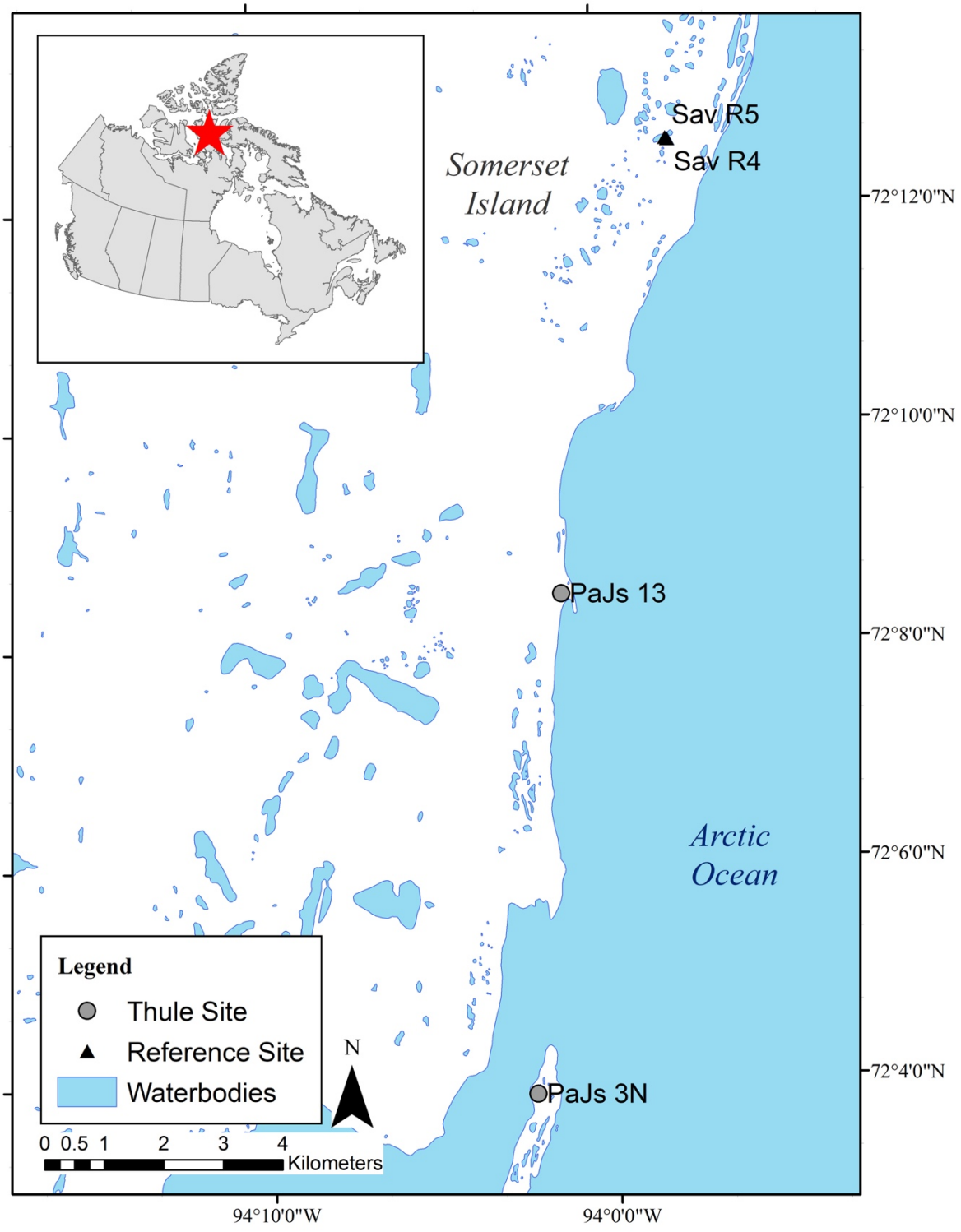

Figure 3.1: Map of Thule-influenced ponds, PaJs 3N and PaJs 13, and reference ponds, Sav R4 and Sav R5, located on Somerset Island, Nunavut, Canada.

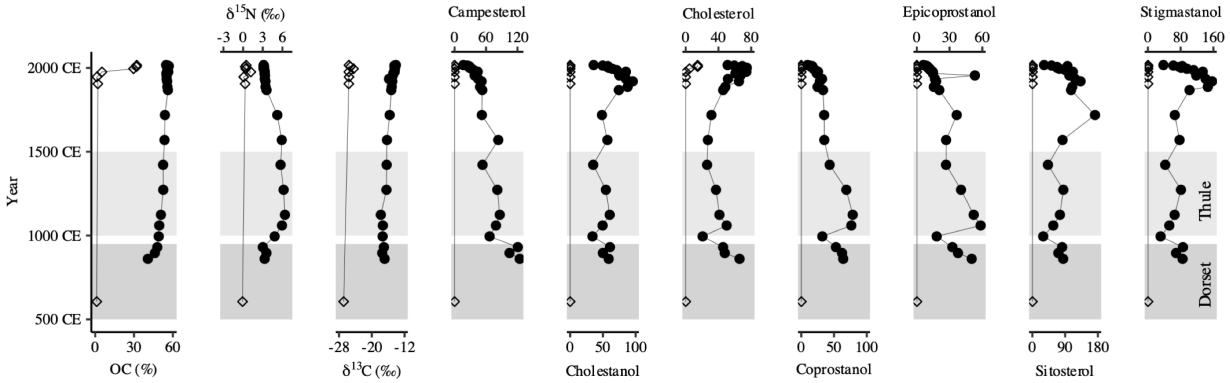

Figure 3.2: Stable isotope and sterol and stanol (µg g^{-1} dw) profiles in the influenced pond, PaJs 3N (●), and the reference pond, Sav R4 (◇). The light gray shaded area signifies the time of Thule presence at PaJs 3N. The dark gray shaded area signifies the time of Dorset presence at PaJs 3N.

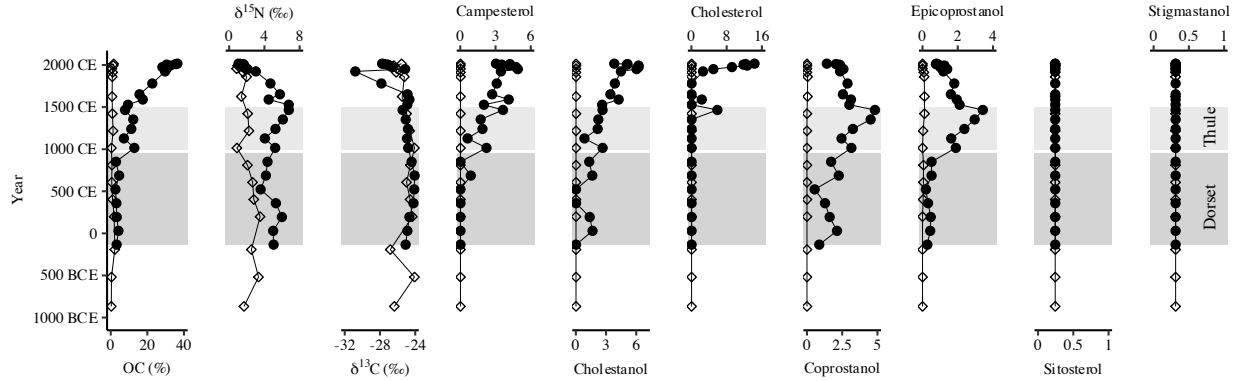

Figure 3.3: Stable isotope and sterol and stanol (µg g^{-1} dw) profiles in the influenced pond, PaJs 13 (●), and the reference pond, Sav R5 (◇). The light gray rectangle signifies the time of Thule presence and the dark gray shaded area signifies the time of Dorset occupation at PaJs 13.

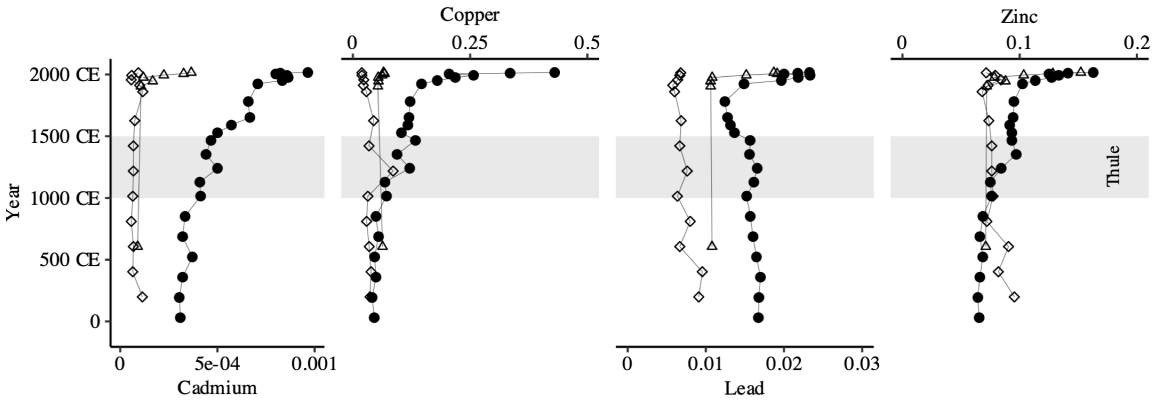

Figure 3.4: Metal concentrations normalized to titanium concentrations in the influenced pond, PaJs 13 (●), and the reference ponds, Sav R4 (△) and Sav R5 (◇). The shaded area signifies the time of Thule presence at PaJs 13.

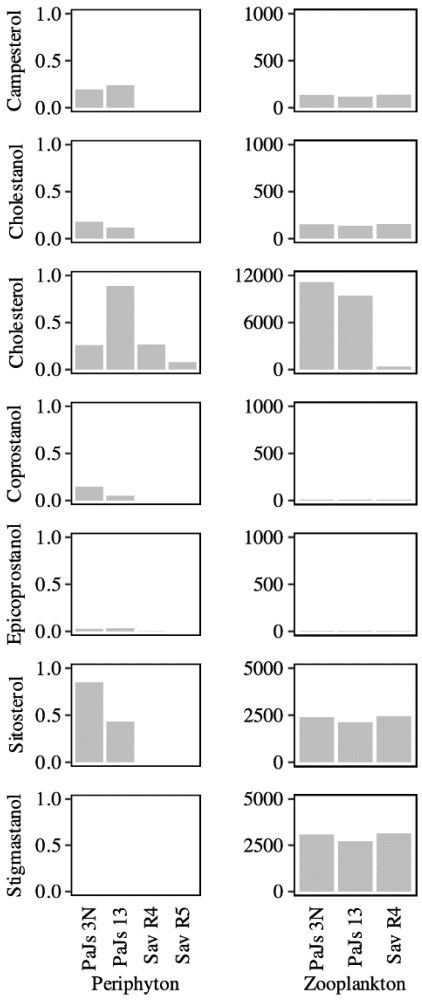

Figure 3.5: Sterols and stanols (µg g^{-1} dw) in periphyton and zooplankton from the influenced ponds, PaJs 3N and PaJs 13, and the reference ponds, Sav R4 and Sav R5. Note the difference in the y-axis scale.

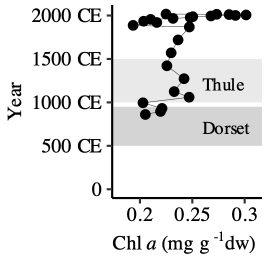

Figure 3.6: Inferred chl *a* in PaJs 3N. The light gray area signifies the time of Thule presence and the dark gray area signifies the time of Dorset presence.

Supplementary information

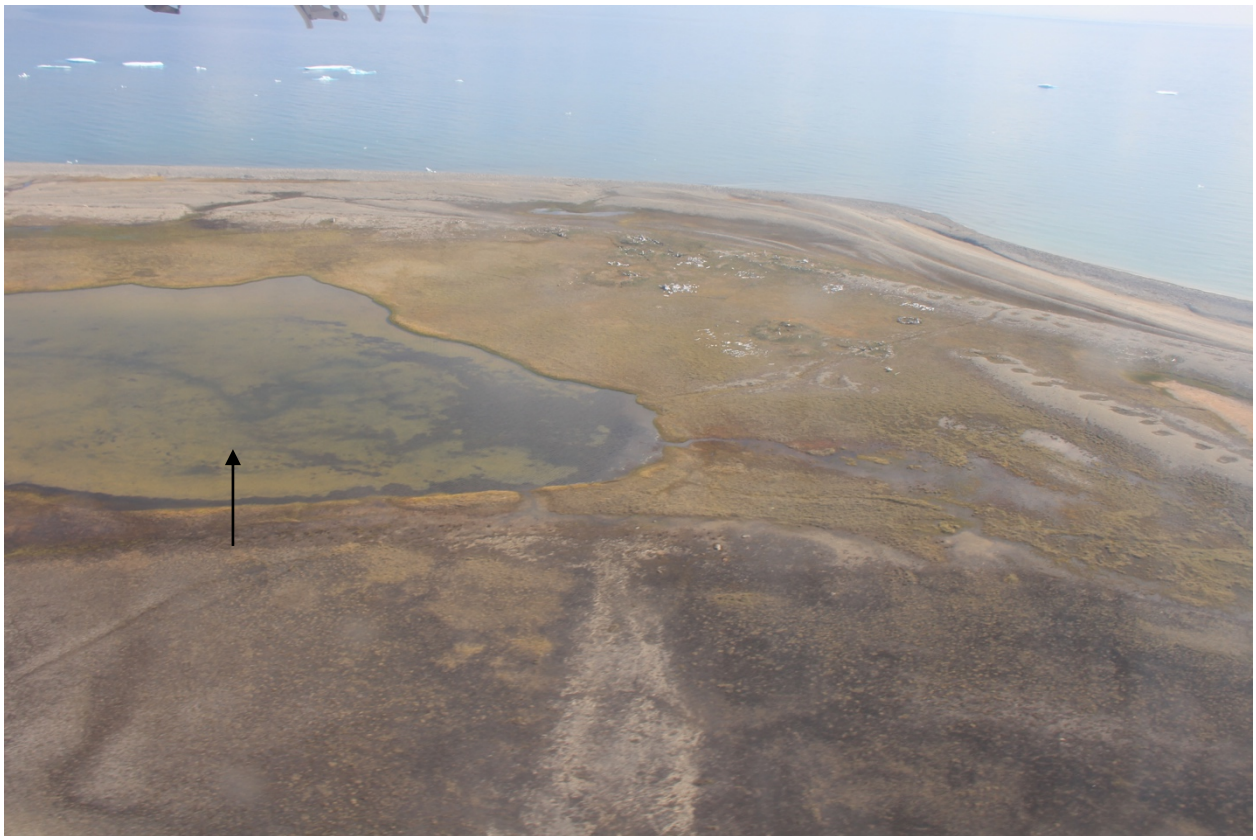

Figure S3.1: Aerial photograph of PaJs 13 (as indicated by the arrow), located on Somerset Island. Note the whalebones to the north west of the pond. Photo credit: LEK.

Figure S3.2: Photograph of PaJs 3N, located on Somerset Island. Photo credit: LEK.

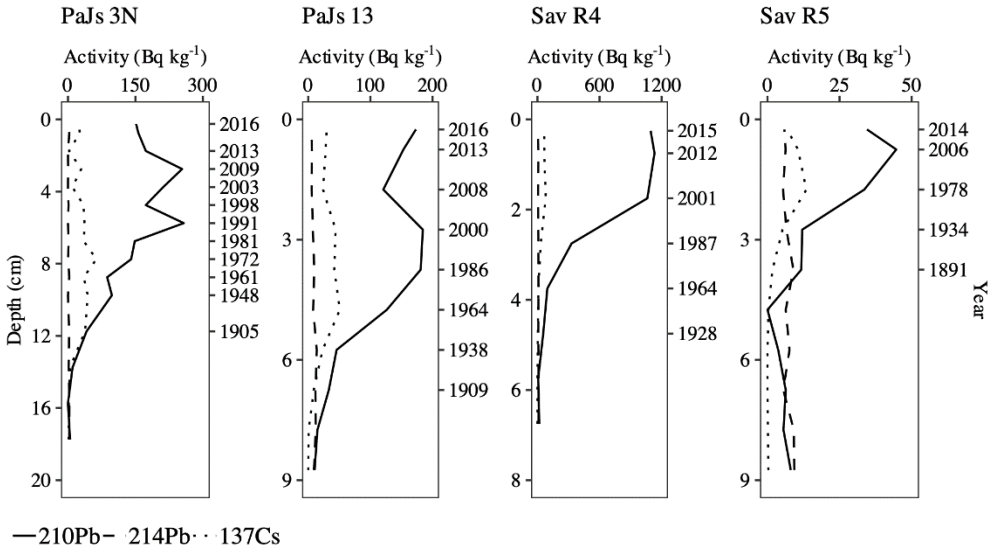

Figure S3.3: ^{210}Pb, ^{214}Pb, and ^{137}Cs activity in the influenced ponds, PaJs 3N and PaJs 13, and the reference ponds, Sav R4 and Sav R5. ^{210}Pb dates are plotted on the right y-axis as calculated by the constant rate of supply model.

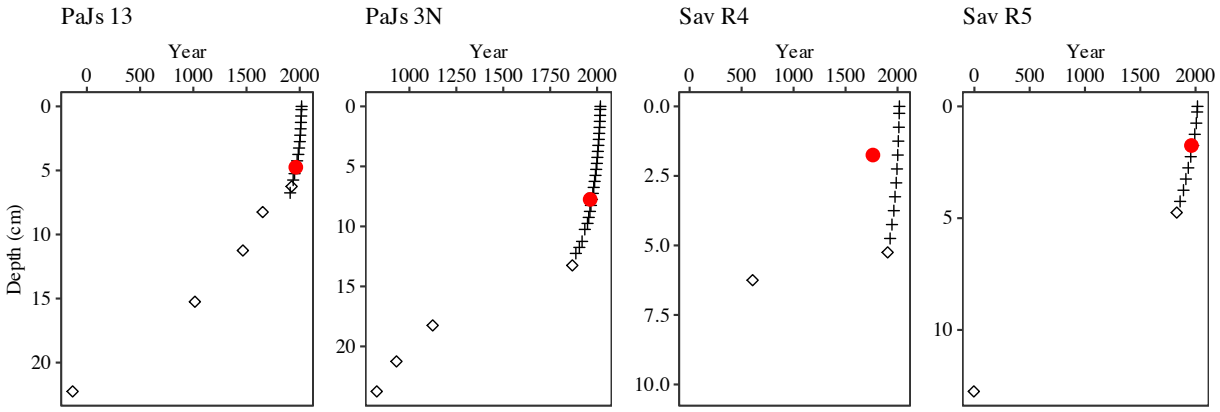

Figure S3.4: ^{210}Pb (+), peak ^{137}Cs (red circle), and ^{14}C (diamond) dates in the sediment cores. A 640-, 453-, 655-, and 1,748-year reservoir effect for radiocarbon was applied to the ^{14}C dates in PaJs 13, PaJs 3N, Sav R4, and Sav R5, respectively. Reservoir effects were based on the calculated difference between the ^{14}C date on material from the depth where the ^{210}Pb date was approximately 1900 CE.

Table S3.1: Latitude, longitude, and elevation above sea level in the waterbodies from Nunavut, Canada.

Site		Latitude	Longitude	Elevation above sea level (m)
Somerset Island				
	PaJs 13	72° 8'26.81"N	94° 1'16.15"W	4
	PaJs 3N	72° 3'52.64"N	94° 2'21.21"W	1
	Sav R4	72°12'34.78"N	93°57'47.90"W	45
	Sav R5	72°12'35.52"N	93°57'51.54"W	45

Table S3.2: Summary of metal concentrations (µg g^{-1} dw) in each waterbody. The sample size is presented in brackets and represents the number of sediment intervals analyzed. SD = standard deviation.

Pond	Compound	Minimum (µg g^{-1} dw)	Maximum (µg g^{-1} dw)	Mean (µg g^{-1} dw)	SD (µg g^{-1} dw)
PaJs 13 (23)	cadmium	0.08	0.29	0.18	0.05
	copper	23.00	60.00	38.00	11.76
	lead	2.00	9.40	6.17	2.09
	titanium	86.00	560.00	377.22	138.10
	zinc	14.00	42.00	32.17	5.94
Sav R4 (16)	cadmium	0.03	0.35	0.07	0.08
	copper	15.00	36.00	23.19	5.31
	lead	3.40	10.00	5.09	1.78
	titanium	51.00	500.00	391.94	124.30
	zinc	23.00	59.00	32.88	7.75
Sav R5 (16)	cadmium	0.01	0.03	0.02	0.01
	copper	4.60	21.00	8.54	4.46
	lead	1.20	2.10	1.58	0.28
	titanium	190.00	280.00	231.88	25.36
	zinc	14.00	21.00	17.88	1.89

Table S3.3: Summary of sterol and stanol percent recoveries as determined by d6 cholesterol. SD = standard deviation. The sample size is presented in brackets and represents the number of sediment intervals analyzed.

Pond	Minimum	Maximum	Mean	SD
PaJs 3N (24)	97.1	184	138	26.1
PaJs 13 (23)	93.0	171	135	23.2
Sav R4 (16)	86.1	100	94.8	4.58
Sav R5 (16)	74.8	119	103	12.6

Table S3.4: Method detection limit (MDL) (ng g^{-1} dw) of sterols and stanols determined through a calibration curve. Values were previously reported in Gallant et al. 2020, under review (17).

Compound	MDL	MDL/√2
coprostanol	1.08	0.76
epicoprostanol	0.81	0.57
coprostanone	169.49	119.85
cholesterol	52.27	36.96
cholestanol	21.91	15.49
cholestanone	16.90	11.95
desmosterol	123.33	87.21
campesterol	19.36	13.69
fucosterol	35.91	25.39
sitosterol	344.99	243.24
stigmastanol	442.73	312.35

Table S3.5: Summary of sterol and stanol concentrations (ng g^{-1} dw) in each pond. The sample size is presented in brackets and represents the number of sediment intervals analyzed. SD = standard deviation.

Pond	Compound	Minimum (ng g^{-1} dw)	Maximum (ng g^{-1} dw)	Mean (ng g^{-1} dw)	SD (ng g^{-1} dw)
PaJs 3N (24)	campesterol	16700	124000	57000	30100
	cholestanol	34100	95600	61900	16900
	cholestanone	12.0	12200	6520	3110
	cholesterol	20700	74600	52700	16100
	coprostanol	9510	100300	38700	24400
	coprostanone	120	120	120	0
	desmosterol	87.2	87.2	87.2	0
	epicoprostanol	5980	58400	25000	16200
	fucosterol	25.4	25.4	25.4	0
	sitosterol	29800	172000	85300	32200
	stigmastanol	30900	157000	88700	34900
PaJs 13 (23)	campesterol	13.7	4890	2220	1730
	cholestanol	15.5	6230	2950	1980
	cholestanone	12.0	1240	276	390
	cholesterol	37.0	14300	3340	5040
	coprostanol	545	4820	2420	1000
	coprostanone	120	120	120	0
	desmosterol	87.2	87.2	87.2	0
	epicoprostanol	191	3420	1290	880
	fucosterol	25.4	25.4	25.4	0
	sitosterol	243	243	243	0
	stigmastanol	312	312	312	0
Sav R4 (16)	campesterol	13.7	1810	126	449
	cholestanol	15.5	15.5	15.5	0
	cholestanone	12	12.0	12.0	0
	cholesterol	37.0	14600	2140	4990
	coprostanol	0.76	140	17.4	39.2
	coprostanone	120	120	120	0
	desmosterol	87.2	87.2	87.2	0
	epicoprostanol	0.44	124	15.1	35.9
	fucosterol	25.4	25.4	25.4	0
	sitosterol	243	243	243	0
	stigmastanol	312	312	312	0
Sav R5 (16)	campesterol	13.7	13.7	13.7	0
	cholestanol	15.5	15.5	15.5	0
	cholestanone	12.0	12.0	12.0	0
	cholesterol	37.0	37.0	37.0	0
	coprostanol	0.76	46.7	6.04	14.5
	coprostanone	120	120	120	0
	desmosterol	87.2	87.2	87.2	0
	epicoprostanol	0.57	114	36.2	43.4
	fucosterol	25.4	25.4	25.4	0
	sitosterol	243	243	243	0
	stigmastanol	312	312	312	0

Table S3.6: Titanium normalized sediment enrichment factors ($sediment_{EF\_Ti}$), sediment enrichment factors ($sediment_{EF}$), and liver enrichment factors ($liver_{EF}$) in PaJs 13. Thule-influenced sediments = metal composition in sediments deposited between 1000 CE and 1500 CE, n = 5. Background sediments = metal composition in Sav R5 sediments deposited pre-Thule and pre-Dorset, n = 2. All concentrations are presented in µg g^{-1} dw.

	Metal concentration normalized to titanium concentration			Metal concentration			
Metal	Thule-influenced sediments	Background sediments	$Sediment_{EF\_Ti}$	Thule-influenced sediments	Background sediments	$Sediment_{EF}$	$Liver_{EF}$
cadmium	$4.0x10^{-4}$	$1.0x10^{-4}$	4	0.17	0.01	12	3100
copper	0.01	0.06	1.7	36	14	2.6	1.4
lead	0.02	0.01	2.8	6.1	1.4	4.3	0.07
zinc	0.09	0.07	1.2	32	17	1.9	8.2

Table S3.7: Summary of stable isotope values in each waterbody. The sample size is presented in brackets and represents the number of sediment intervals analyzed. SD = standard deviation.

Pond	Compound	Minimum	Maximum	Mean	SD
PaJs 3N (24)	$\delta^{13}C$ (‰)	-17.79	-14.11	-15.59	1.21
	$\delta^{15}N$ (‰)	3.01	6.38	3.99	1.19
	N (%)	2.65	3.47	3.13	0.22
	OC (%)	40.70	56.90	53.25	4.01
PaJs 13 (23)	$\delta^{13}C$ (‰)	-30.80	-24.07	-25.68	1.64
	$\delta^{15}N$ (‰)	1.06	6.77	4.14	1.77
	N (%)	0.12	2.22	0.82	0.70
	OC (%)	2.55	36.40	15.81	12.09
Sav R4 (16)	$\delta^{13}C$ (‰)	-28.37	-24.46	-26.88	1.30
	$\delta^{15}N$ (‰)	-5.30	1.18	-0.19	1.46
	N (%)	0.01	1.54	0.31	0.57
	OC (%)	0.49	32.10	6.87	12.14
Sav R5 (16)	$\delta^{13}C$ (‰)	-26.83	-24.08	-25.27	0.89
	$\delta^{15}N$ (‰)	0.84	3.51	1.99	0.83
	N (%)	0.04	0.26	0.13	0.07
	OC (%)	0.30	2.23	1.00	0.55

Table S3.8: ^{14}C dating results for the four ponds.

Pond	Lab ID	Depth (cm)	^{14}C yr BP	Cal BP	median cal BP	Julian date
PaJs 3N	UOC-9919	13.25	528 ± 16	617-613(1.1%) 553-516 (94.3%)	535	1,415 CE
	UOC-9920	18.25	1329 ± 17	1298-1256 (89.3 %) 1203-1187 (6.1 %)	1279	671 CE
	UOC-9921	21.25	1566 ± 16	1523-1410 (95.4 %)	1472	478 CE
	UOC-9922	23.75	1676 ± 18	1617-1537 (95.4 %)	1577	373 CE
PaJs 13	UOC-9923	6.25	699 ± 16	680-651 (2.2%) 579-572 (2.2 %)	666	1284 CE
	UOC-9924	8.25	1017 ± 18	962-920 (95.4 %)	938	1012 CE
	UOC-9925	11.25	1200 ± 18	1180-1065 (95.4 %)	1124	826 CE
	UOC-9926	15.25	1675 ± 18	1616-1537 (95.4 %)	1575	375 CE
	UOC-9927	22.25	2546 ± 19	2748-2699 (77.3 %) 2633-2616 (7.0 %) 2586-2570 (2.4 %) 2565-2539 (8.0 %) 2525-2520 (0.6 %)	2724	774 BCE
Sav R4	UOC-9933	5.25	782 ± 19	730-677 (95.4 %)	700	1250 CE
	UOC-9934	6.25	2045 ± 22	2106-2086 (3.9 %) 2063-1932 (91.5 %)	1999	49 BCE
	UOC-9935	8.25	18957 ± 69	23060-22570 (95.4 %)	22823	20873 BCE
	UOC-9936	10.25	27552 ± 134	31550-31120 (95.4 %)	31333	29383 BCE
Sav R5	UOC-10788	4.75	1923 ± 69	2040-2018 (1.3 %) 20110-1702 (94.1 %)	1868	82 CE
	UOC-10789	12.75	3438 ± 76	3891-3551 (92.2 %) 3534-3484 (3.2 %)	3703	1753 BCE

Table S3.9: ^{210}Pb dating information for PaJs 3N. Bolded year was determined by extrapolating the ^{210}Pb dates using a 3rd order polynomial equation: $y = -0.0563x^3 + 0.1643x^2 - 3.6596x + 2018.2$.

Depth (cm)	Cumulative dry mass (g cm^{-2})	^{210}Pb (Bq kg^{-1})	^{210}Pb error (Bq kg^{-1})	^{214}Pb (Bq kg^{-1})	^{214}Pb error (Bq kg^{-1})	^{137}Cs (Bq kg^{-1})	^{137}Cs error (Bq kg^{-1})	Age (CRS) (year)	Year (CRS) (year)	Error (CRS) (year)
0								0	2017.57	0.7775
0.25	0.0286	151.44	23.82	2.08	3.98	22.83	3.15	0.6085	2016.96	0.7831
0.75	0.0911	156.42	24.16	3	4.14	26.61	3.6	1.7394	2015.83	0.8123
1.75	0.2261	173.08	25.12	0	3.78	2.52	2.28	4.5389	2013.03	0.9568
2.75	0.3599	253.7	30.25	0.62	3.81	29.53	3.73	8.5653	2009	1.188
3.75	0.4954	211.78	24.45	0	3.5	9.96	2.38	13.6923	2003.87	1.4537
4.75	0.6361	172.98	23.14	1.43	3.48	34.51	4.03	18.8443	1998.72	1.7748
5.75	0.784	257.3	28.58	0.23	3.61	36.95	4.15	26.1927	1991.37	2.321
6.75	0.9401	148.51	20.6	1.6	3.38	35.17	3.76	35.6796	1981.89	3.2448
7.75	1.1051	140.49	23.94	0.47	3.9	63.16	6.33	45.2635	1972.3	4.4162
8.75	1.2758	87.15	19.35	2.8	3.58	35.12	4.14	55.8722	1961.69	6.2072
9.75	1.4519	97.74	20.14	0.24	4.12	44.11	4.77	68.6042	1948.96	9.1165
11.75	1.8103	41.34	18.68	2.52	4.01	37.97	4.29	112.1537	1905.41	28.6946
13.75	2.167	10.34	21.39	1.62	4.48	4.62	2.71		**1852.59**	
15.75	2.537	0	17.82	3.34	3.87	1.79	2.35			

Table S3.10: ^{210}Pb dating information for PaJs 13.

Depth (cm)	Cumulative dry mass (g cm^{-2})	^{210}Pb (Bq kg^{-1})	^{210}Pb error (Bq kg^{-1})	^{214}Pb (Bq kg^{-1})	^{214}Pb error (Bq kg^{-1})	^{137}Cs (Bq kg^{-1})	^{137}Cs error (Bq kg^{-1})	Age (CRS) (year)	Year (CRS) (year)	Error (CRS) (year)
0								0	2017.55	0.7486
0.25	0.0386	173.17	20.48	5.47	2.96	29.42	3.25	1.2518	2016.3	0.7722
0.75	0.1203	153.08	17.85	5.85	2.7	27.98	2.99	3.8142	2013.74	0.871
1.75	0.2993	120.63	15.5	5.49	2.09	23.71	2.67	9.0949	2008.46	1.2128
2.75	0.4939	184.27	20.81	7.3	2.89	43.94	4.21	16.9241	2000.63	1.8522
3.75	0.7041	180.84	20	9.69	2.77	41.77	4.02	31.0324	1986.52	3.0776
4.75	0.9336	126.27	17.76	7.79	2.9	50.75	4.72	53.3548	1964.2	6.1348
5.75	1.1762	45.54	13.14	13.61	2.71	23	2.75	79.0786	1938.47	13.355
6.75	1.5068	32.99	13.62	11.51	2.88	8.81	1.84	108.0398	1909.51	24.8814
7.75	2.0066	14.6	9.42	11.95	2.06	0.54	1.07			
8.75	2.6211	10.12	6.46	9.17	1.41	0.04	0.72			

Table S3.11: ^{210}Pb dating information for Sav R4. Bolded year was determined by extrapolating the ^{210}Pb dates using a 3rd order polynomial equation: $y = -0.5591x^3 + 0.3258x^2 - 7.7253x + 2017.8$.

Depth (cm)	Cumulative dry mass (g cm^{-2})	^{210}Pb (Bq kg^{-1})	^{210}Pb error (Bq kg^{-1})	^{214}Pb (Bq kg^{-1})	^{214}Pb error (Bq kg^{-1})	^{137}Cs (Bq kg^{-1})	^{137}Cs error (Bq kg^{-1})	Age (CRS) (year)	Year (CRS) (year)	Error (CRS) (year)
0								0	2017.55	0.5897
0.25	0.024	1093.21	112.42	5.12	3.77	65.26	8.15	1.6182	2015.93	0.62
0.75	0.0735	1130.94	109.97	8.35	3.3	66.53	7.8	4.9896	2012.56	0.7464
1.75	0.2026	1061.53	79.45	6.4	2.37	80.38	6.82	15.7101	2001.84	1.1922
2.75	0.3904	330.47	27.24	8.61	1.75	32.28	3.04	30.2688	1987.28	1.6616
3.75	0.9548	95.82	10.34	9.23	1.34	9.01	1.15	53.2767	1964.28	3.1444
4.75	2.0552	56.2	7.42	8.24	1.13	4.45	0.8	89.1232	1928.43	7.1151
5.75	3.5585	7.29	5.46	10.76	1.14	1.24	0.59		**1877.86**	
6.75	5.2684	18.51	6.07	10.96	1.19	1.41	0.67			

Table S3.12: ^{210}Pb dating information for Sav R5. Bolded year was determined by extrapolating the ^{210}Pb dates using a 2nd order polynomial equation: y = -5.3111x^2 - 14.599x + 2018.8.

Depth (cm)	Cumulative dry mass (g cm^{-2})	^{210}Pb (Bq kg^{-1})	^{210}Pb error (Bq kg^{-1})	^{214}Pb (Bq kg^{-1})	^{214}Pb error (Bq kg^{-1})	^{137}Cs (Bq kg^{-1})	^{137}Cs error (Bq kg^{-1})	Age (CRS) (year)	Year (CRS) (year)	Error (CRS) (year)
0								0	2017.57	3.5877
0.25	0.2686	34.52	9.07	5.84	1.3	6.82	1.1	3.2003	2014.37	3.7417
0.75	0.8219	44.68	7.5	6.25	1.09	10.58	1.19	10.7436	2006.82	4.6662
1.75	2.0421	33.59	9.13	5.4	1.26	13.49	1.49	38.5761	1978.99	12.714
2.75	3.3558	12.06	7.58	6.56	1.2	5.22	0.93	83.201	1934.37	45.6967
3.75	4.6778	11.71	6.7	8.98	1.17	1.73	0.83	126.5543	1891.01	110.2094
4.75	6.0725	0	4.67	6.33	0.96	0.35	0.44		**1829.62**	
5.75	7.5297	3.71	7.42	7.64	1.17	0	0.74			
6.75	8.994	6.32	5.02	5.47	1	0	0.45			
7.75	10.4883	5.55	8.97	9.14	1.36	0.12	0.9			
8.75	11.9702	8.08	7.27	9.31	1.18	0.33	0.73			

References

1. J. M. Savelle, The Umialiit-Kariyit whaling complex and prehistoric Thule Eskimo social relations in the eastern Canadian Arctic. *Bulletin of National Museum of Ethnology* **27**, 159–188 (2002).
2. J. M. Savelle, The role of architectural utility in the formation of zooarchaeological whale bone assemblages. *J Archaeol Sci* **24**, 869–885 (1997).
3. A. P. McCartney, "Thule Eskimo prehistory along northwestern Hudson Bay" in *Archaeological Survey of Canada*, Mercury Series., (1977).
4. J. Habu, J. M. Savelle, Construction, use and abandonment of Thule whale bone house, Somerset Island, Arctic Canada. *Quat Res* **33**, 1–18 (1994).
5. J. M. Savelle, Cumulative bowhead whale (*Balaena mysticetus*) harvest estimates by prehistoric Thule Inuit in the Canadian Arctic 1200–1500 A.D.: Implications for bowhead whale population modeling and Thule demography. *Bulletin of National Museum of Ethnology* **34**, 26 (2010).
6. P. C. Dawson, Interpreting variability in Thule Inuit architecture: A case study from the Canadian High Arctic. *Am Antiq* **66**, 453–470 (2001).
7. R. H. McGuire, M. B. Schiffer, A theory of architectural design. *J Anthropol Archaeol* **2**, 277–303 (1983).
8. A. P. McCartney, J. M. Savelle, Thule Eskimo whaling in the Central Canadian Arctic. *University of Wisconsin Press* **22**, 23 (1985).
9. J. M. Savelle, A. P. McCartney, Thule Eskimo bowhead whale interception strategies. *World Archaeol* **30**, 437–451 (1999).
10. J. Le Mouël, M. Le Mouël, Aspects of early Thule culture as seen in the architecture of a site on Victoria Island, Amundsen Gulf Area. *ARCTIC* **55** (2002).
11. K. R. Hadley, M. S. V. Douglas, R. McGhee, J. M. Blais, J. P. Smol, Ecological influences of Thule Inuit whalers on high Arctic pond ecosystems: a comparative paleolimnological study from Bathurst Island (Nunavut, Canada). *J Paleolimnol* **44**, 85–93 (2010).
12. L. Howse, J. M. Savelle, A. S. Dyke, New insights from the Dorset type site at Alarniq, Northern Foxe Basin, Arctic Canada: beach level chronology and site use. *Am Antiq* **84**, 531–548 (2019).
13. A. S. Dyke, J. M. Savelle, D. S. Johnson, Paleoeskimo demography and holocene sea-level history, Gulf of Boothia, Arctic Canada. *ARCTIC* **64** (2011).
14. D. Antoniades, *et al.*, Cultural eutrophication, anoxia, and ecosystem recovery in Meretta Lake, High Arctic Canada. *Limnol Oceanogr* **56**, 639–650 (2011).
15. E. M. Stewart, *et al.*, A paleoenvironmental study tracking eutrophication, mining pollution, and climate change in Niven Lake, the first sewage lagoon of Yellowknife (Northwest Territories). *Arctic* **71**, 201–217 (2018).
16. T. J. Tse, *et al.*, Reconstructing long-term trends in municipal sewage discharge into a small lake in northern Manitoba, Canada. *Chemosphere* **103**, 299–305 (2014).
17. L. R. Gallant, L. E. Kimpe, K. E. Hargan, J. M. Blais, Under review: Tracking the history of cultural eutrophication in High Arctic waterbodies. *Anthropocene* (2020).
18. R. Leeming, A. Ball, N. Ashbolt, P. Nichols, Using faecal sterols from humans and animals to distinguish faecal pollution in receiving waters. *Wat Res* **30**, 2893–2900 (1996).
19. V. Campos, R. Fracácio, L. F. Fraceto, A. H. Rosa, Fecal sterols in estuarine sediments as markers of sewage contamination in the Cubatão Area, São Paulo, Brazil. *Aquat Geochem* **18**, 433–443 (2012).

20. R. S. Carreira, A. L. R. Wagener, J. W. Readman, Sterols as markers of sewage contamination in a tropical urban estuary (Guanabara Bay, Brazil): space–time variations. *Estuar Coast Mar Sci* **60**, 587–598 (2004).
21. L. Carreón-Palau, C. C. Parrish, H. Pérez-España, Urban sewage lipids in the suspended particulate matter of a coral reef under river influence in the South West Gulf of Mexico. *Water Res* **123**, 192–205 (2017).
22. R. Leeming, J. S. Stark, J. J. Smith, Novel use of faecal sterols to assess human faecal contamination in Antarctica: a likelihood assessment matrix for environmental monitoring. *Antarct Sci* **27**, 31–43 (2015).
23. K. Prost, J. J. Birk, E. Lehndorff, R. Gerlach, W. Amelung, Steroid biomarkers revisited – Improved source identification of faecal remains in archaeological soil material. *PLoS One* **12**, e0164882 (2017).
24. W. Cheng, *et al.*, Sterols and stanols preserved in pond sediments track seabird biovectors in a High Arctic environment. *Environ Sci Technol* **50**, 9351–9360 (2016).
25. J. R. Glew, J. P. Smol, A push corer developed for retrieving high-resolution sediment cores from shallow waters. *J Paleolimnol* **56**, 67–71 (2016).
26. P. G. Appleby, F. Oldfield, The calculation of lead-210 dates assuming a constant rate of supply of unsupported 210Pb to the sediment. *CATENA* **5**, 1–8 (1978).
27. B. Ramsey, Bayesian analysis of radiocarbon dates. *Radiocarbon* **51**, 337–360 (2009).
28. A. Millard, Conventions for reporting radiocarbon determinations. *Radiocarbon* **56**, 555–559 (2014).
29. W. M. Last, J. P. Smol, "Physical and geochemical methods" in *Tracking Environmental Changes Using Lake Sediments*, (Kluwer Academic Publishers, 2001).
30. A. S. Dyke, R. N. McNeely, J. Hooper, Marine reservoir corrections for bowhead whale radiocarbon age determinations. *Can J Earth Sci* **33**, 1628–1637 (1996).
31. M. Stuiver, G. W. Pearson, T. Braziunas, Radiocarbon age calibration of marine samples back to 9000 cal yr BP. *Radiocarbon* **28**, 980–1021 (1986).
32. C. A. Cooke, M. B. Abbott, A. P. Wolfe, J. L. Kittleson, A millennium of metallurgy recorded by lake sediments from Morococha, Peruvian Andes. *Environ. Sci. Technol.* **41**, 3469–3474 (2007).
33. M. B. Abbott, M. W. Binford, M. Brenner, K. R. Kelts, A 3500 14C yr high-resolution record of water-level changes in Lake Titicaca, Bolivia/Peru. *Quat Res* **47**, 169–180 (1997).
34. C. A. Krone, *et al.*, Elements in liver tissues of bowhead whales (*Balaena mysticetus*). *Mar Mammal Sci* **15**, 123–142 (1999).
35. M. Vighi, A. Borrell, A. Aguilar, Bone as a surrogate tissue to monitor metals in baleen whales. *Chemosphere* **171**, 81–88 (2017).
36. I. D. Bull, M. J. Lockheart, M. M. Elhmmali, D. J. Roberts, R. P. Evershed, The origin of faeces by means of biomarker detection. *Environ Int* **27**, 647–654 (2002).
37. A. Evenset, *et al.*, Historical trends in persistent organic pollutants and metals recorded in sediment from Lake Ellasjøen, Bjørnøya, Norwegian Arctic. *Environ Pollut* **146**, 196–205 (2007).
38. S. K. Brimble, *et al.*, High Arctic ponds receiving biotransported nutrients from a nearby seabird colony are also subject to potentially toxic loadings of arsenic, cadmium, and zinc. *Environ Toxicol Chem* **28**, 2426–2433 (2009).

39. Nriagu, Jerome O, A global assessment of natural sources of atmospheric trace metals. *Letters to Nature* **338** (1989).
40. J. O. Nriagu, J. M. Pacyna, Quantitative assessment of worldwide contamination of air, water and soils by trace metals. *Nature* **333**, 134–139 (1988).
41. J. O. Nriagu, The rise and fall of leaded gasoline. *Sci Total Environ* **92**, 13–28 (1990).
42. D. Martin-Creuzburg, P. Merkel, Sterols of freshwater microalgae: potential implications for zooplankton nutrition. *J Plankton Res* **38**, 865–877 (2016).

Chapter 4: A bat guano deposit in Jamaica recorded agricultural changes and metal exposure over the last > 4,300 years

Lauren R. Gallant[a], Christopher Grooms[b], Linda E. Kimpe[a], John P. Smol[b], Wieslaw Bogdanowicz[c], R. Stefan Stewart[d], Elizabeth L. Clare[e], M. Brock Fenton[f], Jules M. Blais[a]

[a] Department of Biology, University of Ottawa, Ottawa, ON, K1N 6N5, Canada

[b] Paleoecological Environmental Assessment and Research Lab (PEARL), Department of Biology, Queen's University, Kingston, ON, K7L 3N6, Canada

[c] Museum and Institute of Zoology, Polish Academy of Sciences, 00-679 Warszawa, Poland

[d] Jamaican Caves Organization, Ewarton, Jamaica

[e] School of Biological Sciences, University of Bristol, Bristol BS8 IUG, UK

[f] Department of Biology, University of Western Ontario, London, ON, N6A 5B7, Canada

This article is published as: Gallant, L. R. *et al.* A bat guano deposit in Jamaica recorded agricultural changes and metal exposure over the last >4300 years. *Palaeogeography, Palaeoclimatology, Palaeoecology* **538**, 109470 (2020).

Statement of author contributions:

Gallant, Lauren R: study design, lab work, data analysis and interpretation, and manuscript preparation. Grooms, Christopher: sample collection and peer review. Kimpe, Linda E: data analysis and interpretation. Smol, John P: study design and peer review. Bogdanowicz, Wieslaw: study design and sample collection, lab work, data analysis and interpretation, and peer review. Stewart, R. Stefan: study design and sample collection. Clare, Elizabeth L: study design, sample

collection, and peer review. Fenton, M. Brock: study design, sample collection, and peer review. Blais, Jules M: study design, data analysis and interpretation, manuscript preparation, and peer review.

Keywords: carbon, nitrogen, lead, mercury, cadmium, isotopes

Abstract

Bats are excellent ecological indicators because they are long-lived, globally distributed, and show predictable responses to environmental stressors. Unaltered bat guano deposits, although rare, can serve as environmental archives to reveal changes in dietary patterns over millennial time scales. We inferred changes in agricultural and industrial practices using a continuous 4,300-year-old bat guano deposit from Jamaica. Cadmium, mercury, lead, and zinc increased during the Industrial Revolution, (which began in ca. 1760), a period characterized by elevated emissions of metals to the atmosphere. Beginning in the early 20th century, decreases in $^{206}Pb/^{207}Pb$ isotopes tracked the history of leaded gasoline use. Metal concentrations in the bat guano deposit exceeded those recorded in two nearby lake sediment cores from Jamaica. Carbon, nitrogen, and sulfur stable isotope profiles in bat guano tracked the agricultural history of Jamaica, specifically the introduction of nitrogen fertilizers, sugarcane, and possibly fungicides. Bat populations are under stress globally, and such intact guano deposits provide potentially critical information on long-term changes in their food source and exposure to metals.

1 Introduction

Present across all continents except Antarctica, there are ~1,300 species of bats that comprise ~20% of all mammal taxa (Fenton and Simmons 2014). Bats occupy a range of trophic levels, and serve as pollinators, natural insecticidal agents, and seed dispersers (Kunz et al. 2011). Furthermore, at peak lactation, bats can consume over 100% of their body mass in a single night (Kunz et al. 2011). Bats may be exposed to high concentrations of metals, some of which passes in their guano (Afonso et al. 2016). Caves in which they roost can house large guano deposits that may provide long-term records of bat exposure to metals. If intact deposits can be located, radiometric dating methods can be combined with stratigraphic elemental analyses to infer long-term changes in metal exposure.

1.1 Using bat guano deposits to infer bat exposure to metals

Many anthropogenic activities contribute to the concentration of metals in the environment (Nriagu and Pacyna 1988). In particular, the onset of the Industrial Revolution in the late 1700s and the introduction of leaded gasoline in the early 20th century contributed to atmospheric metal concentrations in aerosols and soils (Nriagu 1990). Atmospherically released metals can enter food webs, resulting in elevated concentrations of metals in bats (Pikula et al. 2010). Detectable concentrations of metals were recovered previously from bat guano deposits. For example, lead and copper concentrations in a 30,000-year-old bat guano deposit in the Philippines reached peak concentrations of ~10 and >1000 ppm, respectively (Bird et al. 2007). Similarly, copper concentrations in a 13,000-year-old bat guano deposit from Borneo reached ~8,000 ppm, with lower concentrations of other metals such as chromium, vanadium, and zinc (Wurster et al. 2017). Copper, lead, and zinc profiles were also reported for a ~3,000-year-old bat guano deposit in Romania (Onac et al. 2015). Given the concentrations to which metals can be detected in bat

guano deposits, and the well-recorded release of metals to the atmosphere from industrial activity, it is interesting that metal concentrations in the aforementioned bat guano deposits did not fluctuate coeval with industrial practices.

Lake sediment cores are commonly used to infer past environmental conditions and have been employed to document increases in the metal concentrations that resulted from past human activities (e.g.: Cooke et al. 2007; Cooke and Abbott 2008; Laird et al. 2014). For example, 11th century metallurgy and 16th century silver mining in the Andes left a legacy of higher concentrations of zinc and copper, and lead in Peruvian lake sediments, respectively (Cooke et al. 2007). 20th century deposits are commonly enriched in metals, owing to high levels of industrial activity (Cooke and Abbott 2008; Engstrom et al. 2014).

1.2 Tracking past agricultural changes using bat guano deposits

Several studies examined stratigraphic variations of $\delta^{15}N$ and $\delta^{13}C$ in bat guano deposits that ranged in age from mid-20th century to 32,000 yr BP (Wurster et al. 2007; Wurster et al. 2017; Widga and Colburn 2015; Bird et al. 2007; Mizutani et al. 1992). $\delta^{13}C$ values in bat guano have been correlated to precipitation and photosynthetic pathway type, where higher values associated with greater summer precipitation and C4 grasses (Wurster et al. 2007). Accordingly, $\delta^{13}C$ values in bat guano deposits were lowest during periods of drought (Wurster et al. 2017; Onac et al. 2014). $\delta^{13}C$ values in guano have also been used to track bat dietary preferences, with lower $\delta^{13}C$ values indicative of a diet dominated by C3 vegetation (Widga and Colburn 2015). A fall in $\delta^{13}C$ values in a bat guano deposit was also correlated to agricultural practices: historically elevated $\delta^{13}C$ values (C4 plants) corresponded to a period of deforestation and lower present-day $\delta^{13}C$ values (C3 plants) corresponded to forests (Bird et al. 2007). $\delta^{15}N$ values may be more susceptible to diagenesis, and as a result, it is difficult to associate $\delta^{15}N$ profiles with past climate

conditions (Wurster et al. 2017; Bird et al. 2007). Despite difficulties associated with interpretation of nitrogen stable isotopes, greater $\delta^{15}N$ values in bat guano deposits have been associated with insectivorous bats feeding at higher trophic level (Bird et al. 2007). $\delta^{15}N$ was also used to identify the dietary proportions of aquatic and terrestrial vegetation in a bat guano deposit (Ahmad and Davies 2017).

1.3 Objectives

Bat guano was widely mined for gunpowder and fertilizer, such that long sequences of bat guano deposits are now scarce. Consequently, bat guano is rarely used as an archive for paleoenvironmental inference. We present results from one of only a few intact guano deposits remaining in Jamaica, the Home Away from Home (HOM) cave. We set out to analyze a continuous record of bat guano in a core from the cave for stable and radiogenic isotopes and metals. Specifically, our aim was to gain insights into past agricultural practices (using $\delta^{15}N$, $\delta^{13}C$, and $\delta^{34}S$) and industrial activity (using cadmium, lead, mercury, and zinc) in this part of Jamaica over the past four millennia. Lake sediment cores are frequently used to infer past environmental conditions, and we compared the history recorded in the bat guano deposit to histories from two, nearby, Jamaican lake sediment cores. Our guano analyses revealed a history of bat community exposure to contaminants, stemming from a range of anthropogenic activities over the last ~4,300 years.

2 Materials and methods

2.1 Study sites

The bat guano core was collected from Home Away from Home (HOM) cave, in Trelawny Parish, Jamaica. The exact location of the cave is kept confidential for conservation reasons, but

inquiries from qualified researches can be sent to the Jamaican Caves Organization. The cave is well protected from local disturbances, as it is accessible only with technical climbing gear. There is no evidence of human activity beyond the cave entrance. The cave temperature ranges between 25 and 30°C and humidity approaches 100% during the rainy season. The HOM core was taken from the deepest deposit within the cave, located approximately 30 m beneath the entrance. An estimated 5,000 bats currently occupy HOM cave. Five bat species were identified using a combination of sonar (Song-Meter SM2BAT), mist netting, and a taxonomic key created by Dr. M. Brock Fenton and students: insectivorous *Pteronotus parnelli*, *Macrotus waterhousii*, and *Mormoops blainvillii*, nectivorous *Glossophaga soricina*, and frugivorous *Artibeus jamaicensis*. The HOM core was collected by excavation at the apex of the tallest guano deposit. 10 x10-cm cross-sections of bat guano were collected at 1-cm intervals to a depth of 129 cm. Samples were stored in Whirl Pak® bags at -20°C until analysis.

Sediment cores were collected from Crystal Lake (18° 27’ 39.71’’ N, 77 22’ 47.63’’ W) and Wakefield Lake (18° 24' 47.30" N, 77° 43' 42.95" W) using a 3-inch Glew and Smol (Glew and Smol 2016) deep water corer. Cores were sectioned into 0.5-cm intervals, that were refrigerated at 4°C and then freeze-dried for analysis. Crystal Lake is located 512 m from the ocean and 33 km east of HOM cave. It is relatively free from human activity, with the exception of local fishing and a highway to the north. Wakefield Lake is located 9.5 km northwest of HOM cave, within a town that floods frequently and is thought to have existed only since the 1800s.

2.2 ^{210}Pb and ^{14}C dating

^{210}Pb dating and ^{137}Cs measurements on guano from the HOM deposit were accomplished using an Ortec High Purity Germanium Gamma Spectrometer (Oak Ridge, TN, USA) at the University of Ottawa. Measurements on samples from the lake cores were run on gamma

detectors at Queen's University. Certified Reference Materials, obtained from International Atomic Energy Association (Vienna, Austria), were used for efficiency corrections, and results were analyzed using ScienTissiME (Barry's Bay, ON, Canada). ^{137}Cs measurements were made to confirm ^{210}Pb dates calculated using the CRS (constant rate of supply) model. ^{214}Pb activity, which was used as a proxy for supported ^{210}Pb activity, remained relatively low and constant throughout each profile. In the bat guano deposit, an average background value of 56.5 Bq kg^{-1} was used to construct the dating profile. In the Crystal and Wakefield lake sediment cores, ^{210}Pb approached background at 16.25 cm and 32.25 cm, respectively (Fig S4.3). ^{214}Pb activity was averaged in the lake sediment cores; activity was set to a value of 37.11 Bq kg^{-1} for Crystal Lake and 47.49 Bq kg^{-1} for Wakefield Lake.

Lipid-treated (lipids removed using dichloromethane and methanol) and un-treated samples from three selected depths in the guano profile (14.5, 56.5, and 85.5 cm) were ^{14}C-dated by accelerator mass spectrometry at the Poznań Radiocarbon Laboratory in Poland. Because ^{14}C dates from the paired lipid-treated and untreated samples were similar (Table S4.1), ^{14}C dates were run on untreated samples at other depths in the profile. Radiocarbon dates were calculated using OxCal 2013 and age calibrations were conducted using OxCal 4.1.5 software.

2.3 Metals

Metals were extracted by digesting freeze-dried guano in HNO_3 and H_2O_2 in a DigiPREP Jr. (SCP Science, Baie D'Urfé, QC, Canada) in accordance with USEPA Method 3050b. Samples were analyzed for total metals using an Agilent inductively coupled plasma mass spectrometer (ICP-MS) (Santa Clara, CA, USA). Reference material was NIST 8704 Buffalo River Sediment. Method detection limits are shown in Table S4.2. The standard error of triplicates in the lake sediment samples ranged between 0.02 and 5.82 μg kg^{-1} for each metal (Table S4.3). Samples

were re-analyzed for lead isotopes by ICP-MS; the standard error of triplicates in the lake sediment samples ranged between 0.001 and 0.097. Approximately 10 mg of freeze-dried bat guano was analyzed for total mercury on a NIC Mercury Analyzer 3000 (Bryan, TX, USA), using USEPA method 7473. Reference material was NRC MESS-3 Marine Sediment 91+/-9 ng g^{-1} total mercury; the method detection limit was 0.2 ng g^{-1}. In addition to normalizing the total metal concentrations to organic carbon, the metal concentrations were also normalized to titanium concentrations to account for natural weathering and ensure that any fluctuations in the metal profiles were reflective of anthropogenic activity. This standardization accounts for the natural variations in metal flux within the guano deposit as some total metals are immobilized within titanium lattices (Last and Smol 2001).

2.4 Carbon, nitrogen, and sulfur isotopes

Percent carbon, nitrogen, and sulfur were analyzed using a Micro Cube elemental analyzer at the Ján Veizer Stable Isotope Laboratory (formerly G.G. Hatch SIL), located at the University of Ottawa. TOC was determined by analyzing samples after they were acid desiccated using HCl. Organic $\delta^{13}C$ (‰ V-PDB), hereafter, referred to as $\delta^{13}C$, and $\delta^{15}N$ (‰ air) were analyzed using an elemental analyzer interfaced to an isotope ratio mass spectrometer (IRMS). Samples were normalized to the following internal standards: C-51 Nicotiamide ($\delta^{15}N$: +0.07 ‰, $\delta^{13}C$: -22.95 ‰), C-52 ammonium sulphate and sucrose ($\delta^{15}N$: +16.58 ‰, $\delta^{13}C$: -11.94 ‰), and C-54 caffeine ($\delta^{15}N$: -16.61 ‰, $\delta^{13}C$: -34.46 ‰). The blind standard was C-55 glutamic acid ($\delta^{15}N$: -3.98 ‰, $\delta^{13}C$: -28.53 ‰). Results are reported in delta notation (δ) where δ = ((Rx-Rstd))/Rstd)*1000; R = ratio of the abundance of the heavy to light isotope, x = sample, and std = standard. $\delta^{15}N$ values were calibrated to the following international standards: IAEA-N1 (+0.4 ‰), IAEA-N2 (+20.3 ‰), USGS-40 (-4.52 ‰), and USGS-41 (+47.57 ‰). $\delta^{13}C$ values were

calibrated to the following international standards: IAEA-CH-6 (-10.4 ‰), NBS-22 (-29.91 ‰), USGS-40 (-26.24 ‰), and USGS-41 (+37.76 ‰). Analytical precision was ±0.2 ‰ using glutamic acid. $\delta^{34}S$ (‰ VCDT) was analyzed using a Vario Micro Cube elemental analyzer (Langenselbold, Germany) interfaced *via* a conflo IV to a Thermo Finnigan Delta XP IRMS (Bremen, Germany).

3 Results and discussion

3.1 Dating an ancient bat guano deposit

'Unsupported' ^{210}Pb reached radiogenic background at a depth of 14.5 cm in the HOM core (see Methods), corresponding to ca. 1900 CE. We used ^{137}Cs to corroborate the ^{210}Pb dating profile: ^{137}Cs was produced solely from nuclear weapons testing, and most lake sediments show highest activity in 1963 CE, associated with the peak in such testing. ^{137}Cs activity peaked at 8.5 cm depth in the guano, corroborating that the depth corresponded to the early-1960s, as determined by ^{210}Pb dating (Fig S4.1). Although ^{137}Cs dating is widely used in lake and peat deposits, it has not been attempted previously in bat guano archives. Our study reveals that it is possible to reconstruct the history of nuclear weapons testing using ^{137}Cs in bat guano and that it can be used to validate ^{210}Pb dating models.

At 14.5 cm, there was a 580-year difference between the ^{210}Pb date (1900 CE) and the calibrated ^{14}C date (1320 CE). The difference between the ^{210}Pb and ^{14}C dates may be attributed to the dissolution of the limestone cave onto the bat guano deposit, which would contribute dead carbon (carbon lacking ^{14}C) into the system and/or from the bat diet itself, where bats feeding on aquatic insects can incorporate any reservoir effect from the environment into their system. Consequently, we applied a 580-year reservoir effect correction to this bat guano deposit to account for the different dates given by the ^{210}Pb and ^{14}C dating methods. A 2,000-year reservoir

effect correction was applied to a bat guano deposit from the Philippines, to account for the deposition of weathered graphite from a marble cave (Bird et al. 2007). After accounting for the reservoir effect in our guano deposit, the calibrated ^{14}C date on the oldest layer (128.5 cm) was 2307 BCE, indicating the HOM core spans the last ~4,300 years.

3.2 History of metal exposure to bats

The increase in lead concentrations in the HOM core coincided with the onset of the Industrial Revolution ca. 1760 CE, a period of increased mining, coal combustion, and waste incineration (Fig 4.1). (Clark 1979) reported lead concentrations (61-65 μg g^{-1} dw) in guano collected from bats living in proximity to a highway, suggesting that leaded gasoline was the major contributor of lead to the bat's diet.

Lead isotope analyses, e.g. the $^{206}Pb/^{207}Pb$ ratio, were used to "fingerprint" the source of additional lead (Komarek et al. 2008; Teutsch et al. 2001). The ratio decreased in the bat guano deposit from 1.512 to 1.142 starting in the 1920s CE (Fig 4.1). Values approached those typical of leaded gasoline from Australia (~1.04), Europe (1.115), Mexico (1.202-1.204), the United States (1.04-1.39), and Canada (0.92-1.19) (Weiss et al. 1999; Erel et al. 1997; Sañudo-Wilhelmy and Flegal 1994; Sturges and Barrie 1987). Similar $^{206}Pb/^{207}Pb$ values were observed in the Jamaican lake sediments (Table S4.3, Figs 4.2 and 4.3). Neither lake sediment core was old enough to capture pre-industrial lead. Nevertheless, lead ratio values in the lake sediments were more similar to values in 20th-century bat guano than to values in pre-industrial guano (Fig 4.3). $^{208}Pb/^{206}Pb$ can identify the source of Pb used in leaded gasoline because isotope ratios from North American ores (2.06) were generally lower than values in European ores (2.145) (Teutsch et al. 2001). Accordingly, industrial-period $^{206}Pb/^{207}Pb$ (1.228) and $^{208}Pb/^{206}Pb$ (1.994) values in the bat guano (Table S4.4) generally reflect leaded gasoline from North America. Despite the

absence of major roads within several kilometers of the HOM deposit, the lead isotope profile suggests that the lead was carried into the foraging area of the bats and transferred to them through their food web. The slight increase in the lead isotopic ratio at the beginning of the 21st century may reflect a lagged response to removal of lead from gasoline in the early-mid 1980s (Fig 4.1). Notably, the average crustal $^{206}Pb/^{207}Pb$ ratio (~1.2) is similar to the ratio in pre-industrial guano (Weiss et al. 1999; Farmer et al. 2000). The $^{208}Pb/^{207}Pb$ vs $^{206}Pb/^{207}Pb$ profile (Fig 4.3) further supported the shift from a natural to anthropogenic lead source, as lower values of both ratios indicated anthropogenic origin (Emmanuel and Erel 2002). $^{206}Pb/^{204}Pb$ can also distinguish between natural (18.5-19.5) and anthropogenic (16-18.5) lead sources (Hansmann and Köppel 2000). Accordingly, $^{206}Pb/^{204}Pb$ decreased in industrial-era guano (Fig 4.1) and was typically < 18.5 in the lake sediments (Table S4.3).

The range of mercury concentrations in this bat guano deposit (Table S4: 0.09-1.72 μg g^{-1} dw OC) resembled those reported in fresh bat guano samples collected from historically industrialized areas (0.12-0.26 μg g^{-1} dw) and from rural environments (0.08-0.11 μg g^{-1} dw) (O'Shea et al. 2001). Mercury concentrations rose in this deposit at the onset of the Industrial Revolution and the rise in mercury concentrations we recorded in guano from the 20th century is consistent with the timing of an increase in Hg concentrations observed in North American lake sediments (Engstrom et al. 2014). Interestingly, the slow rise in mercury beginning in ~1400 BCE coincided with the earliest record of mercury mining in Peru (Cooke et al. 2009). Mercury amalgamation was introduced to Jamaica in ~1600 CE and may have contributed to the rise in mercury observed within the HOM core. Notably, bat guano had higher mercury than other mammalian faeces, such as that of otters (0.02-0.17 μg g^{-1} dw (Ramos-Rosas et al. 2013)). Elevated mercury concentrations were also observed in bat livers (14.0-151 μg g^{-1} dw (Nam et al.

2012)), hair (0.04-145.27 μg g^{-1} dw (Becker et al. 2018)), and brains (0.41-18.7 μg g^{-1} dw (Nam et al. 2012)).

Zinc concentrations in the HOM core (Table S4.4) generally exceeded those observed in fresh bat guano (64-1,080 μg g^{-1} dw (Zukal et al. 2015)). Furthermore, zinc bioaccumulates and is readily transferred from the lithosphere to biota (Brimble et al. 2009), which explains the much lower zinc concentrations observed in the Jamaican lake sediment cores (Table S4.3: 4.93-15.7 μg g^{-1} dw). Anthropogenic emissions of zinc were reflected within this bat guano deposit. The concentration of zinc peaked at 6,200 μg g^{-1} total organic carbon (TOC) during the Industrial Revolution, during which bauxite mining was introduced to Jamaica (Rainford and Richards 2008). Similarly, Norwegian Arctic lake sediment cores influenced by seabird guano showed an increase in zinc concentrations as a result of the Industrial Revolution (196 μg g^{-1} dw in pre-industrial deposits to a peak of 434 μg g^{-1} dw in 1996) (Evenset et al. 2007).

Previously reported cadmium concentrations in bat guano (0.03-8.5 μg g^{-1} dw (Zukal et al. 2015)) and Jamaican lake sediments (Table S3: 0.03-0.28 μg g^{-1} dw) were much lower than those in the HOM core (Table S4.4). The concentration of cadmium in the bat guano deposit (median = 92.8 μg g^{-1} dw) also exceeded that found in the hair, livers, and kidneys of bats (0.02-0.10 μg g^{-1} dw) (Hernout et al. 2016). Elevated cadmium concentrations in the HOM core may reflect the naturally high cadmium concentrations in soils from Jamaica (298-978 μg g^{-1} dw) compared to soils in other countries (Garrett et al. 2008). About 67% of Jamaica is covered by limestone, which often contains phosphate-bearing minerals such as phosphorite, with cadmium concentrations as high as 6,000 μg g^{-1} dw (Garrett et al. 2008; Garrett et al. 2010; Draper 1986). Moreover, soil collected above white limestone typically has 32 times more cadmium than average Jamaican soil (Garrett et al. 2008). Consequently, bats at HOM cave are exposed to

naturally elevated cadmium concentrations in the soil as well as elevated cadmium in the white limestone cave they inhabit. The cadmium rise in the HOM core was comparable to the 3-fold increase in cadmium observed in Peruvian lake sediments, which was attributed to industrial activity (Cooke and Abbott 2008).

3.3 Stable isotopes and dietary trends

The $\delta^{15}N$, $\delta^{13}C$, and $\delta^{34}S$ composition in this deposit reflects agricultural practices over the past ~4,300 years. In this deposit, $\delta^{13}C$ averaged -26.5 ‰ until the 1670s CE, at which point, $\delta^{13}C$ increased, reaching a maximum value of -22.09 ‰ at 2.5 cm (Fig 4.4). Typical C3 plants have lower $\delta^{13}C$ values (-24 to -34 ‰) than C4 plants (-12 to -23 ‰) (Smith and Epsten 1971), and thus the HOM core appears to have carried a C3 plant signal throughout with a slight C4 component. $\delta^{13}C$ in bat guano can fluctuate with the relative abundance of C4 grasses (Wurster et al. 2007). Thus, although $\delta^{13}C$ values in the most recently deposited bat guano did not reach the average $\delta^{13}C$ values found in C4 plants, the increase in $\delta^{13}C$ likely indicates a shift toward a more C4 plant-based diet. The rise coincided with the agricultural history of Jamaica. The Taíno people, who first arrived in Jamaica in ~650 CE, used maize, a C4 plant, which may have contributed to the first gradual increase in $\delta^{13}C$ (Santos et al. 2013; Mickleburgh and Pagan-Jimenez 2012). Christopher Columbus subsequently introduced sugarcane, another C4 plant, to the Caribbean in the early 16th century (Found and Berbés-Blázquez 2012), which would have contributed further to the rise in $\delta^{13}C$ observed in the HOM core. Notably, there is a sugarcane plantation ~3 km north of HOM cave, thus foraging bats may consume insects supported by a C4-influenced diet.

The median $\delta^{15}N$ value was +12.9 ‰ (range: +9.8 to +18.5 ‰) throughout the guano deposit (Fig 4.4). $\delta^{15}N$ increased steadily in ca. 10th century CE, reached a value of +16.3 ‰ in

the 1870s CE, and then decreased to the lowest value of +9.8 ‰ by 2008 CE. Declining $\delta^{15}N$ in post-industrial deposits may reflect NO_x emissions from coal combustion, as coal $\delta^{15}N$ values are approximately 0 ‰ (Ding et al. 2018; Peterson and Fry 1987). $\delta^{15}N$ can also decrease with increasing anthropogenic emissions from fossil fuel combustion and synthetic fertilizers (Freyer 1978). World-wide use of synthetic nitrogen fertilizers incorporate atmospheric nitrogen and thus have lower $\delta^{15}N$ values (-1.7 to +3.9 ‰) (Vitoria et al. 2004). Lower $\delta^{15}N$ values observed post-1870 CE may also be influenced by decomposition (Peterson and Fry 1987). The slow and gradual rise in $\delta^{15}N$ pre-1870 CE may have resulted from increased ^{15}N from intensive manure fertilization, which can increase $\delta^{15}N$ values to ~+7 ‰ (Bogaard et al. 2013). Manure-based fertilizers were first used by Neolithic farmers (Bogaard et al. 2013), and elevated $\delta^{15}N$ values have also been observed in manure-influenced soils from the Bronze Age (Simpson et al. 1999). Consequently, consumption of plants and insects that were in contact with manure fertilizers and subsequently, synthesized fertilizers, could account for the shifts in the $\delta^{15}N$ values in the HOM core.

Changes in dietary $\delta^{34}S$ are reflected in bat guano (Salvarina et al. 2013), so long-term trends in dietary sulfur accumulation should also be traceable in the HOM core. The median $\delta^{34}S$ value was +18.0 ‰ (ranging from +9.7 to +22.4 ‰) (Fig 4.4). $\delta^{34}S$ was relatively constant pre-1930 CE, and then decreased post-1930 CE, and reached a minimum of +9.7 ‰ in ca. 1990 CE. The $\delta^{34}S$ values post-1930 CE began to approach sulfate $\delta^{34}S$ values associated with coal combustion, which are typically < +10 ‰ (Guo et al. 2016). Therefore, the HOM core could be tracking the increase in industrially sourced sulfur. The decrease in $\delta^{34}S$ could also be attributed to the use of fertilizer. With the exception of superphosphate fertilizers, which display a wide range of $\delta^{34}S$ values, from -4.2 to +17.2 ‰ (Chalk et al. 2017)), most fertilizers tend to have $\delta^{34}S$

values < +12 ‰ (Chalk et al. 2017). In particular, the prominent decrease in $\delta^{34}S$ in the early 1930s CE coincided with the introduction of a $CuSO_4$ fungicide, Bordeaux mixture, introduced to Central America to combat plant pathogenic fungi in the genus *Cercospora* (Wardlaw 1941). Bordeaux mixture typically contains 257-276 g kg^{-1} of copper (Arena et al. 2018), which may account for the elevated copper concentrations in the HOM core (Table S4.4). Soil-enriched copper has been observed in Bordeaux-sprayed areas, in one instance reaching 4,000 μg g^{-1} dw (Thrupp 1991). Copper is readily bound to organic matter (Couto et al. 2015), which may explain the greater copper concentrations in the bat guano relative to the soil. In the HOM core, Cu/Ti peaked in guano deposited in ca. 50 BCE (Fig 4.1), possibly the result of the mobility of copper in the deposit. Bordeaux mixture has been seen to leach 40 cm down-core in lake sediments, which can be attributed to the more mobile Cu^{2+} in the presence of dissolved organic matter (Couto et al. 2015). Cu^{2+} is prevalent in soils (> +43.5 %) when the pH is closer to neutral (4 to 7) (Komarek et al. 2009). Fresh bat guano typically has pH values ranging from 5.1 to 8.0 (Shahack-Gross et al. 2004; Wurster et al. 2015); the pH then becomes more acidic over time, ranging from 2.7 to 5.3 (Wurster et al. 2015). Consequently, the copper observed in the HOM core may have leached downwards as Cu^{2+} until the pH increased to the point that it no longer favoured the mobile Cu^{2+} form. The use of fertilizers and fungicides, as well as the increase in anthropogenic activity in the 20th century, likely drove the decrease in $\delta^{34}S$ values observed in the HOM core.

4 Conclusions

The HOM core provided a rare glimpse into the past ~4,300 years of tropical bat exposure to multiple anthropogenic influences, most notably metal contamination and changing agricultural practices. Bats that used this remote Jamaican cave were exposed to anthropogenic

metals, highlighting the importance of emission controls to reduce the risk of exposure to these contaminants. Bat populations around the world are under stress and declining as a consequence of human activities. Guano archives, although scarce, provide new insights into past diets and contaminant exposure. As such, these deposits can be used to monitor the spatial and temporal movement of contaminants that affect bats, humans, and other species.

Acknowledgements

The authors thank the Jamaican Caves Organization and the individuals involved in sample collection as well as NEPA for the permits.

Funding: This study was supported by Natural Sciences and Engineering Research Discovery Grants (RGPIN-217112-2013 and RGPIN-2018-04248) to JMB and grant number 2011/01/B/NZ8/02988 from the Polish National Science Centre to WB.

The authors declare no competing interests.

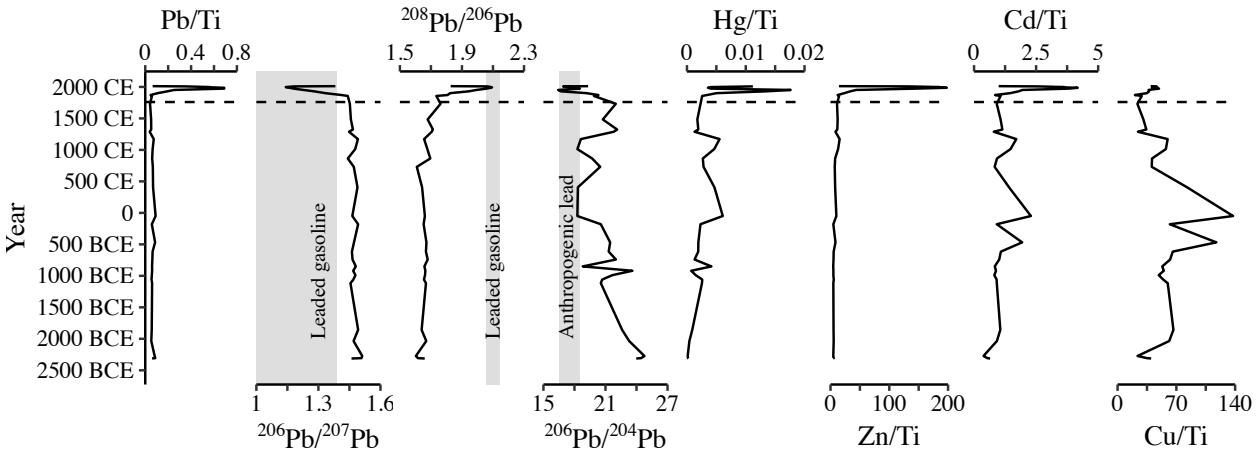

Figure 4.1: Lead ratios and metal concentrations in the HOM core. Metal concentrations are normalized to titanium in order to account for natural weathering. The dashed line separates bat guano deposited before and after 1760 (the year of the start of the Industrial Revolution). ^{210}Pb and ^{14}C years are presented on the y-axis. The shaded area indicates the range of values reported in leaded gasoline for $^{206}Pb/^{207}Pb$ (Sturges and Barrie 1987) and $^{208}Pb/^{206}Pb$ (Teutsch et al. 2001), and in the case of $^{206}Pb/^{204}Pb$, anthropogenic lead (Hansmann and Köppel 2000).

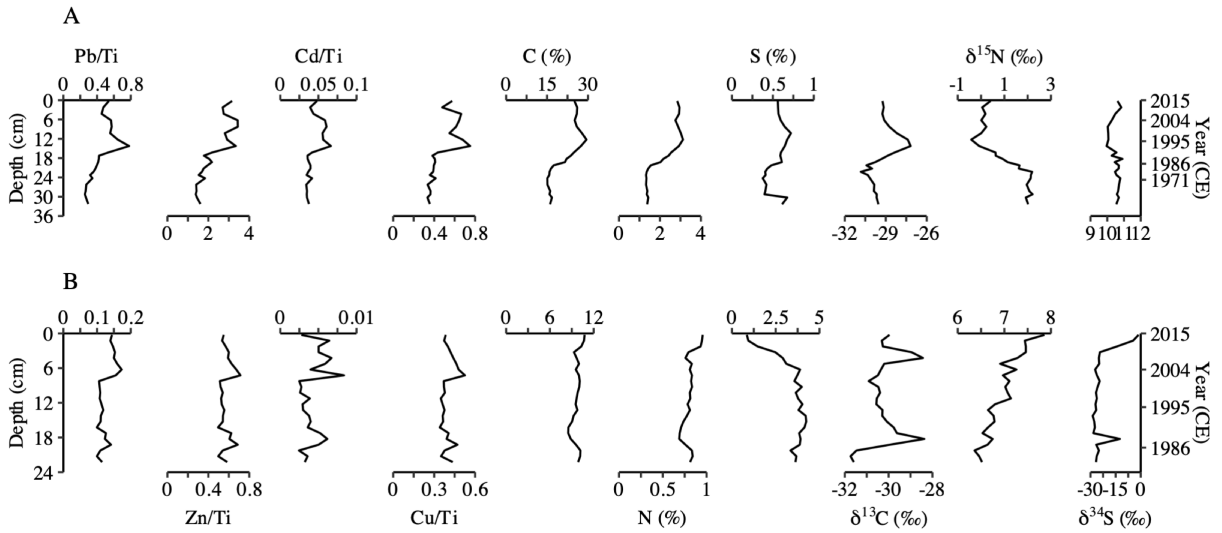

Figure 4.2: Metal, elemental, and stable isotope profiles in Wakefield Lake (panel A) and Crystal Lake (panel B) sediment cores. Metal concentrations are normalized to titanium to account for natural weathering. Select ^{210}Pb dates are presented on the right y-axis.

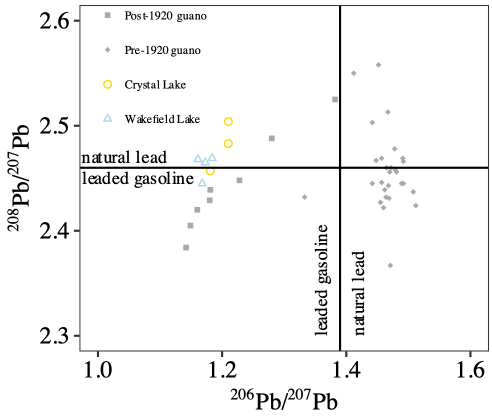

Figure 4.3: Pb isotope ratios in the HOM core in pre-1920 deposited guano and post-1920 deposited guano. Pb ratios in lake sediments from Crystal Lake and Wakefield Lake are also plotted. Lines divide the stable isotope values of naturally occurring lead from leaded gasoline (Emmanuel and Erel 2002).

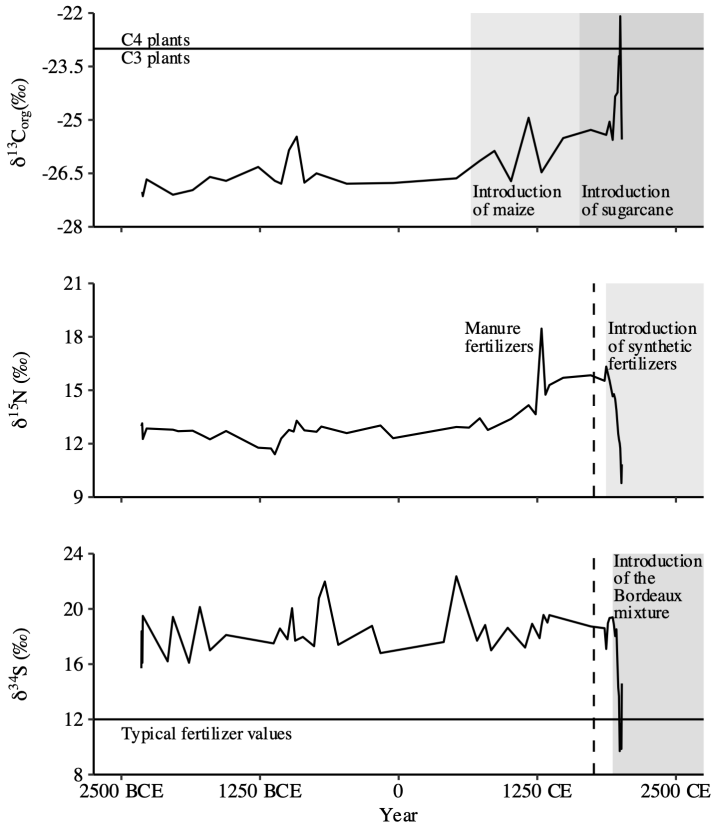

Figure 4.4: Stable isotope profiles in the HOM deposit graphed along the ^{210}Pb and ^{14}C dates. The dashed line indicates the year 1760 CE, the start of the Industrial Revolution. Org = organic.

Supplementary information

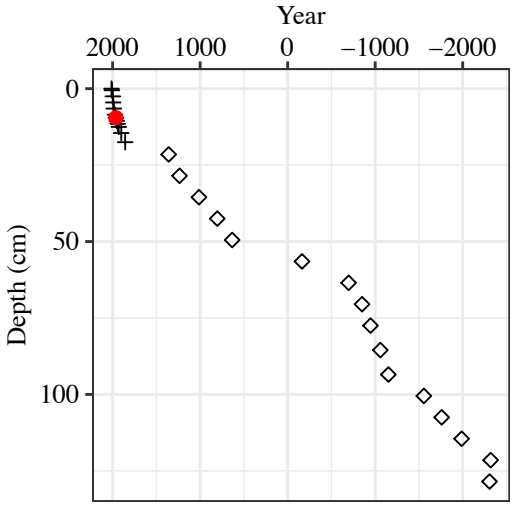

Figure S4.1: ^{210}Pb (+), peak ^{137}Cs (red circle), and ^{14}C (squares) dates in the bat guano deposits. A 580-year reservoir effect for radiocarbon was applied to the ^{14}C dates, based on the calculated difference between the ^{14}C date on material from the depth where the ^{210}Pb date was 1900 CE.

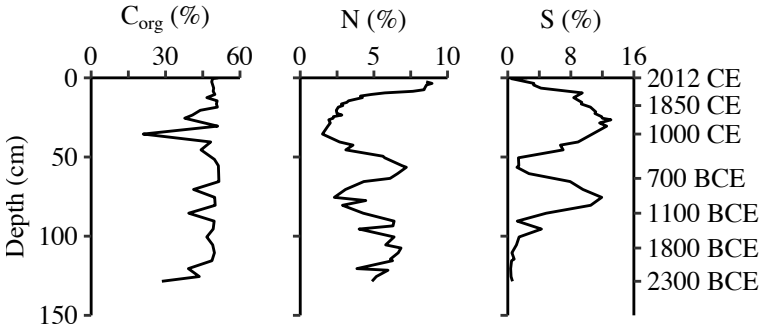

Figure S4.2: Percentage of organic carbon (C_{org}), nitrogen, and sulfur in the HOM deposit. Select estimated ^{210}Pb and ^{14}C dates are presented on the right y-axis.

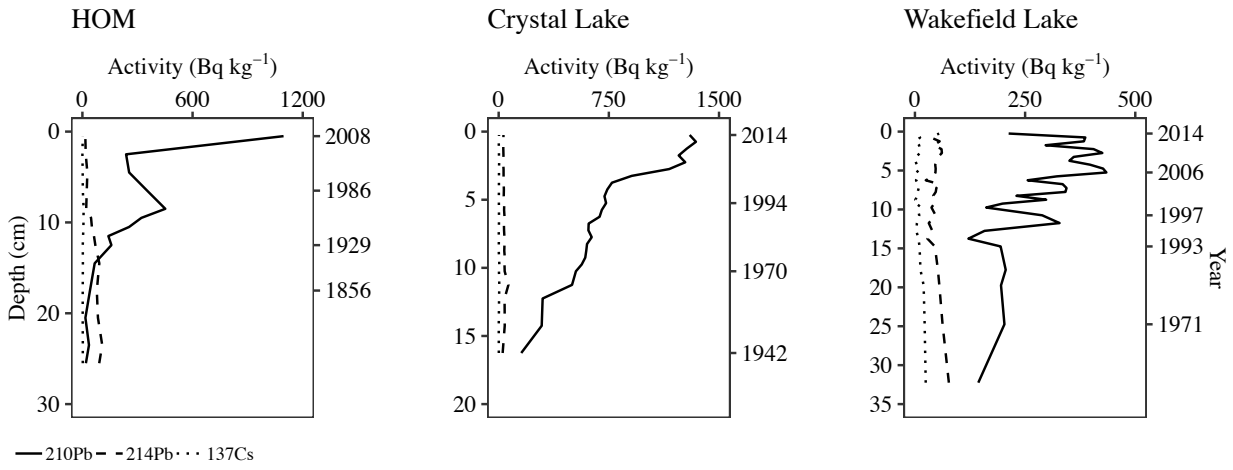

Figure S4.3: ^{210}Pb, ^{214}Pb, and ^{137}Cs activity in the HOM core, Crystal Lake, and Wakefield Lake. The constant rate of supply (CRS) model is used to infer year and is shown on the right y-axes.

Table S4.1: ^{14}C dates for lipid-treated and untreated bulk guano samples.

Depth (cm)	Lipid treated	Untreated
14.5	675 ± 30 BP	745 ± 30 BP
56.5	2625 ± 35 BP	2570 ± 35 BP
85.5	3310 ± 35 BP	3415 ± 25 BP

Table S4.2: Method detection limits (MDLs) for metals, presented in counts per second (CPS), calculated using 5 blanks.

Analyte	Standard deviation of the blanks (CPS)	Slope of calibration curve	MDL ($\mu g\ kg^{-1}$)
Cu	117543	14530	24.27
Zn	1918	2350	2.45
Cd	3.2	3381	0.00
Pb	588	26445	0.07
Ti	21	243	0.26

Table S4.3: Metal concentrations, metal ratios, and Pb isotope ratios in the lake sediments. All values are in μg g^{-1} dw. Sample size indicated by 'n'. min = minimum, max = maximum.

Crystal lake

n = 23	Pb	Zn	Cd	Cu
Median	1.31	5.92	0.04	4.13
Min-max	1.00-2.01	4.93-7.73	0.03-0.09	3.21-5.39
Median (metal/Ti)	0.12	0.55	0.004	0.38
Min-max (metal/Ti)	0.10-0.17	0.49-0.71	0.002-0.008	0.34-0.53
n = 3	$^{206}Pb/^{207}Pb$	$^{208}Pb/^{206}Pb$	$^{208}Pb/^{207}Pb$	$^{206}Pb/^{204}Pb$
Median	1.210	2.069	2.483	18.21
Min-max	1.181-1.210	2.051-2.081	2.457-2.504	18.13-18.60

Wakefield lake

n = 22	Pb	Zn	Cd	Cu
Median	2.27	11.60	0.23	2.49
Min-max	1.92-3.18	9.30-15.68	0.17-0.28	1.97-3.58
Median (metal/Ti)	0.42	2.00	0.04	0.41
Min-max (metal/Ti)	0.26-0.78	1.38-3.44	0.03-0.07	0.33-0.75
n = 4	$^{206}Pb/^{207}Pb$	$^{208}Pb/^{206}Pb$	$^{208}Pb/^{207}Pb$	$^{206}Pb/^{204}Pb$
Median	1.171	2.098	2.467	18.13
Min-max	1.161-1.184	2.086-2.125	2.445-2.469	17.70-18.46

Table S4.4: Metal concentrations, metal ratios, and Pb isotope ratios in the bat guano deposit. All values are in μg g^{-1} dry unless identified with '*', indicating mg g^{-1}. TOC = total organic carbon, min = minimum, max = maximum, CE = common era.

	Pb	Hg	Zn	Cd	Cu
Median (μg g^{-1})	8.04	0.18	997	92.8	3.92*
Min-max (μg g^{-1})	2.17-26.2	0.04-0.85	312-3,060	32.1-247	0.58-15.2*
Median (μg g^{-1} TOC)	17.9	0.41	2050	213	10.7*
Min-max (μg g^{-1} TOC)	4.27-81.7	0.09-1.72	627-6,190	65.6-503	1.18-32.7*
Median (metal/Ti)	0.06	0.002	8.37	1.04	45.8
Min-max (metal/Ti)	0.04-0.70	0-0.02	3.54-198	0.38-4.18	20.6-138
Pre-1850 CE median	0.06	0.002	5.44	0.92	54.3
Post-1850 CE median	0.25	0.004	43	1.95	39.4

	$^{206}Pb/^{207}Pb$	$^{208}Pb/^{206}Pb$	$^{208}Pb/^{207}Pb$	$^{206}Pb/^{204}Pb$
Median	1.461	1.678	2.446	20.52
Min-max	1.142-1.512	1.603-2.094	2.367-2.558	16.42-24.77
Pre-1850 CE median	1.469	1.664	2.446	21.45
Post-1850 CE median	1.228	1.994	2.439	18.09

Table S4.5: Average and standard error of Wakefield Lake (depth of sample = 21.5 cm, n = 3) and Crystal Lake (depth of sample = 13.5 cm, n = 3).

	Wakefield Lake		Crystal Lake	
Analyte	Average ($\mu g\ kg^{-1}$)	Standard error ($\mu g\ kg^{-1}$)	Average ($\mu g\ kg^{-1}$)	Standard error ($\mu g\ kg^{-1}$)
Cu	23.0	0.83	43.2	0.87
Zn	105	2.94	65.1	1.89
Cd	2.31	0.09	0.35	0.02
Pb	22.7	0.62	13.8	0.33
Ti	60.7	1.65	124	5.82
$^{206}Pb/^{207}Pb$	1.172	0.001	1.194	0.007
$^{208}Pb/^{206}Pb$	2.113	0.005	2.086	0.007
$^{208}Pb/^{207}Pb$	2.476	0.005	2.489	0.006
$^{206}Pb/^{204}Pb$	18.37	0.097	18.05	0.089

References

Afonso, E., P. Tournant, J. C. Foltete, P. Giraudoux, P. E. Baurand, S. Roue, V. Canella, D. Vey, and R. Scheifler. 2016. "Is the lesser horseshoe bat (*Rhinolophus hipposideros*) exposed to causes that may have contributed to its decline? A non-invasive approach." *Global Ecology and Conservation* 8 (October): 123–37.

Ahmad, Khaldoun, and Caroline Davies. 2017. "Stable isotope ($\delta^{13}C$ and $\delta^{15}N$) based interpretation of organic matter source and paleoenvironmental conditions in Al-Azraq basin, Jordan." *Appl. Geochem.* 78 (March): 49–60.

Arena, M., D. Auteri, S. Barmaz, G. Bellisai, A. Brancato, D. Brocca, L. Bura, et al. 2018. "Peer review of the pesticide risk assessment of the active substance copper compounds copper(I), copper(II) variants namely copper hydroxide, copper oxychloride, tribasic copper sulfate, copper(I) oxide, Bordeaux Mixture." *EFSA* 16 (1): 5152.

Becker, D. J., M. M. Chumchal, H. G. Broders, J. M. Korstian, E. L. Clare, T. R. Rainwater, S. G. Platt, N. B. Simmons, and M. B. Fenton. 2018. "Mercury bioaccumulation in bats reflects dietary connectivity to aquatic food webs." *Environ. Pollut.* 233 (February): 1076–85.

Bird, Michael I., Ella M. Boobyer, Charlotte Bryant, Helen A. Lewis, Victor Paz, and W. Edryd Stephens. 2007. "A long record of environmental change from bat guano deposits in Makangit Cave, Palawan, Philippines." *Earth and Environmental Science Transactions of the Royal Society of Edinburgh* 98 (1): 59–69.

Bogaard, A., R. Fraser, T. H. E. Heaton, M. Wallace, P. Vaiglova, M. Charles, G. Jones, et al. 2013. "Crop manuring and intensive land management by Europe's first farmers." *Proc. Natl. Acad. Sci. U. S. A*. 110 (31): 12589–94.

Brimble, Samantha K., Karen L. Foster, Mark L. Mallory, Robie W. Macdonald, John P. Smol, and Jules M Blais. 2009. "High Arctic ponds receiving biotransported nutrients from a nearby seabird colony are also subject to potentially toxic loadings of arsenic, cadmium, and zinc." *Environ. Toxicol. Chem.* 28 (11): 2426.

Chalk, P. M., C. T. Inacio, and D. Chen. 2017. "Tracing S dynamics in agro-ecosystems using S-34." *Soil Biol. Biochem* 114 (November): 295–308.

Clark, D. R. 1979. "Lead concentrations: Bats vs terrestrial small mammals collected near a major highway." *Environ. Sci. Technol.* 13 (3): 338–41.

Cooke, Colin A., and Mark B. Abbott. 2008. "A paleolimnological perspective on industrial-era metal pollution in the Central Andes, Peru." *Sci. Total Environ.* 393 (2–3): 262–72.

Cooke, Colin A., Mark B. Abbott, Alexander P. Wolfe, and John L Kittleson. 2007. "A millennium of metallurgy recorded by lake sediments from Morococha, Peruvian Andes." *Environ. Sci. Technol.* 41: 3469–74.

Cooke, Colin A., Prentiss H. Balcom, Harald Biester, Alexander P. Wolfe, and Mark Brenner. 2009. "Over three millennia of mercury pollution in the Peruvian Andes." *Proc. Natl. Acad. Sci. U.S.A.* 106 (22): 8830–34.

Couto, R. D., L. Benedet, J. J. Comin, P. Belli, S. R. Martins, L. C. Gatiboni, M. Radetski, C. M. de Valois, V. G. Ambrosini, and G. Brunetto. 2015. "Accumulation of copper and zinc fractions in vineyard soil in the mid-western region of Santa Catarina, Brazil." *Environ. Earth Sci.* 73 (10): 6379–86.

Ding, Dianshi, Guijian Liu, Biao Fu, and Wenjun Wang. 2018. "New insights into the nitrogen isotope compositions in coals from the Huainan Coalfield, Anhui Province, China: Influence of the distribution of nitrogen forms." *Energy Fuels* 32: 9380–87.

Draper, Grenville. 1986. “Blueschists and associated rocks in eastern Jamaica and their significance for Cretaceous plate-margin development in the northern Caribbean.” *Geol. Soc. Am. Bull.* 97 (1): 48–60.

Emmanuel, S, and Y. Erel. 2002. “Implications from concentrations and isotopic data for Pb partitioning processes in soils.” *Geochim. Cosmochim. Acta* 66 (14): 2517–27.

Engstrom, D. R., W. F. Fitzgerald, C. A. Cooke, C. H. Lamborg, P. E. Drevnick, E. B. Swain, S. J. Balogh, and P. H. Balcom. 2014. “Atmospheric Hg emissions from preindustrial gold and silver extraction in the Americas: A Reevaluation from lake-sediment archives.” *Environ. Sci. Technol.* 48 (12): 6533–43.

Erel, Yigal, Alain Veron, and Ludwik Halicz. 1997. “Tracing the transport of anthropogenic lead in the atmosphere and in soils using isotopic ratios.” *Geochim. Cosmochim. Acta* 61 (21): 4495–4505.

Evenset, A., G. N. Christensen, J. Carroll, A. Zaborska, U. Berger, D. Herzke, and D. Gregor. 2007. “Historical trends in persistent organic pollutants and metals recorded in sediment from Lake Ellasjoen, Bjornoya, Norwegian Arctic.” *Environ. Pollut.* 146 (1): 196–205.

Farmer, John G., Lorna J. Eades, Margaret C. Graham, and Jeffrey R. Bacon. 2000. “The changing nature of the $^{206}Pb/^{207}Pb$ isotopic ratio of lead in rainwater, Atmospheric particulates, pine needles and leaded petrol in Scotland, 1982-1998.” *J. Environ. Monit.* 2 (1): 49–57.

Fenton, Brock M., and Nancy B. Simmons. 2014. *A World of Science and Mystery*. University of Chicago Press.

Found, William, and Marta Berbés-Blázquez. 2012. “The sugar-cane landscape of the Caribbean Islands: Resilience, adaptation and transformation of the plantation social–ecological system.” In *Resilience and the Cultural Landscape*, edited by Tobias Plieninger and Claudia Bieling, 164–84. Cambridge: Cambridge University Press.

Freyer, H. D. 1978. “Preliminary ^{15}N studies on atmospheric nitrogenous trace gases.” *Pure Appl. Geophys.* 116 (2–3): 393–404.

Garrett, R. G., A. R. D. Porter, and P. A. Hunt. 2010. “An occurrence of cadmiferous phosphorite soil concretions in Jamaica.” *Appl. Geochem.* 25 (7): 1047–55.

Garrett, R. G., A. R. D. Porter, P. A. Hunt, and G. C. Lalor. 2008. “The presence of anomalous trace element levels in present day Jamaican soils and the geochemistry of Late-Miocene or Pliocene phosphorites.” *Appl. Geochem.* 23 (4): 822–34.

Glew, J.R., and J.P. Smol. 2016. “A push corer developed for retrieving high-resolution sediment cores from shallow waters.” *J. Paleolimnology* 56: 67–71.

Guo, Q. J., G. X. Zhu, H. Strauss, M. Peters, T. B. Chen, J. X. Yang, R. F. Wei, L. Y. Tian, and X. K. Han. 2016. “Tracing the sources of sulfur in Beijing soils with stable sulfur isotopes.” *Journal of Geochemical Exploration* 161 (February): 112–18.

Hansmann, W., and V. Köppel. 2000. “Lead-isotope as tracers of pollutants in soils.” *Chem. Geol.* 171 (1–2): 123–44.

Hernout, B. V., K. E. Arnold, C. J. McClean, M. Walls, M. Baxter, and A. B. A. Boxall. 2016. “A national level assessment of metal contamination in bats.” *Environ. Pollut.* 214 (July): 847–58.

Komarek, M., V. Ettler, V. Chrastny, and M. Mihaljevic. 2008. “Lead isotopes in environmental sciences: A review.” *Environ. Int.* 34 (4): 562–77.

Komarek, M., A. Vanek, V. Chrastny, J. Szakova, K. Kubova, P. Drahota, and J. Balik. 2009. "Retention of copper originating from different fungicides in contrasting soil types." *J. Hazard. Mater.* 166 (2–3): 1395–1402.

Kunz, Thomas H., Elizabeth Braun de Torrez, Dana Bauer, Tatyana Lobova, and Theodore H. Fleming. 2011. "Ecosystem services provided by bats: Ecosystem services provided by bats." *Ann. N. Y. Acad. Sci.* 1223 (1): 1–38.

Laird, Kathleen R., Biplob Das, and Brian F. Cumming. 2014. "Enrichment of uranium, arsenic, molybdenum, and selenium in sediment cores from boreal lakes adjacent to northern Saskatchewan uranium mines." *Lake and Reservoir Management* 30 (4): 344–57.

Last, W.M., and J.P. Smol. 2001. "Physical and Geochemical Methods." In *Tracking Environmental Changes Using Lake Sediments*. Vol. 2. Dordrecht, The Netherlands: Kluwer Academic Publishers.

Mickleburgh, H. L., and J. R. Pagan-Jimenez. 2012. "New insights into the consumption of maize and other food plants in the pre-Columbian Caribbean from starch grains trapped in human dental calculus." *J. Archaeol. Sci.* 39 (7): 2468–78.

Mizutani, Hiroshi, Donald A McFarlane, and Yuko Kabaya. 1992. "Nitrogen and carbon isotope studies of a bat guano core from Eagle Creek Cave, Arizona, USA." *Journal of the Mass Spectrometry Society of Japan* 40 (1): 57–65.

Nam, D. H., D. Yates, P. Ardapple, D. C. Evers, J. Schmerfeld, and N. Basu. 2012. "Elevated mercury exposure and neurochemical alterations in little brown bats (*Myotis lucifugus*) from a site with historical mercury contamination." *Ecotoxicology* 21 (4): 1094–1101.

Nriagu, Jerome O. 1990. "The rise and fall of leaded gasoline." *Sci. Total Environ.* 92: 13–28.

Nriagu, Jerome O, and Jozef M. Pacyna. 1988. "Quantitative assessment of worldwide contamination of air, water and soils by trace metals." *Nature* 333: 134–39.

Onac, Bogdan P., Ferenc L. Forray, Jonathan G. Wynn, and Alexandra M. Giurgiu. 2014. "Guano-derived $\delta^{13}C$ -based paleo-hydroclimate record from Gaura Cu Musca Cave, SW Romania." *Environ Earth Sci* 71 (9): 4061–69.

Onac, Bogdan P., Simon M. Hutchinson, Anca Geantă, Ferenc L. Forray, Jonathan G. Wynn, Alexandra M. Giurgiu, and Ioan Coroiu. 2015. "A 2500-yr late Holocene multi-proxy record of vegetation and hydrologic changes from a cave guano-clay sequence in SW Romania." *Quat. Res.* 83 (3): 437–48.

O'Shea, T. J., A. L. Everette, and L. E. Ellison. 2001. "Cyclodiene insecticide, DDE, DDT, arsenic, and mercury contamination of big brown bats (*Eptesicus fuscus*) foraging at a Colorado superfund site." *Arch. Environ. Contam. Toxicol.* 40 (1): 112–20.

Peterson, B. J., and B. Fry. 1987. "Stable isotopes in ecosystem studies." *Annu. Rev. Ecol. Evol. Syst.* 18: 293–320.

Pikula, J., J. Zukal, V. Adam, H. Bandouchova, M. Beklova, P. Hajkova, J. Horakova, R. Kizek, and L. Valentikova. 2010. "Heavy metals and metallothionein in Vespertilionid bats foraging over aquatic habitats in the Czech Republic." *Environ. Toxicol. Chem.* 29 (3): 501–6.

Rainford, Oral B., and Rohan A. Richards. 2008. "Sustainable Development and the Industrial Minerals Sector: Integrating the Principles of Sustainable Development within Jamaica's Industrial Minerals Sector." Biannual publication Volume 3, Number 1. Business, Finance & Economics in Emerging Economies. Caribbean Centre for Money & Finance.

Ramos-Rosas, N. N., C. Valdespino, J. Garcia-Hernandez, J. P. Gallo-Reynoso, and E. J. Olguin. 2013. "Heavy metals in the habitat and throughout the food chain of the neotropical otter,

Lontra longicaudis, in protected Mexican wetlands." *Environ. Monit. Assess.* 185 (2): 1163–73.

Salvarina, I., E. Yohannes, B. M. Siemers, and K. Koselj. 2013. "Advantages of using fecal samples for stable isotope analysis in bats: Evidence from a triple isotopic experiment." *Rapid Commun. Mass Spectrom.* 27 (17): 1945–53.

Santos, A. L., M. T. Gardner, and P. Allsworth-Jones. 2013. "Treponematosis in Pre-Columbian Jamaica: A biocultural approach to the human cranium found in Bull Savannah." *J. Archaeol. Sci.* 40 (1): 490–96.

Sañudo-Wilhelmy, Sergio A., and A.Russell Flegal. 1994. "Temporal variations in lead concentrations and isotopic composition in the Southern California Bight." *Geochim. Cosmochim. Acta* 58 (15): 3315–20.

Shahack-Gross, Ruth, Francesco Berna, Panagiotis Karkanas, and Steve Weiner. 2004. "Bat guano and preservation of archaeological remains in cave sites." *J. Archaeol. Sci.* 31 (9): 1259–72.

Simpson, I. A., R. Bol, I. D. Bull, R. P. Evershed, K. J. Petzke, and S. J. Dockrill. 1999. "Interpreting early land management through compound specific stable isotope analyses of archaeological soils." *Rapid Commun. Mass Spectrom.* 13 (13): 1315–19.

Smith, Bruce N, and Samuel Epsten. 1971. "Two categories of $^{13}C/^{12}C$ ratios for higher plants." *Plant Physiology* 47: 380–84.

Sturges, W. T., and L. A. Barrie. 1987. "Lead 206/207 isotope ratios in the atmosphere of North America as tracers of US and Canadian emissions." *Nature* 329 (6135): 144–46.

Teutsch, N., Y. Erel, L. Halicz, and A. Banin. 2001. "Distribution of natural and anthropogenic lead in Mediterranean soils." *Geochim. Cosmochim. Acta* 65 (17): 2853–64.

Thrupp, Lori Ann. 1991. "Long-term losses from accumulation of pesticide residues: A case of persistent copper toxicity in soils of Costa Rica." *Geoforum* 22 (1): 1–15.

Vitoria, L., N. Otero, A. Soler, and A. Canals. 2004. "Fertilizer characterization: Isotopic data (N, S, O, C, and Sr)." *Environ. Sci. Technol.* 38 (12): 3254–62.

Wardlaw, C. W. 1941. "The banana in Central America II. The control of Cercospora leaf disease." *Nature* 147: 344–49.

Weiss, Dominik, William Shotyk, Peter G. Appleby, Jan D. Kramers, and Andriy K. Cheburkin. 1999. "Atmospheric Pb deposition since the Industrial Revolution recorded by five Swiss peat profiles: Enrichment factors, fluxes, isotopic composition, and sources." *Environ. Sci. Technol.* 33 (9): 1340–52.

Widga, C., and M. Colburn. 2015. "Paleontology and paleoecology of guano deposits in Mammoth Cave, Kentucky, USA." *Quat. Res.* 83 (3): 427–36.

Wurster, C. M., D. A. McFarlane, and M. I. Bird. 2007. "Spatial and temporal expression of vegetation and atmospheric variability from stable carbon and nitrogen isotope analysis of bat guano in the southern United States." *Geochim. Cosmochim. Acta* 71 (13): 3302–10.

Wurster, Christopher M., Niels Munksgaard, Costijn Zwart, and Michael Bird. 2015. "The biogeochemistry of insectivorous cave guano: A case study from insular Southeast Asia." *Biogeochemistry* 124 (1–3): 163–75.

Wurster, Christopher M., Hamdi Rifai, Jordahna Haig, Jupiri Titin, Geraldine Jacobsen, and Michael Bird. 2017. "Stable isotope composition of cave guano from eastern Borneo reveals tropical environments over the past 15,000 Cal yr BP." *Palaeogeogr. Palaeoclimatol. Palaeoecol.* 473 (May): 73–81.

Zukal, Jan, Jiri Pikula, and Hana Bandouchova. 2015. “Bats as bioindicators of heavy metal pollution: History and prospect.” *Mamm. Biol.* 80 (3): 220–27.

Chapter 5: A 4,300-year history of bat foraging habits determined from a guano deposit in a Jamaican cave

Gallant, Lauren R[a]; Fenton, M. Brock[b]; Grooms, Christopher[c]; Bogdanowicz, Wieslaw[d], Stewart, R. Stefan[e], Clare, Elizabeth L.[f], Smol, John P[c]; and Blais, Jules M[a]

[a] Department of Biology, University of Ottawa, Ottawa, ON, K1N 6N5, Canada

[b] Department of Biology, University of Western Ontario, London, ON, N6A 5B7, Canada

[c] Paleoecological Environmental Assessment and Research Lab (PEARL), Department of Biology, Queen's University, Kingston, ON, K7L 3N6, Canada

[d] Museum and Institute of Zoology, Polish Academy of Sciences, 00-679 Warszawa, Poland

[e] Jamaican Caves Organization, Ewarton, Jamaica

[f] School of Biological and Chemical Sciences, Queen Mary University of London, London UK, E14NS

This article is being prepared for submission to Nature.

Author statement of contributions:

Gallant, Lauren R: study design, sample collection, lab work, data analysis and interpretation, and manuscript preparation. Fenton, M. Brock: study design, sample collection, peer review. Grooms, Christopher: sample collection and peer review. Bogdanowicz, Wieslaw: study design, sample collection, and peer review. Stewart, R. Stefan: sample collection and peer review. Clare, Elizabeth L: study design, sample collection, and peer review. Smol, John P: study design and

peer review. Blais, Jules M: study design, data analysis and interpretation, manuscript preparation, and peer review.

Keywords: sterols, stanols, ratios, isotopes, carbon, nitrogen

Abstract

We examined feeding strategies in bats based on the composition of sterols, stanols, and stable isotopes of carbon ($\delta^{13}C$) and nitrogen ($\delta^{15}N$) of bat guano in relation to a bat's dietary preferences for fruits, insects, or mammalian blood. In general, the guano of bats with animal-based diets had lower C/N ratios and higher cholesterol/(cholesterol+sitosterol) ratios than those with plant-based diets. We then examined the same suite of analytes in a ~4,300-year-old bat guano deposit from Jamaica to infer long-term changes in feeding strategies for this bat assemblage. Our multi-proxy analysis, based on a concordance of sterol ratios, $\delta^{13}C$, and C/N in the ~4,300-year old deposit, revealed two periods of increased frugivory relative to insectivory. Periods of increased frugivory relative to insectivory were observed at ca. 1000-500 BCE and ca. 700-1900 CE. These periods were characterized by wetter conditions in Central America, which we hypothesized favoured vegetation growth, and therefore resulted in greater frugivory relative to insectivory. This study demonstrated that dietary sources of stable isotopes, sterols, and stanols were reflective of different feeding habits in bat guano and provided a first glimpse of foraging habits in bats extending back over the past four millennia.

1 Introduction

Bats occupy a range of trophic niches reflecting diverse feeding strategies and diets[1]. Bats can consume up to 100 % of their body weight per day[1], such that lipids and stable isotopes of carbon and nitrogen in bat guano are representative of their recent diet[2–4]. In addition, changes in $\delta^{15}N$ values often reflect a bat's trophic position[5,6], with higher values in more carnivorous individuals[6]. Similarly, $\delta^{13}C$ values fluctuate based on diet. C3 plants have lower $\delta^{13}C$ values and are commonly found in more temperate environments, whereas C4 and Crassulacean acid metabolism (CAM) plants have greater $\delta^{13}C$ values and are typically found in more arid locations[7-9]. Previous studies have used stable isotopes to characterize the chemical composition of bat guano in different bat species based on their dietary preferences[10,11] and therefore long-term changes in foraging habits may be observed by coring and radiometrically dating bat guano deposits in caves inhabited by bats.

Whilst stable isotope analyses have been useful in trophic reconstructions, sterols and stanols offer a more specific means of determining differences in the chemical composition of bat guano based on dietary trends. Zoosterols (animal-derived) and phytosterols (plant-derived) play key roles in metabolism, cell signaling pathways, and membrane fluidity[12]. The zoosterol, cholesterol, is found in all mammals and constitutes a large percentage of the sterol profile in all mammalian faeces[13]. Coprostanol, produced by the microbial breakdown of cholesterol in higher mammals and birds, is detectable in faeces, and can thus be used as a paleolimnological marker as elevated concentrations are present in sewage-influenced lake sediments[13,14]. Faecal cholesterol concentrations generally increase in higher trophic level mammals[13] and, as such, increased concentrations of cholesterol and its metabolite coprostanol are expected in bats feeding at higher trophic levels.

Phytosterols can also be used to differentiate between dietary habits. Desmosterol is used to synthesize both sitosterol and stigmastanol in insects[15] and makes up a large proportion of total sterols in algae[16,17]. Sitosterol is highly concentrated in most plants[18–20] and reached concentrations of ~ 50 μg g^{-1} dw in High Arctic mosses[21] and 17 g kg^{-1} dw in plant-based oils[22]. Despite variable sitosterol concentrations in plants[22], sitosterol composes a large portion of mammalian dietary sterols and stanols, and thus sitosterol concentrations in mammalian faeces can exceed > 200 μg g^{-1} dw[23]. In mammals, sitosterol undergoes microbial reduction to stigmastanol and stigmastanol concentrations tend to be higher in herbivores relative to omnivores owing to dietary intake; e.g.: 1400 μg g^{-1} dw in sheep faeces compared to 160 μg g^{-1} dw in human faeces[23]. Therefore, phytosterol profiles in guano should reflect differences in the dietary consumption of phytosterols by bats.

We hypothesized that these differences in sterol and stanol patterns among plants and animals would reflect different feeding habits in the guano of bats that feed on a range of plants, insects, small vertebrates, and mammalian blood. We thus predicted that frugivorous bat guano would have greater concentrations of phytosterols than insectivorous and sanguinivorous bat guano and that sanguinivorous bat guano would have greater concentrations of zoosterols than insectivorous and frugivorous bat guano.

1.1 Objectives

We determined the $\delta^{13}C$, $\delta^{15}N$, C/N, sterol, and stanol composition of frugivorous, insectivorous, and sanguinivorous bat guano. We then used this information to infer long-term dietary shifts between the two main feeding categories (frugivorous and insectivorous, because sanguinivorous bats were absent) of a bat colony in Jamaica by analyzing these constituents in a ~4,300-year-old bat guano deposit.

2 Materials and Methods

2.1 Site description and guano collection

Fresh guano was collected from bats in Orange County, Belize, in May of 2016 and 2017, with permission from the Forest Department, Ministry of Agriculture, Fisheries, Forestry, the Environment and Sustainable Development, Belize and exported from Belize under an export permit issued to LRG from the Forest Department (reference numbers: WL/1/1/16(20) and WL/2/7/17(24)) and samples were imported to Canada under a permit to LRG issued by The Canadian Food Inspection Agency (A-2018-00359-4). Bats were captured using mist nets and identified to species in the field. Individual bats were then placed in cloth bags, genus was confirmed, and guano samples were collected. Bats were subsequently fed and released at their place of capture. Guano samples were air-dried in 2 mL microcentrifuge tubes and sealed until analysis. In total, we collected 37 samples from 18 different species. Chiropterologists assigned a feeding strategy (frugivorous, insectivorous, or sanguinivorous) to each bat based on previous studies that observed the feeding strategy and/or examined morphological traits associated with dietary requirements. In total, 1 sanguinivorous (3 samples), 12 insectivorous (23 samples), and 5 frugivorous (11 samples) species were collected (Table S5.1). Notably, we classified *Trachops cirrhosus* as an insectivorous bat, but it is also known to feed on small vertebrates[24].

A bat guano core was collected from Home Away from Home (HOM) cave, in the Parish of Trelawny, Jamaica. The GPS coordinates of the cave are confidential for conservation purposes, but inquiries from researchers may be sent to the Jamaican Caves Organization. A full description of the cave and collection methods can be found in Gallant et al.[25]. In brief, the cave is isolated from human activity with no evidence of human disturbance beyond the cave entrance. The cave is home to five species of bats, totaling ~ 5,000 individuals. The following

species of bats were identified using a combination of sonar (Song-Meter SM2BAT), mist netting, and a taxonomic key created by MBF and students: insectivorous *Pteronotus parnelli*, *Macrotus waterhousii*, and *Mormoops blainvillii*; nectivorous *Glossophaga soricina*; and frugivorous *Artibeus jamaicensis*. Notably, we classified *Glossophaga soricina* as a frugivorous bat for data analysis. No sanguinivorous bats were observed in the cave. A 129 cm core, sectioned into 1 cm intervals (10 cm by 10 cm cross-section), was excavated from the apex of the bat guano deposit. Samples were stored in Whirl-Pak® bags at -20°C until analysis.

2.2 ^{210}Pb and ^{14}C dating

The bat guano deposit was ^{210}Pb and ^{14}C dated at the University of Ottawa and the Poznań Radiocarbon Laboratory in Poland, respectively. Full methods and results are presented in Gallant et al.[25].

2.3 Sterols and stanols

Sterols and stanols were analyzed in the bat guano following the protocol outlined in Gallant et al. (under review)[26]. Briefly, sterols and stanols were extracted from 0.1 g of freeze-dried bat guano. Sterols and stanols were extracted by rinsing the material with dichloromethane (DCM) and sonicating the sample for ten minutes. Samples were evaporated to 1 mL and eluted through a 1 g LC-Si SPE columns (Sigma-Aldrich, Oakville, ON, Canada) using 20 mL of DCM. Samples were evaporated to dryness under nitrogen and a 10-fold dilution in toluene was created. Samples were derivatized for two hours at 60°C using 100 µL of 99 % N,O-bis(trimethylsilyl)trifluoroacetamide) + 1% trimethylchlorosilane. 100 ng of p-terphenyl-d_{14} (Cambridge Isotope Laboratories, Tewksbury, MA, USA) was added as a recovery standard.

Percent recoveries were determined by adding 100 ng of a ‘3-mix’ solution (5a-androstan-3-ol, 5a-pregnan-3b-ol, and 5a-pregnan-3-one) to seven replicates of 0.2 g of one

guano sample prior to sonication. The samples were extracted, and the remaining guano was evenly divided into two. 100 ng of the 3-mix solution was added to one half of the remaining guano and 100 ng of a '14-mix' solution (5α-androstan-3β-ol, 5α-pregnan-3β-ol, 5α-pregnan-3-one, 5β-cholestan-3β-ol, 5β-cholestan-3α-ol, 5β-cholestan-3-one, cholest-5-en-3β-ol, 5α-cholestan-3β-ol, 5α-cholestan-3-one, cholest-5,24-dien-3β-ol, campest-5-en-3β-ol, stigmasta-5,24-dien-3β-ol, β-sitosterol, 5α-stigmastan-3β-ol) was added to the other half of the remaining guano. Both sets of samples, and an additional sample containing only 100 ng of the 14-mix, were extracted following the same protocol. Percent recoveries were calculated by subtracting the concentration of each compound in the 3-mix-spiked guano from the 14-mix-spiked guano and dividing by the concentration of each compound in the 14-mix. The mean percent recovery (n = 7) of the 3-mix was 89.1 % (5a-androstan-3-ol: 87.6 %, 5a-pregnan-3b-ol: 85.0 %, and 5a-pregnan-3-one: 94.6 %). The mean and standard deviation (SD) percent recovery of the sterols and stanols was 92.1 ± 4.3 %, ranging from 87.0 to 103 % (Table S5.2). Owing to high and consistent percent recoveries, samples were not recovery corrected.

All samples were injected on an Agilent 6890 gas chromatograph – 5973 mass selective detector in electron impact, selected ion monitoring mode (Agilent 19091J-433 HP-5 5% phenyl methyl siloxane 29.8 m x 250 μm x 0.25 μm column). Analytical conditions include: a pulsed splitless injection at 250°C at 17.75 psi (17.17 psi for the fresh bat guano samples), DB-5MS (Agilent, Santa Clara, CA, USA), oven start at 150°C, ramp 1 at 8°C $minute^{-1}$ to 250°C, ramp 2 at 12°C $minute^{-1}$ to 300°C held for 12 minutes. Mass selective conditions as follows: transfer line 300°C, source 230°C, quad 150°C. Sterol concentrations were volume corrected to p-terphenyl-d_{14} using MSD ChemStation D.02.00.275.

We measured the guano samples for eleven sterols and stanols: coprostanol (5β-cholestan-3β-ol), epicoprostanol (5β-cholestan-3α-ol), coprostanone (5β-cholestan-3-one), cholesterol (cholest-5-en-3β-ol), cholestanol (5α-cholestan-3β-ol), cholestanone (5α-cholestan-3-one), campesterol (campest-5-en-3β-ol), desmosterol (3β-cholesta-5,24-dien-3-ol), fucosterol (stigmasta-5,24-dien-3β-ol), sitosterol (β-sitosterol), and stigmastanol (5α-stigmastano-3β-ol). Analytes were blank corrected and corrected to their respective method detection limits (MDLs) (Tables S5.3 and S5.4).

2.4 Stable isotopes

Fresh bat guano samples were analyzed for organic carbon and nitrogen stable isotopes following the protocol in Gallant et al.[25]. Guano samples were not acidified for organic $\delta^{13}C$ because values (mean ± SD) in a paired subset of acidified (-24.8 ± 0.5 ‰, n = 10) and unacidified (-25.2 ± 0.4 ‰, n = 10) bat guano samples were essentially identical. Carbon and nitrogen isotopes were therefore determined simultaneously on non-acidified samples.

3 Results

3.1 Stable isotopes by diet

Mean ± SD carbon to nitrogen ratio (C/N) values were 25 ± 13 (n = 9) in frugivorous, 4.7 ± 1.1 (n = 17) in insectivorous, and 5.7 ± 1.2 (n = 2) in sanguinivorous bat guano (Fig 5.1). Mean $\delta^{15}N$ was 4.8 ± 2.8 ‰ (n = 9) in frugivorous, 4.8 ± 2.2 ‰ (n = 17) in insectivorous, and 5.9 ± 3.4 ‰ (n = 2) in sanguinivorous bat guano. Mean $\delta^{13}C$ was -28 ± 0.2 ‰ (n = 9) in frugivorous, -27 ± 0.8 ‰ (n = 17) in insectivorous, and -18 ± 0.8 ‰ (n = 2) in sanguinivorous bat guano.

3.2 Sterol and stanol ratios by diet

We examined two sterol and stanol ratios in bat guano to identify different foraging habits: a trophic level index: cholesterol/ (cholesterol+sitosterol), and an expanded index: (cholesterol+cholestanol)/(cholesterol+cholestanol+sitosterol+stigmastanol). These ratios can provide information on whether their diets are more plant- or animal-based. Frugivorous bat guano was characterized by low trophic level and expanded index values and high C/N values, whereas the opposite was true of insectivorous bat guano. Mean trophic level index values increased with trophic level with values of 0.6 ± 0.3 (n = 11) in frugivorous, 0.8 ± 0.3 (n = 23) in insectivorous, and 1 (n = 2) in sanguinivorous bat guano (Fig 5.1). Likewise, mean expanded index values increased with trophic level with values of 0.6 ± 0.3 (n = 11) in frugivorous, 0.8 ± 0.3 (n = 23) in insectivorous, and 1 (n = 2) in sanguinivorous bat guano (Fig 5.1).

3.3 Historical stable isotope composition

The stable isotope composition of the bat guano deposit was previously reported in Gallant et al.[25]. In summary, $\delta^{13}C$ values in the bat guano deposit ranged from -27.1 to -22.1 ‰ and $\delta^{15}N$ values ranged from 9.8 to 18.5 ‰ (Fig 5.2). The C/N ratio ranged from 4.8 to 27, with two peaks of 22 (ca. 900 BCE) and 27 (ca. 1200 CE). Trophic level and expanded index values were generally low in guano deposited between ca. 1700 BCE and ca. 1300 BCE (0.7, 0.5, n = 1), ca. 1000 BCE and ca. 500 BCE (0.7 ± 0.1, 0.6 ± 0.1, n = 4), and ca. 700 CE and ca. 1900 CE (0.4 ± 0.2, 0.5 ± 0.1, n = 9), respectively (Fig 5.2). Notably, C/N peaks coincided with the periods of decreased trophic level and expanded index values.

3.4 Sterols and stanols

Mean sterol and stanol concentrations in fresh guano (Fig S5.1) where generally greater than the maximum sterol and stanol concentrations in the guano deposit (Fig 5.3). Mean

coprostanol and epicoprostanol concentrations in insectivorous bat guano were > 7.5 and > 27-fold greater than background concentrations in bat guano deposited prior to 1900. Similarly, the mean cholesterol concentration in fresh insectivorous bat guano was > 48-fold greater than the peak cholesterol concentration in the bat guano deposit. Maximum concentrations in the fresh guano of all three diets always exceeded the maximum concentration in the guano deposit. The lower sterol and stanol concentrations in sub-surface bat guano, relative to the fresh bat guano, suggested some degradation of sterols and stanols through time (Fig 5.3). As such, this further justified the use of the sterol and stanol ratios as fluctuations in the relative proportion of zoosterols and phytosterols may be detectable, despite the lower concentrations.

In the bat guano deposit, concentrations of coprostanol (0.001 to 0.04 μg g^{-1} dw) and epicoprostanol (0.008 to 0.03 μg g^{-1} dw) were generally low until the 1900s, when concentrations peaked at 0.26 and 0.24 μg g^{-1} dw, respectively (Fig 5.3). Coprostanone was generally undetected within the bat guano deposit, with the exception of one surface peak, where the concentration reached 1.8 μg g^{-1} dw. The concentration of cholesterol rose at ca. 1060 BCE (16 μg g^{-1} dw), and the peak cholesterol concentration was observed in the surface sample (57 μg g^{-1} dw). The concentration of cholestanol also exhibited a small increase at approximately the same time (ca. 1600 BCE; 4.0 μg g^{-1} dw) and peaked in the most recently deposited guano (7.5 μg g^{-1} dw).

The concentration of phytosterols fluctuated coeval with changes in the zoosterols (Fig 5.3). Prior to the 20th century, the concentrations of desmosterol, fucosterol, and sitosterol were below the MDL; peak concentrations of these sterols occurred in the most recently deposited guano (4.0 μg g^{-1} dw, 3.7 μg g^{-1} dw, and 12 μg g^{-1} dw, respectively). Campesterol peaked slightly at ca. 1060 BCE and reached its maximum concentration in the most recently deposited guano

(8.6 μg g^{-1} dw). The concentration of stigmastanol was elevated between ca. 2040 BCE and ca. 730 CE (peak concentration of 4.1 μg g^{-1} dw at ca. 1600 BCE) and the highest concentration occurred in the most recently deposited guano (7.2 μg g^{-1} dw).

When sterols and stanols were normalized to organic carbon, profiles were nearly identical to the dry weight normalized concentrations (Fig S5.2), indicating the composition of organic carbon was not a major influence on the sterol and stanol composition of the bat guano deposit. Consequently, we examined all sterols and stanols in μg g^{-1} dw in order to maintain consistency between the fresh bat guano (where low sample volume precluded acidification) and the bat guano deposit.

4 Discussion

4.1 Stable isotopes and C/N by diet

We recorded different mean $\delta^{13}C$ values in sanguinivorous bat guano (-18 ‰), relative to frugivorous (-28 ‰) and insectivorous (-27 ‰) bat guano (Fig 5.1). This is likely because insectivorous bats consumed aquatic insects while frugivorous bats largely consumed C3 plants, which would have contributed to more negative $\delta^{13}C$ values[27]. Sanguinivorous bats, however, largely feed on mammals such as domesticated cattle, which feed on C4 grains that have more positive $\delta^{13}C$ values[28,29], thus resulting in greater $\delta^{13}C$ values in their guano. Indeed, the values recorded in this study approach those in the wing tissue of *Desmodus rotundus* feeding on livestock[29]. Mean $\delta^{15}N$ values in sanguinivorous bat guano (5.9 ‰) were only slightly greater than those in insectivorous (4.8 ‰) and frugivorous (4.8 ‰) bat guano (Fig 5.1). We thus surmised that both the sanguinivorous and insectivorous bats in this study were feeding on primary consumers, which resulted in similar $\delta^{15}N$ values in their guano. Stable isotopes of

carbon and nitrogen in fresh bat guano thus reflected the foraging habits of bats but did not reflect trophic level (Fig 5.1).

We found that C/N values best reflected trophic level, as evidenced by greater C/N values in frugivorous bat guano relative to insectivorous and sanguinivorous bat guano (Fig 5.1). Insectivorous bats feed on aquatic insects, which was supported by C/N values below 10 in their fresh guano (Fig 5.1). Conversely, C/N values greater than 10 indicate a greater input of terrestrial vegetation[30], and indeed, C/N values in fresh guano from frugivorous bats ranged from 19.4 to 30.3 as expected for bats feeding on terrestrial fruits. Furthermore, fruit pulp is generally low in nitrogen (<1%)[31], and as such, we observed greater C/N ratios in bats feeding predominantly on fruits. These results suggested that while dietary stable isotopes were variable within a trophic level, the dietary proportion of carbon and nitrogen were more stable within a trophic level and as such, C/N may better reflect a bat's trophic level. For example, percent nitrogen in fruits ranged from 0.07 to 3.2 while $\delta^{15}N$ values ranged from -0.85 to 13.5 ‰[32].

4.2 Examining historical foraging habits

We observed a remarkable concordance between C/N, $\delta^{13}C$, and trophic level index values in the 4,300-year-old bat guano deposit consistent with frugivorous and insectivorous foraging (Fig 5.2). Based on this multi-proxy evidence, we observed two periods of increased frugivory relative to insectivory in the bat guano deposit: ca. 1000-500 BCE and ca. 700-1900 CE) (Fig 5.2). There is no record of sanguinivorous bats in Jamaica[33], thus we attributed greater C/N values in the bat guano deposit to an increase in the relative contribution of frugivory to insectivory-based foraging**.**

Greater $\delta^{13}C$ values recorded in our bat guano deposit also tracked two periods of increased frugivory/insectivory-based foraging (Fig 5.2). Fruits are fat-depleted relative to

insects[34], so frugivorous bats tend to have greater $\delta^{13}C$ values than insectivorous bats. Conversely, fat is typically enriched in ^{12}C relative to ^{13}C resulting in lower $\delta^{13}C$ values in animal tissues consuming a fat-rich diet[34,35]. Furthermore, $\delta^{13}C$ values of bananas and cane sugar are approximately -23.7 ‰ and -10.4 ‰, respectively[36], and thus an increase in frugivory/insectivory could result in greater $\delta^{13}C$ values. We thus concluded that $\delta^{13}C$ values in this guano deposit increased in response to periods of greater frugivory/insectivory-based foraging habits of the bat colony.

We also employed the use of sterol and stanol ratios in order to examine long-term changes in the foraging habits of the bat colony (Fig 5.2). The trophic level index can be used to infer the influence of higher trophic level species because cholesterol concentrations tend to be greater in higher trophic level mammals[23]. Furthermore, cholesterol concentrations were generally greater in insectivorous bat guano relative to frugivorous bat guano (Fig S5.1). We thus predicted that a higher trophic level index in the bat guano deposit would indicate greater insectivory/frugivory. Indeed, the trophic level index values were generally lower in the guano deposit during periods of higher C/N and $\delta^{13}C$ values (Fig 5.2), suggesting a greater influence of frugivory/insectivory-based foraging.

Sterols are susceptible to *in situ* degradation under aerobic conditions[37]. In order to account for the degradation of sterols within the bat guano deposit, we also examined an expanded index that included the stanol degradation products, cholestanol and stigmastanol (Fig 5.2). This index was used in a study, which tracked the presence of bird guano in lake sediments[38]. The expanded index and trophic level index in our bat guano deposit tracked one another almost exactly. This was expected because the concentrations of cholestanol and stigmastanol fluctuated coeval with their precursor sterols (Fig 5.3), thus the relative contribution

of stanols in the guano deposit did not change through time. Indeed, cholestanol and stigmastanol have been shown to be highly stable in lake sediments over time[39] and our results suggested that these stanols were more stable within the bat guano deposit relative to the other sterols and stanols. Consequently, elevated C/N and $\delta^{13}C$ values, coincident with decreased sterol and stanol ratios within the bat guano deposit, tracked two periods of increased frugivory over the past 4,300 years, which is precisely what we would predict if sterol and C/N ratios were each inversely tracking the bat colony's frugivory/insectivory ratio (Fig 5.2).

4.3 Increased frugivory and climate

These periods of increased frugivory/insectivory occurred during periods of wetter climactic conditions in the Caribbean, as evidenced by lower $\delta^{18}O$ values in ostracod shells; drier conditions were recorded between these wetter periods, as characterized by higher $\delta^{18}O$ values and higher Sr/Ca values, (as a result of increased evaporation and decreased precipitation)[40,41]. Following a period of increased precipitation in ca. 1250 BCE, there was a dry period, as determined by increased plants of the genus *Cepcropia* and *Trema*, and the establishment of dry forests[40]. The wetter period, beginning in ca. 700 CE, was characterized by lower $\delta^{18}O$ and $\delta^{13}C$ values in micrite and the establishment of new ostracod species, signifying a flooding event[41]. Sr/Ca values also decreased during this period, indicating decreased evaporation and increased precipitation[41]. Periods of increased precipitation favour increased plant growth[42,43], and thus we hypothesize that we observed an increase in frugivory-based foraging owing to increased food availability. Furthermore, bats are known to modify their foraging habits based on climactic conditions[44] and thus we suspect that periods of wetter conditions favoured frugivory over insectivory owing to increased primary fruit production.

Increased $\delta^{13}C$ values also coincided with periods of wetter climactic conditions. While lower $\delta^{13}C$ are usually associated with C3 plants, C4 grasses having a minimum water requirement such that C4 grasses do not necessarily flourish under dry conditions[45]. Furthermore, some C3 plants are able to survive on sub-surface water stores, and thus $\delta^{13}C$ values may not necessarily increase in response to increased precipitation[46]. Similar results were observed in a bat guano deposit from the United States, where $\delta^{13}C$ values increased in association with increased summer precipitation[3,8].

The $\delta^{15}N$ values within the bat guano deposit did not decrease to reflect lower trophic level foraging (Fig 5.2). Instead, researchers have postulated that greater $\delta^{15}N$ values in bat guano may reflect the consumption of C4 nectars, which have elevated $\delta^{15}N$ values (e.g. 13.5 ‰ in cane sugar)[32]. Moreover, $\delta^{15}N$ values in the bat guano deposit (9.8 to 18.5 ‰) were greater than those in the fresh bat guano (e.g. mean of 5.9 ‰ in sanguinivorous bats), suggesting influence by other factors. Indeed, we previously related fluctuations in $\delta^{15}N$ in this bat guano deposit to changes in fertilizer use as early as 1100 CE[25,47,48].

5 Conclusions

We determined the sterol, stanol, and stable isotope composition in fresh bat guano and a ~4,300-year-old bat guano deposit. Increased C/N and $\delta^{13}C$ values coupled with decreased sterol ratio values in the bat guano deposit marked two periods of greater frugivory/insectivory foraging habits by the bat colony. We were further able to associate wetter climactic conditions to these periods of increased frugivory/insectivory as a result of increased fruit availability. We found that stable isotopes of carbon and nitrogen in fresh guano best reflected bat foraging habits while C/N values in fresh bat guano most effectively identified trophic level as frugivorous bats generally consumed less nitrogen, regardless of the stable isotope composition of their diet**.** The

concentration of cholesterol in fresh bat guano increased according to trophic level and thus may be useful in identifying different feeding strategies in bats based on the chemical composition of their guano. Concentrations of campesterol, sitosterol, and stigmastanol in fresh guano were generally similar among frugivorous and insectivorous bats but were absent in sanguinivorous bats. We surmised that sterols, stanols, and stable isotopes in bat guano were reflective of a bat's diet and that the chemical analysis of intact bat guano deposits permits inference of long-term changes in feeding patterns and thus demographic changes in bat community composition.

Acknowledgements

The authors thank the field work crew for their help in capturing and identifying bats in Belize. In particular, we thank Dr. Nancy Simmons for organizing and coordinating the field seasons. We thank the staff at Lamanai Outpost Lodge for lodging and support. This study was supported by Natural Sciences and Engineering Research Council of Canada Grants (RGPIN-217112-2013 and RGPIN-2018-04248) to JMB and grant number 2011/01/B/NZ8/02988 from the Polish National Science Centre to WB.

The authors declare no competing interests.

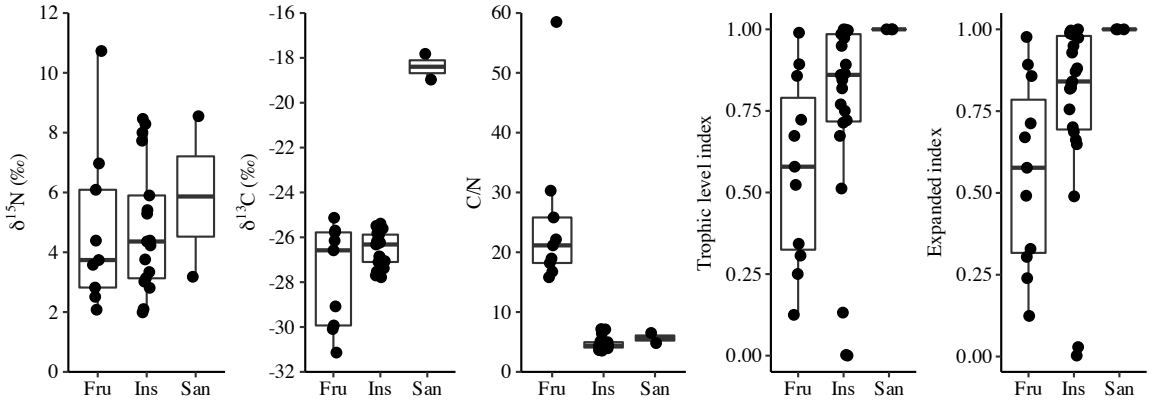

Figure 5.1: Boxplot of nitrogen and carbon stable isotopes, the ratio of carbon to nitrogen (C/N), the trophic level index (cholesterol / (cholesterol + sitosterol)), and the expanded index ((cholesterol + cholestanol) / (cholesterol + cholestanol + sitosterol + stigmastanol)) in fresh bat guano. Fru = frugivorous, Ins = insectivorous, San = sanguinivorous.

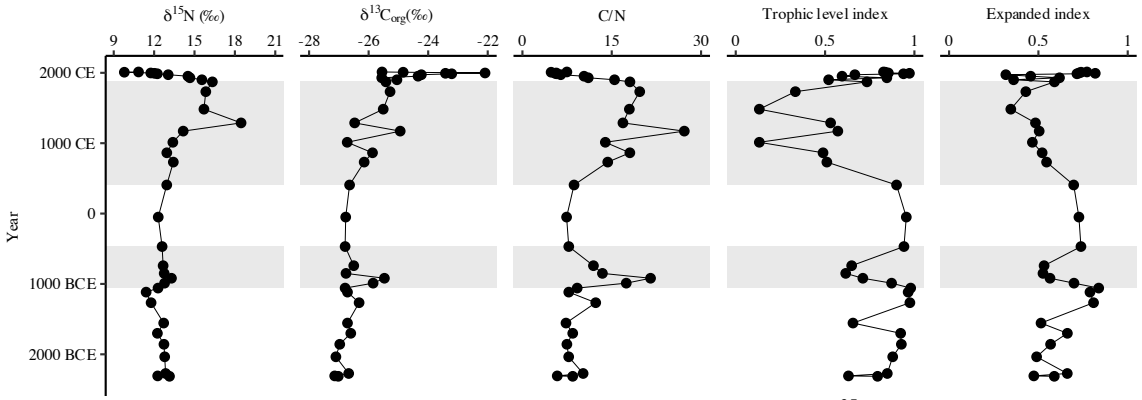

Figure 5.2: Stable isotope profiles (as previously published in Gallant et al.[25]), sterol ratios, and the C/N ratio in the bat guano deposit. Gray shaded areas represent periods with a greater influence of frugivory relative to insectivory foraging habits. Trophic level index = cholesterol / (cholesterol + sitosterol). Expanded index = (cholesterol + cholestanol) / (cholesterol + cholestanol + sitosterol + stigmastanol).

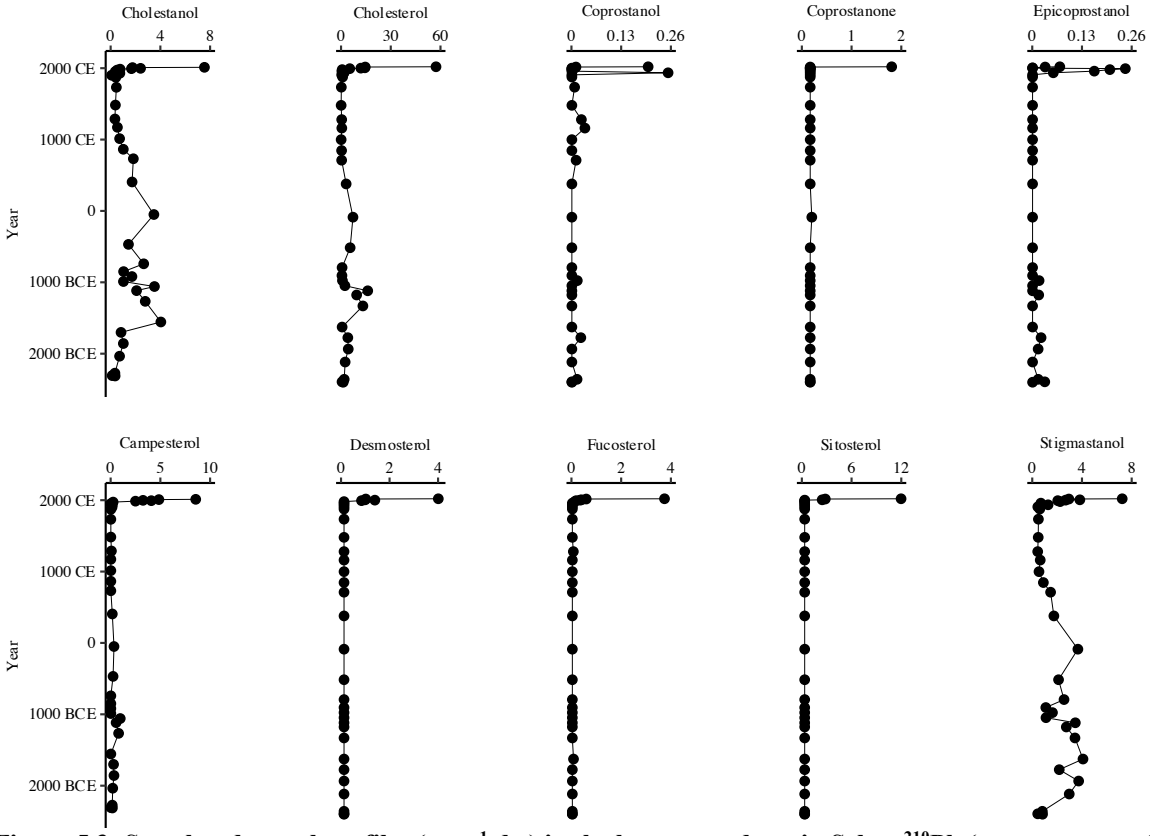

Figure 5.3: Sterol and stanol profiles (µg g^{-1} dw) in the bat guano deposit. Select ^{210}Pb (constant rate of supply model) and ^{14}C dates are shown on the y-axis.

Supplementary information

We examined the sterol and stanol composition of guano from frugivorous, insectivorous, and sanguinivorous bats to determine whether the chemical composition of bat guano was characteristic of foraging behaviour. Phytosterol concentrations of campesterol, fucosterol, sitosterol, and stigmastanol, were greater in frugivorous (27 ± 19, 0.68 ± 0.95, 82 ± 110, and 3.2 ± 5.4 μg g^{-1} dw, n = 11) and insectivorous guano (91 ± 230, 25 ± 60, 120 ± 300, and 16 ± 57 μg g^{-1} dw, n = 23) than in sanguinivorous guano (0.02, 0.03, 0.31, and 0.40 μg g^{-1} dw, n = 3), respectively (Fig S5.1). Mean zoosterol concentrations of coprostanol (0.35 ± 1.2 μg g^{-1} dw, n = 23) and epicoprostanol (0.82 ± 3.8 μg g^{-1} dw, n = 23) were highest in insectivorous bat guano, and nearly absent in frugivorous and sanguinivorous guano (<0.013 ± 0.04 μg g^{-1} dw in all instances, n = 11). Mean cholestanol and cholesterol in guano increased according to trophic level: 0.10 ± 0.3 and 260 ± 620 μg g^{-1} dw in frugivorous guano (n = 11), 16 ± 29 and 2,800 ± 5400 μg g^{-1} dw in insectivorous guano (n = 23), and 46 ± 1.4 and 23,000 ± 5700 μg g^{-1} dw in sanguinivorous guano (n = 3), respectively. Mean desmosterol was greatest in insectivorous guano (1.5 ± 4.9 μg g^{-1} dw, n = 11) and below the MDL in frugivorous and sanguinivorous guano (0.12 ± 0.0 μg g^{-1} dw, n = 23). Notably, only 3 of the 23 insectivorous guano samples had detectable concentrations of desmosterol.

Insectivorous and sanguinivorous bats occupy a higher trophic level than frugivorous bats and thus we predicted that their guano would have higher concentrations of zoosterols than frugivorous bat guano. Accordingly, cholesterol was generally more concentrated in insectivorous bat guano than in frugivorous bat guano (Fig S5.1). Sanguinivorous bat guano had the highest cholesterol concentrations, which can be attributed to the consumption of blood of domesticated animals, where cholesterol concentrations are approximately 27 to 60 μg L^{-1} [49].

Cholestanol is found in insects as it can play an important role in maintaining cell structure[12,19], but it is also present in mammals at low concentrations (< 0.2 % of cholesterol)[50]. In faeces, the proportion of cholestanol is greater (ratio of cholestanol to cholesterol of 1:4 in cattle faeces and 1:8 in human faeces), with concentrations of 90 μg g^{-1} dw in cattle faeces and 96 μg g^{-1} dw in human faeces[23]. Cholestanol is not commonly found in plants[19] and not surprisingly, cholestanol was more concentrated in insectivorous bat guano than in frugivorous bat guano (Fig S5.1). We expected sanguinivorous bats to have higher cholestanol concentrations owing to their higher cholesterol concentrations (because greater cholesterol concentrations should result in greater cholestanol concentrations if the same proportion of cholesterol is transformed). However, cholestanol concentrations in sanguinivorous bat guano (45 to 48 μg g^{-1} dw) fell within the range observed in insectivorous bat guano (20 to 99 μg g^{-1} dw), suggesting that the proportion of cholesterol converted to cholestanol is not the same among all bat species.

Coprostanol is formed from the reduction of cholesterol in the gut of higher mammals[14]. Accordingly, coprostanol in frugivorous bat guano reached a maximum of 0.07 μg g^{-1} dw, versus a minimum of 5.4 μg g^{-1} dw in insectivorous bat guano. Given that sanguinivorous bats occupy a similar trophic level to insectivorous bats[51] and that cholesterol was elevated in sanguinivorous bat guano, it was unexpected that coprostanol in sanguinivorous bat guano was nearly equal to that in frugivorous bat guano (Fig S5.1). In humans, the proportion of cholesterol converted to coprostanol is highly variable, ranging from nearly none to nearly all[52], and thus the lower coprostanol concentrations may also reflect a low conversion rate of cholesterol to coprostanol in *Desmodus rotundus*.

Campesterol is elevated in vegetation (e.g., 50 to 660 μg g^{-1} dw in plant oils)[22] as well as in insects, composing anywhere from 0.6 to 95 % of the total sterol composition[12]. Given the

elevated campesterol concentrations in the diets of both frugivorous and insectivorous bats, it follows that campesterol concentrations were similar between frugivorous and insectivorous bat guano (Fig S5.1). The variability of campesterol concentrations in insects was also evident within insectivorous bat guano, where campesterol concentrations ranged from 0.018 μg g^{-1} dw (equal to that in frugivorous bat guano) to 1050 μg g^{-1} dw. Conversely, campesterol concentrations are generally low in mammalian blood (e.g. campesterol composed < 8.5 % of total sterols in mice blood[53]) and as such, campesterol concentrations were below the MDL in sanguinivorous bat guano.

Sitosterol is commonly the most abundant phytosterol in vegetation[12] and can make up a significant proportion of the total sterol burden in insects[54-56]. Sitosterol concentrations were similar among frugivorous (0.3 to 200 mg g^{-1} dw) and insectivorous (0.3 to 250 mg g^{-1} dw; with the exception of one sample with a concentration of 1,500 mg g^{-1} dw) bat guano. The similar sitosterol concentrations recorded in frugivorous and insectivorous bat guano reflected the consumption of primary producers by frugivorous bats and insects, respectively (Fig S5.1). Stigmastanol is produced from the reduction of sitosterol in the mammalian gut[23] and accordingly, stigmastanol concentrations were similar among frugivorous and insectivorous bat guano as a result of similar sitosterol concentrations (Fig S5.1). Sitosterol was low in sanguinivorous bat guano, which is reflective of the low blood sitosterol concentrations previously seen in mice (e.g. sitosterol composed < 22 % of total sterols in mice blood)[53]. Furthermore, intestinal absorption of sitosterol is < 5 % in humans[57] thus suggesting little opportunity for dietary transfer of sitosterol to sanguinivorous bats. It thus follows that stigmastanol concentrations were also low in sanguinivorous bat guano as a result of limited sitosterol.

In the process of synthesizing cholesterol, sitosterol is converted to fucosterol and subsequently desmosterol in the gut of insects[54,58,59]. Freshwater diatoms have measurable concentrations of fucosterol[60,61] and other algae are largely composed of fucosterol and desmosterol[62,63]. Fucosterol and desmosterol were present in similar proportions within *Daphnia magna*[59] and fucosterol concentrations in algae were reported at 48 μg g^{-1} dw[64]. As such, fucosterol and desmosterol concentrations were greater in insectivorous bat guano relative to frugivorous bat guano as expected if fucosterol and desmosterol were transferred from aquatic insects to insectivorous bats (Fig S5.1).

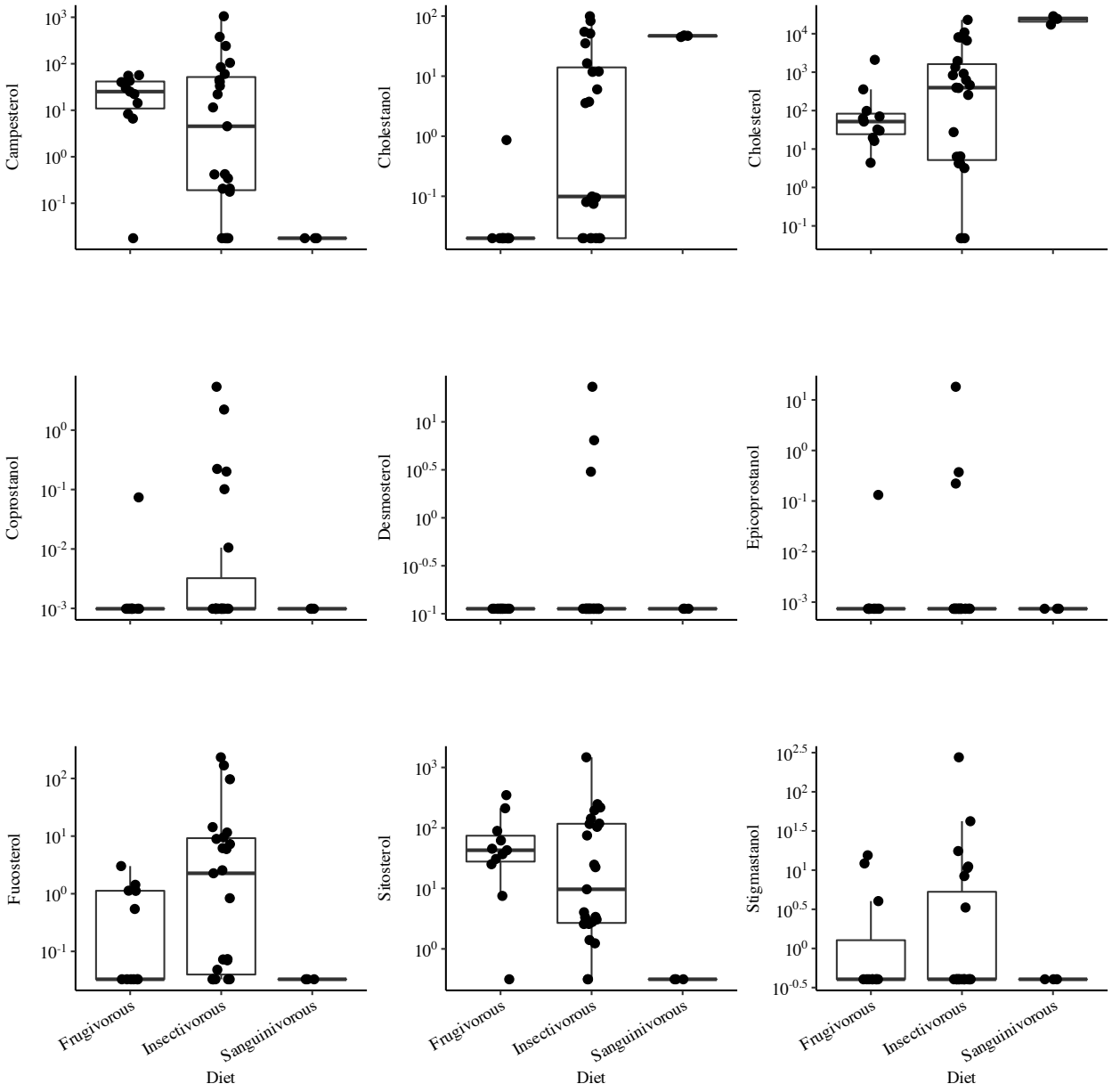

Figure S5.1: Boxplot of sterols and stanols (µg g^{-1} dw) in fresh bat guano samples collected in Belize.

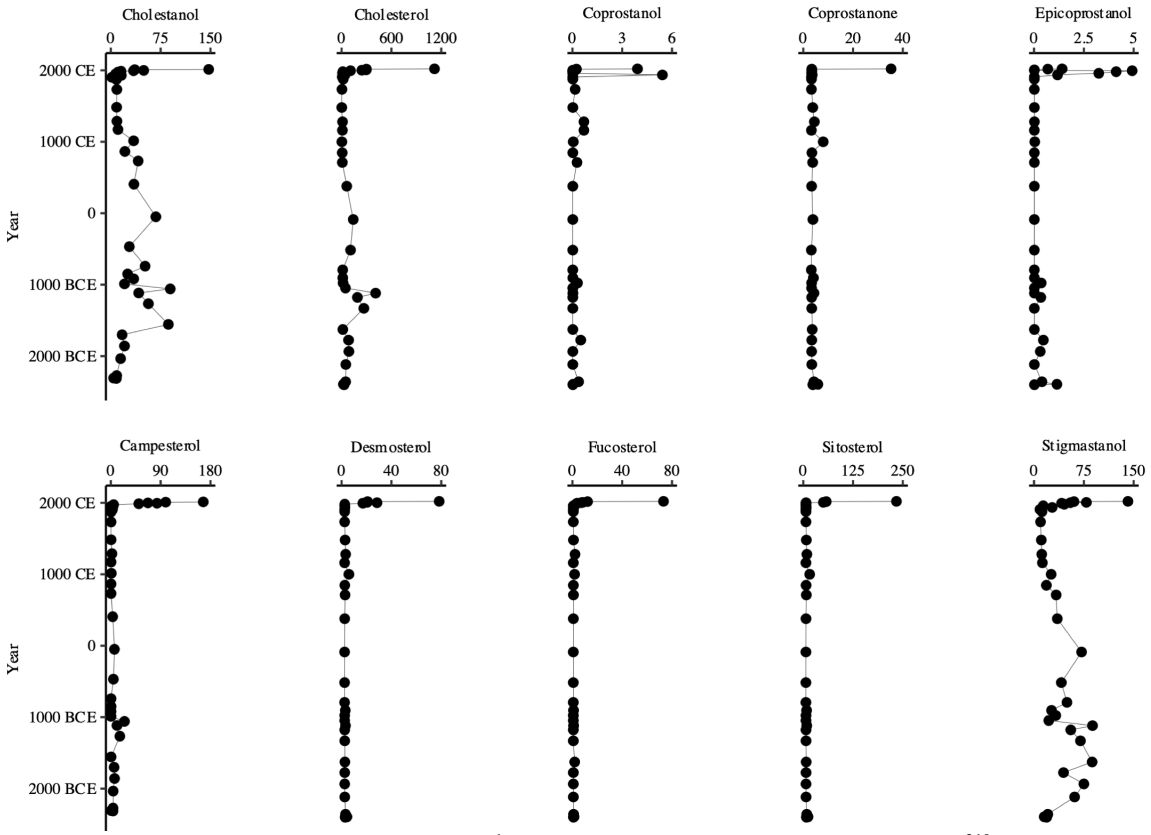

Figure S5.2: Sterol and stanol profiles (ng g^{-1} OC dw) in the bat guano deposit. Select ^{210}Pb (constant rate of supply model) and ^{14}C dates are shown on the y-axis.

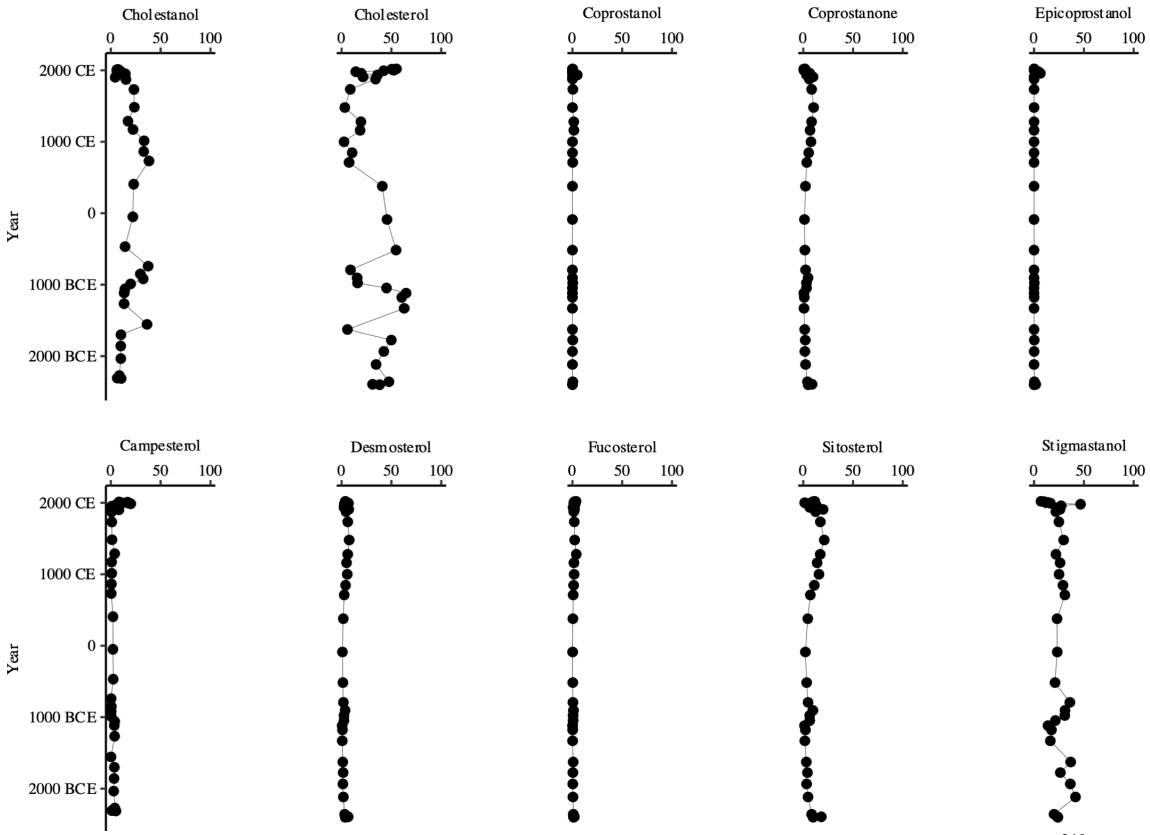

Figure S5.3: Percent relative abundance of sterols and stanols in the bat guano deposit. Select ^{210}Pb (constant rate of supply model) and ^{14}C dates are shown on the y-axis.

Table S5.1: List of bat species and their diet for guano samples collected from Belize. Each guano sample was collected from a different bat.

Bat species	Diet	Number of guano samples
Desmodus rotundus	sanguinivorous	3
Trachops cirrhosus	insectivorous	1
Pteronotus mesoamericanus	insectivorous	3
Pteronotus davyi	insectivorous	3
Mimon cozumelae	insectivorous	2
Micronycteris schmidtorum	insectivorous	1
Saccopteryx bilineata	insectivorous	1
Gardnerycteris crenulatum	insectivorous	1
Rhogeesa anaeus	insectivorous	3
Myotis keaysi	insectivorous	3
Eptesicus farinalis	insectivorous	3
Lophastoma evotis	insectivorous	1
Pteronotus personatus	insectivorous	1
Carollia perspicillata	frugivorous	3
Artibeus jamaicensis	frugivorous	1
Glossophaga soricina	frugivorous	1
Sturnira lilium	frugivorous	3
Carollia sowelli	frugivorous	3

Table S5.2: Average percent recovery of sterols and stanols in one interval of bat guano from the deposit, extracted seven times.

Compound	Recovery (%)
coprostanol	90.8
epicoprostanol	90.1
coprostanone	91.6
cholesterol	88.1
cholestanol	91.8
cholestanone	90.1
desmosterol	87.0
campesterol	93.1
fucosterol	90.7
sitosterol	103.2
stigmastanol	97.0

Table S5.3: Method detection limit (MDL) (ng g^{-1} dw) of sterols and stanols in the bat guano deposit.

Compound	MDL	MDL/√2
coprostanol	1.51	1.07
epicoprostanol	1.13	0.80
coprostanone	237.83	168.17
cholesterol	73.55	51.87
cholestanol	30.75	21.74
cholestanone	23.71	16.77
desmosterol	173.07	122.38
campesterol	27.17	19.21
fucosterol	50.39	35.63
sitosterol	482.71	341.32
stigmastanol	619.85	438.30

Table S5.4: Method detection limit (MDL) (ng g^{-1} dw) of sterols and stanols in the fresh bat guano.

Compound	MDL	MDL/√2
coprostanol	1.40	0.99
epicoprostanol	1.05	0.74
coprostanone	219.11	154.94
cholesterol	67.58	47.79
cholestanol	28.33	20.03
cholestanone	21.84	15.45
desmosterol	159.44	112.74
campesterol	25.03	17.70
fucosterol	46.42	32.83
sitosterol	445.72	314.46
stigmastanol	571.07	403.81

References

1. Kunz, T. H., Braun de Torrez, E., Bauer, D., Lobova, T. & Fleming, T. H. Ecosystem services provided by bats: Ecosystem services provided by bats. *Ann N Y Acad Sci* **1223**, 1–38 (2011).
2. Salvarina, I., Yohannes, E., Siemers, B. M. & Koselj, K. Advantages of using fecal samples for stable isotope analysis in bats: evidence from a triple isotopic experiment. *Rapid Commun Mass Spectrom* **27**, 1945–1953 (2013).
3. Wurster, C. M., McFarlane, D. A. & Bird, M. I. Spatial and temporal expression of vegetation and atmospheric variability from stable carbon and nitrogen isotope analysis of bat guano in the southern United States. *Geochim Cosmochim Acta* **71**, 3302–3310 (2007).
4. Wurster, C. M. *et al.* Stable isotope composition of cave guano from eastern Borneo reveals tropical environments over the past 15,000 cal yr BP. *Palaeogeogr. Palaeoclimatol. Palaeoecol.* **473**, 73–81 (2017).
5. Siemers, B. M., Greif, S., Borissov, I., Voigt-Heucke, S. L. & Voigt, C. C. Divergent trophic levels in two cryptic sibling bat species. *Oecologia* **166**, 69–78 (2011).
6. McCutchan Jr., J. H., Lewis Jr., W. M., Kendall, C. & McGrath, C. C. Variation in trophic shift for stable isotope ratios of carbon, nitrogen, and sulfur. *Oikos* **102**, 378–390 (2003).
7. O'Leary, M. H. Carbon isotope fractionation in plants. *Phytochemistry* **20**, 553–567 (1981).
8. Wurster, C. M. *et al.* Stable carbon and hydrogen isotopes from bat guano in the Grand Canyon, USA, reveal Younger Dryas and 8.2 ka events. *Geology* **36**, 683 (2008).
9. Miron M., L. L. Effect of diet quality on carbon and nitrogen turnover and isotopic discrimination in blood of a New World nectarivorous bat. *J Exp Biol* **209**, 541–548 (2006).
10. Widga, C. & Colburn, M. Paleontology and paleoecology of guano deposits in Mammoth Cave, Kentucky, USA. *Quat Res* **83**, 427–436 (2015).
11. Mizutani, H., McFarlane, D. A. & Kabaya, Y. Nitrogen and carbon isotope studies of a bat guano core from Eagle Creek Cave, Arizona, USA. *J Mass Spectrom Soc Jpn* **40**, 57–65 (1992).
12. Behmer, S. T. & Nes, W. D. Insect sterol nutrition and physiology: A global overview. in *Adv Insect Physiol* vol. 31 1–72 (Elsevier, 2003).
13. Leeming, R., Ball, A., Ashbolt, N. & Nichols, P. Using faecal sterols from humans and animals to distinguish faecal pollution in receiving waters. *Wat Res* **30**, 2893–2900 (1996).
14. Bull, I. D., Lockheart, M. J., Elhmmali, M. M., Roberts, D. J. & Evershed, R. P. The origin of faeces by means of biomarker detection. *Environ Int* **27**, 647–654 (2002).
15. Yamada, J. *et al.* 24-methyl- and 24-ethyl-delta(24(25))-cholesterols as immediate biosynthetic precursors of 24-alkylsterols in higher plants. *Tetrahedron* **53**, 877–884 (1997).
16. Taipale, S. J., Hiltunen, M., Vuorio, K. & Peltomaa, E. Suitability of phytosterols alongside fatty acids as chemotaxonomic biomarkers for phytoplankton. *Front Plant Sci* **7**, (2016).
17. Lopes, G., Sousa, C., Bernardo, J., Andrade, P. B. & Valentão, P. Sterol profiles in 18 macroalgae of the Portuguese coast. *J Phycol* **47**, 1210–1218 (2011).
18. Bull, I. D., Evershed, R. P. & Betancourt, P. P. An organic geochemical investigation of the practice of manuring at a Minoan site on Pseira Island, Crete. *Geoarchaeology* **16**, 223–242 (2001).

19. Jing, X., Grebenok, R. J. & Behmer, S. T. Sterol/steroid metabolism and absorption in a generalist and specialist caterpillar: Effects of dietary sterol/steroid structure, mixture and ratio. *Insect Biochem Molec* **43**, 580–587 (2013).
20. Nes, W. D. *et al.* Sterol utilization and metabolism by Heliothis zea. *Lipids* **32**, 1317–1323 (1997).
21. Cheng, W. *et al.* Sterols and stanols preserved in pond sediments track seabird biovectors in a High Arctic environment. *Environ Sci Technol* **50**, 9351–9360 (2016).
22. Piironen, V., Lindsay, D. G., Miettinen, T. A., Toivo, J. & Lampi, A.-M. Review Plant sterols: biosynthesis, biological function and their importance to human nutrition. *J Sci Food Agric* 28 (2000).
23. Prost, K., Birk, J. J., Lehndorff, E., Gerlach, R. & Amelung, W. Steroid biomarkers revisited – Improved source identification of faecal remains in archaeological soil material. *PLoS One* **12**, e0164882 (2017).
24. Cramer, M. J., Willig, M. R. & Jones, C. Trachops cirrhosus. *Mamm Species* **656**, 1–6 (2001).
25. Gallant, L. R. *et al.* A bat guano deposit in Jamaica recorded agricultural changes and metal exposure over the last >4300 years. *Palaeogeogr. Palaeoclimatol. Palaeoecol.* **538**, 109470 (2020).
26. Gallant, L. R., Kimpe, L. E., Hargan, K. E. & Blais, J. M. Submitted: Tracking the history of cultural eutrophication in High Arctic waterbodies. *Anthropocene* (2020).
27. Cryan, P. M., Stricker, C. A. & Wunder, M. B. Evidence of cryptic individual specialization in an opportunistic insectivorous bat. *J Mammal* **93**, 381–389 (2012).
28. DeNiro, M. J. & Epstein, S. Influence of diet on the distribution of carbon isotopes in animals. *Geochim Cosmochim Acta* **42**, 495–506 (1978).
29. Voigt, C. C. & Kelm, D. H. Host preference of the common vampire bat (*Desmodus rotundus*; Chiroptera) assessed by stable isotopes. *J Mammal* **87**, 1–6 (2006).
30. Meyers, P. A. Applications of organic geochemistry to paleolimnological reconstructions: a summary of examples from the Laurentian Great Lakes. *Org Geochem* **34**, 261–289 (2003).
31. Herbst, L. H. The role of nitrogen from fruit pulp in the nutrition of the frugivorous bat *Carollia perspicillata*. *Biotropica* **18**, 39 (1986).
32. Voigt, C. C. & Matt, F. Nitrogen stress causes unpredictable enrichments of ^{15}N in two nectar-feeding bat species. *J Exp Biol* **207**, 1741–1748 (2004).
33. *Bat management plan for Jamaica*. (2011).
34. Voigt, C. C., Rex, K., Michener, R. H. & Speakman, J. R. Nutrient routing in omnivorous animals tracked by stable carbon isotopes in tissue and exhaled breath. *Oecologia* **157**, 31–40 (2008).
35. Tieszen, L. L., Boutton, T. W., Tesdahl, K. G. & Slade, N. A. Fractionation and turnover of stable carbon isotopes in animal tissues: Implications for delta13C analysis of diet. *Oecologia* **57**, 32–37 (1983).
36. Voigt, C. C. Low turnover rates of carbon isotopes in tissues of two nectar-feeding bat species. *J Exp Biol* **206**, 1419–1427 (2003).
37. Daughton, C. G. Real-time estimation of small-area populations with human biomarkers in sewage. *Sci Total Environ* **414**, 6–21 (2012).
38. Hargan, K. E. *et al.* Sterols and stanols as novel tracers of waterbird population dynamics in freshwater ponds. *Proc. R. Soc. B* **285**, 20180631 (2018).

39. Nishimura, M. & Koyama, T. The occurrence of stanols in various living organisms and the behavior of sterols in contemporary sediments. *Geochim Cosmochim Acta* **41**, 379–385 (1977).
40. Hodell, D. A. *et al.* Reconstruction of Caribbean climate change over the past 10,500 years. *Nature* **352**, 790–793 (1991).
41. Holmes, J. A., Street-Perrott, F. A., Ivanovich, M. & Perrott, R. A. A late Quaternary palaeolimnological record from Jamaica based on trace-element chemistry of ostracod shells. *Chem Geol* **124**, 143–160 (1995).
42. Zeppel, M. J. B., Wilks, J. V. & Lewis, J. D. Impacts of extreme precipitation and seasonal changes in precipitation on plants. *Biogeosciences* **11**, 3083–3093 (2014).
43. Zheng, Y. *et al.* Effects of burial in sand and water supply regime on seedling emergence of six species. *Ann Bot* **95**, 1237–1245 (2005).
44. Frick, W. F. *et al.* Climate and weather impact timing of emergence of bats. *PLoS ONE* **7**, e42737 (2012).
45. Collatz, G. J., Berry, J. A. & Clark, J. S. Effects of climate and atmospheric CO_2 partial pressure on the global distribution of C4 grasses: present, past, and future. *Oecologia* **114**, 441–454 (1998).
46. Paruelo, J. M. & Lauenroth, W. K. Relative abundance of plant functional types in grasslands and shrublands of North America. *Ecol Appl* **6**, 1212–1224 (1996).
47. Bogaard, A. *et al.* Crop manuring and intensive land management by Europe's first farmers. *Proc Natl Acad Sci* **110**, 12589–12594 (2013).
48. Simpson, I. A. *et al.* Interpreting early land management through compound specific stable isotope analyses of archaeological soils. *Rapid Commun Mass Spectrom* **13**, 1315–1319 (1999).
49. Molefe, K. & Mwanza, M. Serum biochemistry in cows of different breeds presented with reproductive conditions. *Onderstepoort J Vet Res* **86**, (2019).
50. Mast, N. *et al.* Cytochrome P450 27A1 deficiency and regional differences in brain sterol metabolism cause preferential cholestanol accumulation in the cerebellum. *J Biol Chem* **292**, 4913–4924 (2017).
51. Casotti, G., Gerardo Herrera M., L., Flores M., J. J., Mancina, C. A. & Braun, E. J. Relationships between renal morphology and diet in 26 species of new world bats (suborder microchiroptera). *Zoology* **109**, 196–207 (2006).
52. Veiga, P. *et al.* Correlation between faecal microbial community structure and cholesterol-to-coprostanol conversion in the human gut. *FEMS Microbiol Lett* **242**, 81–86 (2005).
53. Wilund, K. R. *et al.* No association between plasma levels of plant sterols and atherosclerosis in mice and men. *ATVB* **24**, 2326–2332 (2004).
54. Gilbert, L. I., Rybczynski, R. & Warren, J. T. Control and biochemical nature of the ecdysteroidogenic pathway. *Annu Rev Entomol* **47**, 883–916 (2002).
55. Clayton, R. B. The utilization of sterols by insects. *J Lipid Res* **5**, (1964).
56. Charlet, M., Roussel, J.-P., Rinternecht, E., Berchtold, J.-P. & Costet, M.-F. Development and morphogenetic alterations in larvae of *Locusta migratoria* reared on plant diet with a selectively modified sterol profile. *J Insect Physiol* **34**, 787–796 (1988).
57. Gould, R. G., Jones, R. J., LeRoy, G. V., Wissler, R. W. & Taylor, C. B. The absorption of B-sitosterol in humans. *Metabolism* **18**, 652–662 (1969).
58. Ikekawa, N., Morisaki, M. & Fujimoto, Y. Sterol metabolism in insects: dealkylation of phytosterol to cholesterol. *Acc Chem Res* **26**, 139–146 (1993).

59. Martin-Creuzburg, D., Oexle, S. & Wacker, A. Thresholds for sterol-limited growth of *Daphnia magna*: A comparative approach using 10 different sterols. *J Chem Ecol* **40**, 1039–1050 (2014).
60. Martin-Creuzburg, D. & Merkel, P. Sterols of freshwater microalgae: potential implications for zooplankton nutrition. *J Plankton Res* **38**, 865–877 (2016).
61. Martin-Creuzburg, D., Sperfeld, E. & Wacker, A. Colimitation of a freshwater herbivore by sterols and polyunsaturated fatty acids. *Proc. R. Soc. B* **276**, 1805–1814 (2009).
62. Mouritsen, O. G. *et al.* Effects of seaweed sterols fucosterol and desmosterol on lipid membranes. *Chem Phys Lipids* **205**, 1–10 (2017).
63. Patterson, G. W. Phylogenetic distribution of sterols. in *Isopentenoids and other natural products* (ed. Nes, W. D.) vol. 562 90–108 (J Am Chem Soc, 1994).
64. Pereira, C. M. P. *et al.* Extraction of sterols in brown macroalgae from Antarctica and their identification by liquid chromatography coupled with tandem mass spectrometry. *J Appl Phycol* **29**, 751–757 (2017).

General conclusions

Study outcomes

Chapter 2

The objective of Chapter 2 was to reconstruct the history of wastewater input in three High Arctic waterbodies. We used a multi-proxy approach to study sediments from three waterbodies, R-12, R-13, and Meretta Lake, in which wastewater from an airport was released over the span of several decades. We examined sterol, stanol, metal ratios (metals normalized to titanium), $\delta^{15}N$, and $\delta^{13}C$ in sediment cores influenced by wastewater input and compared the results to those in a reference pond (Little Char). Increased $\delta^{15}N$, coprostanol, cholesterol, and cholestanol tracked wastewater deposition over the last eighty years. Campesterol and sitosterol (phytosterols), increased at the time of wastewater input as a result of increased plant growth in response to the addition of wastewater nutrients. Sterol concentrations in sediments from Little Char were always lower than the concentrations recorded in the wastewater-influenced waterbodies. Sterol concentrations in R-12 and R-13 sediments returned to pre-wastewater concentrations following the cessation of wastewater input, whereas elevated sterol concentrations persisted in Meretta Lake, possibly owing to the longer period of wastewater input than that in R-12 and R-13. Sterols and stanols thus not only tracked the historical influence of wastewater discharge on these waterbodies, but also provided insight into recovery. In R-12, copper and lead ratios increased coeval with wastewater, while arsenic, cadmium, chromium, nickel, and zinc increased more than 15 years after the onset of wastewater input. This study highlighted the importance of using multiple proxies when studying paleo-archives. Our results provided compelling evidence that these paleolimnological approaches may be used

to track human occupation in an Arctic environment, which raises the possibility that they may be applied to other prehistoric archeological investigations in Arctic environments.

Chapter 3

The objective of chapter 3 was to reconstruct the presence of past human habitation in Canada's High Arctic by examining the chemical composition of pond sediments. Specifically, we looked to see if we track changes in sterols, stanols, stable isotopes ($\delta^{15}N$, $\delta^{13}C$), metal ratios (metals normalized to titanium), and chlorophyll *a* (chl *a*) in sediment influenced by the Dorset people (as early as ca. 550 BCE until ca. 1250 CE) and the Thule people (from ca. 1000 to ca. 1600 CE). We examined two known influenced ponds, PaJs 13 and PaJs 3N, (identified based on the presence of whalebone structures around the ponds), and two reference ponds, Sav R4 and Sav R5. The zoosterols, coprostanol and epicoprostanol, and $\delta^{15}N$ values increased in pre-Thule influenced sediments, marking the earlier arrival of the Dorset people as early as ca. 860 CE. These same proxies then peaked in Thule-influenced sediments at ca. 1000 CE, coeval with the timing of previously suggested Thule occupation [1,2], as opposed to the more recently suggested date of ca. 1200 CE [3]. Cadmium, copper, and zinc ratios increased in Thule-influenced sediments from PaJs 13, whereas metal ratios were low and stable in Dorset-era sediments and reference pond sediments. These proxies thus tracked not only the presence of human settlements in High Arctic ponds, but also their level of influence on the environment. The Thule people flensed whales whereas the Dorset did not, and consequently we see greater changes in sterols, stanols, and metals in association with Thule occupation relative to Dorset occupation. This chapter demonstrated that the same proxies used in Chapter 2 to reconstruct wastewater discharge in the last century, can also be used to infer the presence of human settlements in the High Arctic over the past 2000 years. This study provided the first look at

changes in the sterol, stanol, and metal composition of lake sediments as a result of Thule and Dorset occupation in High Arctic ponds. We surmised that the combined analysis of sterols, stanols, stable isotopes, and metal ratios in pond sediments could be used to identify other historically occupied sites to inform archeological and anthropological investigations, and infer the long-term effects of human activity on sediment chemistry.

Chapter 4

Intact bat guano deposits serve as natural archives allowing for the reconstruction of historical environmental conditions through time. The objective of this chapter was to infer historical metal exposure and dietary changes based on the chemical composition of a bat guano deposit. We collected a 4,300-year-old bat guano deposit from the Home Away from Home cave in Jamaica and inferred past agricultural practices (using $\delta^{15}N$, $\delta^{13}C$, and $\delta^{34}S$) and industrial activity (using the ratios of cadmium, lead, mercury, and zinc to titanium). $\delta^{15}N$, $\delta^{13}C$, and $\delta^{34}S$ values tracked the introduction of nitrogen fertilizers, sugarcane, and fungicides, respectively. Cadmium, mercury, lead, and zinc ratios increased in guano, coincident with the onset of the Industrial Revolution in ca. 1760. $^{206}Pb/^{207}Pb$ isotopes tracked the introduction of leaded gasoline in the 1930s and its subsequent removal from the market in the 1970s. Bat populations are under stress globally and this chapter highlighted the importance of emission controls to reduce the risk of exposure to metals. To our knowledge, this was the first study to document ~4,300 years of anthropogenic metal exposure to bats and provide information on historical metal exposure, which could serve useful in highlighting the effects of industrial emissions on wildlife exposures to contaminants, and the importance of emission controls.

Chapter 5

The objective of this chapter was to determine whether differences in the chemical composition of bat guano were affected by their diet. We first characterized the sterol, stanol, and stable isotope profiles in guano from species-identified bats. In doing so, we were the first to characterize these chemical profiles of bat guano for frugivorous, insectivorous, and sanguinivorous bats. We then determined the sterol, stanol, and stable isotope composition in a ~4,300-year-old bat guano deposit. We identified two periods of frugivory-dominated foraging based on coincident decreases in cholesterol/(cholesterol+sitosterol) ratios, decreased $\delta^{13}C$ values, and increased C/N values. We surmised that these two periods, which were characterized by wetter climactic conditions, may have promoted fruit growth, as well as suppressed insect activity and/or decreased a bat's ability to echolocate, resulting in increased frugivory/insectivory-based foraging.

In the fresh bat guano, phytosterols (campesterol, sitosterol, and stigmastanol), $\delta^{13}C$, and $\delta^{15}N$ were similar in frugivorous and insectivorous bat guano owing to the dietary intake of vegetation by the bats themselves or the insects consumed by bats, respectively. As predicted, phytosterols were not detected in sanguinivorous bat guano owing to low phytosterol concentrations in mammalian blood. Cholesterol and cholestanol concentrations were greatest in sanguinivorous bat guano (owing to elevated dietary blood concentrations), followed by insectivorous bat guano, and lastly, frugivorous bat guano (reflecting low cholesterol and cholestanol concentrations in fruits). To our knowledge, this thesis was the first to identify differences in the sterol and stanol profiles in bat guano based on foraging habits. Furthermore, this thesis was the first to infer long-term changes in dietary habits based on the sterol and stanol profiles in a bat deposit. This chapter demonstrated that sterols, stanols, (and their ratios), and stable isotopes were reflective of a bat's diet in species-identified bat guano. Consequently, we

determined that long-term trends in diet could be tracked within a bat guano deposit using the same chemical constituents.

General conclusions

Metal ratios tracked the history of anthropogenic activity

Metal ratios (metals normalized to titanium) in High Arctic lake sediments and a bat guano deposit from Jamaica were greatly influenced by human activity over the past 1000 years, highlighting metal exposure in two very different environments. Metal ratios of cadmium, chromium, copper, lead, nickel, and zinc tracked the influence of wastewater discharge on the metal composition of waterbody sediments as well as recovery in post-wastewater influenced sediments. Differences in sediment metal ratios in wastewater-influenced waterbodies suggested differences in wastewater discharge and/or a dilution effect owing to waterbody size. We also used metal ratios to track the presence of the Thule people in High Arctic ponds owing to increased metal loadings that we suspect were derived mainly from hunted animals, which largely comprised of bowhead whales. Low (or absent) metal ratios in reference pond sediments highlighted the low backgrounds for these metals in the Arctic environment, which likely helped to amplify the Thule/Dorset signal in the sites that were occupied by these peoples. Metal ratios in the bat guano deposit increased coeval with anthropogenic activity during the Industrial Revolution and demonstrated the extent to which bats were exposed to anthropogenic metals. Furthermore, we used lead isotope ratios to track the introduction and subsequent banning of leaded gasoline in the bat guano deposit. This thesis found that metals were consistently a useful proxy for tracking human influence as demonstrated by changes in metals in response to wastewater discharge, human settlements, and mining activity. To our knowledge, we conducted the first analysis documenting increased metals in High Arctic sediments as a result of Thule

occupation. This thesis was also the first to reconstruct historical changes in metal exposure to bats based on the chemical composition of their guano over the past 4,300 years.

Sterols and stanols reflected human activity in lake sediments and bat dietary habits in bat guano

There is a growing interest in the use of sterols and stanols for paleolimnological studies as they may be a source-specific proxy in some circumstances [4–6]; we thus used sterols and stanols to track both human activity in lake sediments and dietary changes in bat guano. Sterols and stanols can function as biomarkers of human presence as the specificity of the sterol composition in vegetation and animals can be used to reconstruct long-term trends in waterbody sediments. Coprostanol has been used for sewage identification in environmental samples as far back as the 1980s [7]. Indeed, we observed increased sediment coprostanol concentrations coincident with wastewater input into High Arctic waterbodies. Other zoosterols (cholesterol, cholestanol, and epicoprostanol) and phytosterols (sitosterol and stigmastanol) also increased in wastewater-influenced sediments. Sterols and stanols also proved useful in tracking the recovery of sediments to pre-wastewater conditions following the cessation of wastewater input. Similarly, sterol and stanol concentrations tracked human occupation in High Arctic waterbodies approximately 2000-years-ago. This thesis found that sterols and stanols were well-preserved in High Arctic waterbody sediments and can be powerful tools for tracking human activities on millennia time scales.

The sterol and stanol composition of excrement is reflective of dietary intake [8–10]. Sterols and stanols offer a more specific means to determine the differences in the chemical composition of bat guano based on dietary trends. Cholesterol and its reduction product, cholestanol, increased in bat guano according to trophic level as predicted given that cholesterol is synthesized *de novo* in mammals and only found in small concentrations in fruits.

Sanguinivorous bats do not consume fruits and consequently, they had the lowest phytosterol concentrations in their guano. Mean phytosterol concentrations were similar among frugivorous and insectivorous bats, reflecting their consumption of fruits and insects that feed on vegetation, respectively. We found that sterol and stanol ratios (the trophic level index and the expanded index) and the C/N ratio distinguished frugivorous from insectivorous bats: these ratios represented the proportion of fruits and insects within a bats' diet, which was reflective of their trophic level. We then examined the composition of sterols and stanols in a 4,300-year-old bat guano deposit in order to characterize historical bat foraging habits. Given the ability of the sterol and stanol ratios to differentiate between frugivory and insectivory-based foraging in fresh bat guano, we employed the use of sterol and stanol ratios to examine long-term dietary changes in the deposit. Both the trophic level and expanded index, coupled with the C/N profile, tracked two periods of increased frugivory relative to insectivory in the bat guano deposit. This thesis demonstrated the use of sterols and stanols as a powerful proxy for a broad range of applications including examining historical anthropogenic activity, monitoring waterbody recovery, and identifying differences in foraging habits.

Future directions

This thesis demonstrated the versatility of sterols and stanols to infer both human activity in waterbody sediments and dietary trends in bat guano. While we used sterols and stanols to track human activity in High Arctic lake sediments ~2000-years-ago, the stability of these compounds suggests that archeological investigations of pre-historic Arctic peoples before this time period are also possible. Furthermore, we used sterols and stanols to record the history of human settlement at ponds known previously to have been occupied by the Thule people, as evidenced by the presence of whalebones in, and adjacent to, these ponds. We thus suggest that

sterols and stanols could also be used to infer the presence of humans (or other biota) in pond sediments, in the absence of physical evidence.

While cholestanol and cholesterol concentrations in guano were distinguishable between bat foraging strategies, differences in other sterols and stanols, (particularly the phytosterols: campesterol, fucosterol, sitosterol, and stigmastanol) were less obvious. In order to better differentiate between foraging habits, we recommend the use of bile acids, which can offer more source specific information [10]. Bile acids were found in greater concentrations in human faeces (relative to sterols and stanols) and thus better tracked historical wastewater discharge [11]. Similarly, bile acids were well-preserved in archaeological soils and were better able to identify the presence of faecal matter [12]. As such, we suggest the combined use of sterols, stanols, and bile acids to reconstruct the effects of human activity and track dietary trends in order to improve the clarity of the results.

Sterols and stanols (with the exception of cholestanol and stigmastanol) were generally low in the bat guano deposit making it difficult to observe long-term trends. We thus employed the use of two sterol and stanol ratios, the trophic level index and the expanded index, in order to examine historical differences in the sterol and stanol composition of the bat guano deposit. It was through the use these ratios that we were able to track periods of frugivory within the 4,300-year-old bat guano deposit. Sterol and stanol ratios are thus powerful tools that can be employed in natural archives to better observe historical changes in diet or human influence.

Closing statement

This thesis aimed to examine changes in the chemical composition of two different natural archives, lake sediments cores and bat guano deposits, for the purpose of reconstructing historical environmental conditions. We demonstrated that our multi-proxy approach was a

powerful tool allowing one to conduct a broad range of analysis in various natural archives. This thesis served to improve our understanding of how human activity has affected the environment and provide future researchers with new tools and methods to continue to monitor and improve the health of the environment.

References

1. Savelle JM. The role of architectural utility in the formation of zooarchaeological whale bone assemblages. J Archaeol Sci. 1997;24: 869–885. doi:10.1006/jasc.1996.0167
2. McCartney AP. Thule Eskimo prehistory along northwestern Hudson Bay. Archaeological Survey of Canada. 1977.
3. Savelle JM. Cumulative bowhead whale (*Balaena mysticetus*) harvest estimates by prehistoric Thule Inuit in the Canadian Arctic 1200–1500 A.D.: Implications for bowhead whale population modeling and Thule demography. Bulletin of National Museum of Ethnology. 2010;34: 26.
4. Bull ID, Lockheart MJ, Elhmmali MM, Roberts DJ, Evershed RP. The origin of faeces by means of biomarker detection. Environ Int. 2002;27: 647–654. doi:10.1016/S0160-4120(01)00124-6
5. Leeming R, Ball A, Ashbolt N, Nichols P. Using faecal sterols from humans and animals to distinguish faecal pollution in receiving waters. Wat Res. 1996;30: 2893–2900.
6. Leeming R, Latham V, Rayner M, Nichols P. Detecting and distinguishing sources of sewage pollution in Australian inland and coastal waters and sediments. In: Eganhouse RP, editor. Molecular markers in environmental geochemistry. Washington, DC: American Chemical Society; 1997. pp. 306–319. doi:10.1021/bk-1997-0671.ch020
7. Vivian CMG. Tracers of sewage sludge in the marine environment: A review. Sci Total Environ. 1986;53: 5–40. doi:10.1016/0048-9697(86)90091-4
8. Prost K, Birk JJ, Lehndorff E, Gerlach R, Amelung W. Steroid biomarkers revisited – Improved source identification of faecal remains in archaeological soil material. Bicho N, editor. PLoS One. 2017;12: e0164882. doi:10.1371/journal.pone.0164882
9. Battistel D, Piazza R, Argiriadis E, Marchiori E, Radaelli M, Barbante C. GC-MS method for determining faecal sterols as biomarkers of human and pastoral animal presence in freshwater sediments. Anal Bioanal Chem. 2015;407: 8505–8514. doi:10.1007/s00216-015-8998-2
10. Birk JJ, Dippold M, Wiesenberg GLB, Glaser B. Combined quantification of faecal sterols, stanols, stanones and bile acids in soils and terrestrial sediments by gas chromatography–mass spectrometry. J Chromatogr A. 2012;1242: 1–10. doi:10.1016/j.chroma.2012.04.027
11. Bull ID, Elhmmali MM, Roberts DJ, Evershed RP. The application of steroidal biomarkers to track the abandonment of a Roman wastewater course at the Agora (Athens, Greece). Archaeometry. 2003;45: 149–161. doi:10.1111/1475-4754.00101
12. Evershed RP, Bethell PH. Application of multimolecular biomarker techniques to the identification of fecal material in archaeological soils and sediments. In: Orna MV, editor. Archaeological Chemistry. Washington, DC: American Chemical Society; 1996. pp. 157–172. doi:10.1021/bk-1996-0625.ch013